UNIVERSITY *of the*
WESTERN CAPE

Graphene based materials for carbon capture

by

Gabrielle Enid Kelly

M.Sc. thesis submitted in partial fulfilment of the requirements for the degree of Magister Scientiae

In the Department of Chemistry, Catalysis Research Group,

University of Western Cape

Supervisors

Prof. Salam Titinchi

Dr Hanna Abbo

Declaration

I declare that "Graphene based materials for carbon capture" is my own work, that it has not been submitted for any degree or examination in any other university, and that all the sources I have used or quoted have been indicated and acknowledged by complete references.

Full name: ……..… Date: ……..

Signed: ……

Acknowledgements

This thesis marks the end of my MSc degree. Throughout the writing of this dissertation I have received a great deal of support and assistance from a number of people and organisations. I would like to first and foremost thank my parents; Mr. K. Kelly and Miss. C. Klein for their understanding and guidance throughout my academic career. I want to express my deepest gratitude for affording me the opportunity to pursue my life goals. To my siblings Mrs. N. Arnold, Mr. C. Klein and Mrs. K. Mandes for their advice, unwavering love and continuous positive reinforcement's. I would like to express my deepest appreciation to Dr. S. Titinchi for allowing me to be part of the Inorganic Catalysis Research team. I am truly thankful for the valuable guidance and vast knowledge which has been passed onto me. It has been a great experience to work under your supervision, also knowing that I could seek assistance at any given time of the day and your door would always be open. To my co-supervisor Dr. H. Abbo whose expertise was invaluable in the formulation of the research topic, thank you for your patience and words of encouragement. To the rest of my colleagues in the Inorganic catalysis team thank you for welcoming me into the group and assisting where possible. Above all to my fiancé, Sharief Petersen for being by my side during the gloomiest days, for always passing on a joke to make me smile, words of wisdom and constant motivation. To my extended family and friends thank you for not allowing me to give up.

This work has been the result of collaborations within different departments of the University of Western Cape and other research institutions. I would like to extend my appreciation to Mr T. Lesch, Chemistry department (UWC), Mr. A. Josephs from the Physics Department (UWC), Dr. R. Bucher from ithemba Labs, for assisting me with

my HR-SEM, EDS and XRD analysis. I also would like to acknowledge Dr. W. Davids from HySA Systems for his immense assistance and giving me the opportunity to do my FT-IR and N_2 Physisorption analysis at the facility.

Finally, I would like to acknowledge the financial assistance received from the National Research Foundation (NRF).

Dedicated to my late father, Kenneth Kelly

Contents

Glossary

APTES	Aminopropyltriethoxy silane
CCS	Carbon Capture and Sequestration
CCS	Carbon Capture and Storage
CFCs	Chlorofluorocarbons
FT-IR	Fourier Transmission Infrared
GHG	Greenhouse gases
GO	Graphene oxide
HCFCs	Hydrochlorofluorocarbons
HFCs	Hydrofluorocarbons
IGCC	Integrated Gasification Combined Cycle
MEA	Monoethanolamine
MOF	Metal Organic Framework
NGCC	Natural Gas Combined Cycle
NO_X	Nitrous oxides
OMS	Ordered mesoporous silica
SEM	Scanning Electron Microscopy
SSNMR	Solid State Nuclear Magnetic Resonance
TEM	Transmission Electron Microscopy
TEPA	Tetraethylenepentamine
TGA	Thermogravic Analysis
TPD	Temperature Programme Desorption
TRIS	Tris(2-aminoethyl) amine
UV	Ultraviolet radiation
VOC's	Volatile organic compounds
XRD	X-ray Diffraction

List of Figures

List of Tables

List of Schemes

Abstract

The adverse effects of CO_2 and greenhouse gas emissions into the atmosphere is believed to be one of the causes of climate change. The seriousness of global warming is encouraging the development of technologies designed to reduce CO_2 emissions. Adsorption in the broadest context can be considered to be a promising method to address this due to the energy saving potential and regenerability, compared to other techniques. In this study, graphite was first oxidized to graphene oxide (GO) with concentrated acid. This was followed by formation of the aminosilanes viz. 3-aminopropyl-triethoxysilane (APTES), tris(2-aminoethyl)amine (TRIS) and guanidine being functionalized onto the surface of graphene oxide (GO). A second series involving the ordered mesoporous materials (OMS) was prepared employing cetyltrimethylammonium bromide (CTAB) and P123 triblock copolymer, as the structure directing agents for the organization of polymerizing silica species. Following the self-assembly of OMS onto GO, the so formed GO-OMS compound was modified with polyethylenimine (PEI).

Several characterization techniques such as X-ray powder diffraction (XRD), Fourier Transform Infra-Red (FT-IR) spectroscopy, high resolution scanning microscopy (HRSEM), high resolution transmission electron microscopy (HRTEM) and N_2 physisoprion employing the Brunauer-Emmett-Teller (BET) analysis to determine specific surface areas of porous solid materials were employed to study the structural, morphological and textural properties of the adsorbents. CO_2 isotherms employing thermogravimetric analysis (TGA) were used to analyse modified GO for CO_2 capture. The CO_2 adsorption uptake of modified GO with aminosilanes and GO-OMS-PEI were studied and compared. CO_2 adsorption characteristics of OMS were studied using CO_2-

thermogravimetric analysis (TGA). The results revealed that the structural integrity of modified GO was not compromised during the functionalization process and showed stable CO_2 adsorption uptake in the adsorption-desorption cycles proving that the modified materials were able to be regenerated.

Keywords

Graphene oxide

APTES (amino propyl triethoxy silane)

TRIS (2-aminoethyl) amine

Guanidine

Ordered mesoporous silica

Polyethylenimine

Chapter 1

Introduction

Chapter 1 outlines the study conducted and briefly describes the importance of alleviating global warming through CO_2 sequestration. It refers to the materials synthesized, which have a great potential to reduce carbon emissions and highlights how the synthesis will be conducted.

Chapter 2 reviews the literature consulted to corroborate the technological approaches implemented by various research groups for CO_2 sequestration. Moreover, it elucidates the major combustion processes and highlights their advantages and disadvantages with respect to its immediate application to fixed point sources. In addition, chapter 2 draws attention to the various supports used for CO_2 capture and subsequently discusses why solid adsorption techniques outperform the others. It further describes GO, the structural models proposed by scientists over the years and their superiority. GO synthesis methods and those of its derivative are also discussed. Finally, this chapter describes the general chemical reactions that take place between the as-synthesized GO and functionalized as-synthesized GO (aminosilanes and OMS/OMS-polymer) as well as their reactions with CO_2.

Chapter 3 highlights in detail the apparatus of various characterization techniques employed for the analysis of as-synthesized GO before and after functionalization.

Chapter 4 illustrates results based on the synthesis of GO material and its functionalization using grafting and self-assembly methods.

Chapter 5 presents and discusses the results obtained from previously mentioned characterization techniques

Chapter 6 encapsulates the conclusions of this investigation and proposes recommendations for future research work.

1.1 Background

Greenhouse gases found in the atmosphere are made up of CO_2, NO, CFCs, HFCs and HCFCs, as well as, CH_4 and O_3 [1]. When greenhouse gases increase in the atmosphere, UV rays become entrapped inside the stratosphere causing a heating effect, referred to as global warming [2]. The alarming global atmospheric CO_2 concentration has escalated by about 80%, from ~21 Gt in 1970 to ~38 Gt in 2004 [3]. South Africa is claimed to be the highest emitter of CO_2 on the African continent and the 12th highest contributor in the world [4]. Eskom, South Africa's leading electricity producer, to date, still uses coal as its primary energy source, with an average of 92% fuel input to generate power [5]. Subsequently, a condemnation by the international community has been assigned to human activities for their negative impacts, facilitating adverse climate change [6]. In addition, fixed point sources such as pulverized coal fired power plants and cement, steel and petrochemical industries have also been identified as major contributors of CO_2 emissions [7]. Numerous critical research reports emphasized that glaciers are melting faster than ever before affecting low lying countries [8]. Sea levels are rising threatening the natural habitats of animal and plant species along ocean boarders and thus leading to their possible extinction [9]. For the past few decades, research studies have suggested that environmental changes could be alleviated by CCS. However economic constraints remain the biggest limitation in this regard. The largest worldwide CO_2 producing conglomerates have often misunderstood the essential affordability of new equipment or the total rebuilding of plants, regardless of their effects on the environment. Hence, newly implemented, affordable, feasible and applicable methods with high CO_2 adsorption capacities need to be developed [10]. To this end, combustion processes have been described as the most reliable technique for CO_2 reduction [11]. The three primary combustion processes documented in literature

include pre-combustion, oxy-combustion and post-combustion. Post combustion has an advantage of not demanding the construction of new plants and can immediately be retrofitted to existing power stations [12]. In addition, the common techniques used to capture CO_2 from flue gases involve cryogenic distillation, adsorption, absorption and membrane separation [13].

Recently, zeolites, MOFs, polymer based sorbents and porous silicates have been considered as effective materials that could be incorporated in the capturing techniques used to reduce CO_2 [14]. Indeed, adsorption techniques employing carbonaceous supports have been recognized as promising remedies because of the active sites available to facilitate functionalization. Basic functional groups, high specific surface areas as well as remarkable sensitivity towards water due to a hydrophilic structure are a few of the principle factors which affect the functionalization of materials used to reduce CO_2 [13].

The current study employs amorphous carbon, GO and mesoporous carbon GO-OMS to selectively adsorb CO_2. Graphite, the starting material from which GO and GO-OMS substrates are synthesized is affordable and readily available. These two materials can be synthesized using strong oxidizing agents to incorporate oxygen containing functional groups onto their basal planes and edges of the layered structure. The presence of oxygen containing functional groups facilitates ionic and non-ionic interactions with a wide selection of molecules [15]. The advantage of the GO's structure is its ability to undergo surface modification. Such modifications take place through grafting of amine functional groups onto the solid support whilst the modification of GO-OMS can take place through self- assembly methods [13]. Grafting and self-assembly have been studied and proven to be inexpensive methods for producing stable materials such as amorphous silica [16] and polymer-modified

graphene sheets [17]. Amine functional groups were grafted onto GO supports through condensation of the coupling agents viz., APTES, TRIS and Guanidine. GO-OMS was synthesized through a two-step self-assembly process employing cationic surfactant CTAB and co-block polymer P123 surfactant [18-20].

The chemical reactions between the basic amine functionalized GO and slightly acidic CO_2, takes place through a two-step zwitterion reaction forming carbamates and bicarbonates as presented in equations 1 and 2 (Scheme 1). R is an alkane group, $RNHCO_2^- - RNH_3^+$ represents a carbonate and $RNH_3 + HCO_3 + RNH_2$ represents a bicarbonate.

$$2(RNH_2) + CO_2 \rightleftharpoons \underset{\text{carbonate}}{RNHCO_2^- - RNH_3^+} \quad \text{..... 1}$$

$$RNHCO_2^- - RNH_3^+ + H_2O \rightleftharpoons \underset{\text{bicarbonate}}{RNH_3 + HCO_3 + RNH_2} \quad \text{..... 2}$$

Scheme 1: Two step zwitterion reaction

1.2 Problem statement

The adverse effects of uncontrolled population increase at the present rate can have major consequences on the environment because of the dependence on coal for power generation [10]. Capturing and sequestering CO_2 through post combustion processes is one of the techniques that could immediately be implemented within existing power plants as an intermediate solution to the building of new power plants. The utilisation of solid carbonaceous adsorbents has proven to be a remediation method to addressing this challenge. The adsorbent materials should be stable at normal conditions of temperature and pressure, have spontaneous adsorption and desorption kinetics and exhibit

regenerability. The scale up of this process could be a promising remediation technique for CO_2 reduction and demand less energy to minimize economic restrictions.

1.3 Hypothesis

The modification of the as-synthesized GO surface support by functionalization with amine groups via silylation to enhance CO_2 adsorption can be employed to reduce GHG emissions and mitigate global warming.

1.4 Research questions

- Is it possible to develop a method to achieve exfoliation of graphite of high quality to produce single layer materials from graphite precursors?
- What are the effects of employing oxidizing precursors to the synthetic process?
- Which aminosilane linkers used for the functionalization of GO would improve the adsorption capacity of CO_2.
- Is it possible to get mesoporous silicas (CTAB and P123) to electrostatically adsorb and self-assemble onto the surface of GO resulting in GM-silica sheets with high surface areas.
- Which method of functionalization provides higher adsorption capacity of CO_2 i.e. self-assembly or grafting?

1.5 Aims and objectives

The purpose of this research aims to investigate different amine solid sorbents for capturing CO_2 using thermal analysis studies.

Therefore, the objectives of this research include:

- The synthesis of GO with a modified method to enhance the exfoliation of GO layers to achieve large quantities of single layer graphene.
- The measurement of adsorption properties of CO_2 in different solid amine adsorbents. A probabilistic comparison is then to be made among these solid sorbents.
- The modification of as-synthesized GO surface via grafting methods by incorporating various aminosilane linkers as well as embedding OMS into the layers of GO with self-assembly methods
- Various characterization techniques will be used to study the properties and structures of as-synthesized GO and their functionalized analogues.
- The utilization of thermal analysis technique, TGA to determine the CO_2 adsorption capacity of as-synthesized functionalized GO and G/Silica composites.

1.6 Research approach

This research focused on modifying and optimizing synthetic methods to produce greater exfoliation between GO layers of high quality. The as-synthesized GO materials will be analysed by different characterization techniques. The crystalline structure, surface areas, pore size, specific functional groups, chemical composition of the individual elements and morphology will be studied using various characterization

techniques. Fourier transform infrared spectroscopy (FT-IR) will be employed to identify organic functional groups which might or might not have been incorporated onto the GO structure when oxygenation occurred. N_2 physisorption employing, Brunauer–Emmett–Teller (BET) and Barrett-Joyner-Halenda (BJH) methods will be used to determine surface areas, pore size and pore volume. Scanning electron microscopy (SEM) will be used to provide images which demonstrate the exfoliation of the individual layers, chemical composition as well as surface topography. Transmission electron miscopy (TEM) will be employed to determine morphology and X-ray diffraction (XRD) to confirm the crystallinity of GO. The functionalization will be achieved through grafting and self-assembly procedures. Initially as-synthesized GO will be functionalized with various functionalities using aminosilane linkers such as APTES, TRIS, and Guanidine. The impregnation of CTAB and P123 into the layers of GO will also be investigated. The above mentioned characterization techniques will be used to prove that the functionalization of GO has taken place. In addition, thermogravimetric analysis (TGA) will be employed to study CO_2 adsorption of as-synthesized GO and functionalized GO analogues

1.7 Scope and limitations of study

The field of carbon based materials has received an enormous amount of interest within material science and catalysis [21]. However, various possibilities and modifications of GO have been proposed in literature [22]. The study covers oxidation of graphite to GO by employing a modified Hummers method which incorporates oxygen containing functional groups into its aromatic structure. Two synthetic methods were employed in this study to try and optimize the oxidation process. The presence of hydroxyl groups found on the edges and basal planes of GO enables grafting to occur with trialkoxy

groups of aminosilanes via silylation reactions. The impregnation of OMS between GO layers was a technique employed to increase the surface area with the self-assembly of PEI. These changes are hypothesized to enhance adsorption of CO_2. Various physicochemical techniques were employed to study GO before and after functionalization takes place. The adsorption behaviour was studied through gravimetric analysis employing thermal decomposition studies in which the samples are subjected to a temperature ramp, in which the change in sample mass of material is affected by the change in time. The morphology of the GO-CTAB and CTAB-PEI were studied with SEM and TEM. However, due to time constraints GO-CTAB and GO-CTAB-PEI were the only samples, selected at random for analysis. Mesoporous silicas have been widely published in literature and have demonstrated good adsorption abilities. Designing and developing new hybrid nanomaterials such as novel G/Silica nanosheet composites have recently been synthesized because of the structural potential both GO and OMS possess and because the materials possess the ability to be integrated into organic-inorganic nanocomposites [23]. Therefore, being able to determine the size and morphology of their structure was important. The recyclability of the as synthesized functionalized materials were limited to three cycles and only three samples were selected at random.

Chapter 2

Introduction

This chapter provides a general overview of the literature covering technological approaches used to sequester CO_2. It touches on the different ways in which CO_2 can be separated, either through absorption or adsorption and discusses a few absorbent and adsorbent materials. Emphasis is placed on adsorption and the effects amine functionalization has on the adsorption capacity of various sorbent materials. Graphene oxide and graphene oxide mesoporous silica was employed as the solid supports in this study.

2.1 Technological approaches to capture CO_2

Technological techniques applied to fossil fuelled power plants can be divided into various categories. This study will briefly discuss pre-combustion, post-combustion and oxy-combustion by taking into account that technology has its own advantages and disadvantages and are at different stages in their development [24].

2.1.1 Pre-combustion capture

Pre-combustion can be classified as a gasification process which occurs before combustion takes place. It is commercially employed and practiced in various industries such as the manufacturing of ammonia and hydrogen from hydrocarbon feed stocks. The production of a primary fuel within a reactor involves reaction of air, oxygen or steam at elevated temperatures and pressures producing a combination of H_2 and CO.

This process is commonly referred to as the synthesis gas process. In addition, steam reacts with the produced CO in a catalytic or water gas shift reaction to obtain CO_2 and an excess of H_2. The blend of H_2 and CO_2 can be separated into their individual streams, one consisting of CO_2 and the other H_2 [25] [26]. A power plant that employs a syngas in its system can be classified as an integrated gasification combined cycle (IGCC). The IGCC process is another route which can be undertaken for the production of electricity. CO_2 released from shift converters in the IGCC process exhibits relatively high partial pressures and for this reason physical solvents can be used as an alternative to chemical solvents. Physical solvents require less energy during regeneration and therefore are a favoured technique. However, one of the drawbacks is that the process requires low temperatures to operate at full capacity. An advantage application of the pre-combustion processes is the evolution of high CO_2 concentrations in addition to high pressures. Thus results in a reduced amount of energy consumed during the capturing process. The fuel conversion steps are more complicated and therefore more expensive than those involved in post-combustion techniques. The upside however is production of a hydrogen-rich fuel that can be employed as a starting material in the production of fuel cells or the introduction of the development of a society using hydrogen to generate power. One of the key disadvantages of the pre-combustion capturing processes is the need for long-term development in various areas to improve the progress of an economy approaching hydrogen [27-29].

2.1.2 Oxy-combustion

Oxy-combustion is a technological capturing process that consumes pure oxygen as an alternative to air. It almost exclusively produces CO_2 and water. CO_2 can be separated

from water through condensation. Since, no flue gas desulphurization unit and NO_x reduction units are needed the CO_2 concentration from the flue gas output streams in oxy-combustion processes are considered to be beneficial. Most of the SOx and NO_x gasses are captured with CO_2 [30]. The conditions of a specific sites' retrofitting limits the oxy-combustion process. High energy costs are required to separate oxygen from air. Oxy-combustion technologies can be considered as a platform for the initiation of a "zero emission cycle" configured to new plants but it unfortunately results in complete redesign of turbines negatively impacting the total cost of operation. This process is still in its early developmental stages due to the high temperatures at which combustion of oxygen takes place for a regular power plant and hence the lack of a full scale display as well as limited experience [31].

2.1.2 Post-combustion capture

Post combustion is a technological capturing process which follows after the combustion of fossil fuels from the flue gas stream. The capturing process can be applied to pulverized coal, oil-fired or gas-fired power plants. The CO_2 found within these flue gases exist as a mixture of inert gases such as argon, NO_x as well as SO_2, oxygen and water. The CO_2 needs to be removed from these gases. Contaminants such as SO_2 are extremely difficult to remove and influence the running of the capturing process. Inhibitors are essential to limit corrosion and oxidative degradation due to residual oxygen in the flue stream [24]. There are carbon capture projects employing amine absorption to sequester CO_2 from power plant flue gases, which have proven to be successful. However, the low concentrations of CO_2 in flue gas streams as well as the difference in pressure and temperature have an impact on the inefficiency of post-

combustion processes, when aqueous amine solvents are employed [32]. Alternative methods have been investigated to improve some of the approaches of post-combustion sequestration. Consequently, post combustion capture still remains one of the most widely applied processes from an economic point of view because the process can be retrofitted to existing power plants and does not require the replacing and rebuilding by new equipment. It is also flexible in that if the capturing site retrofitted to a power plant stops working, the power plant can still continue and fully function [33] (Fig 1).

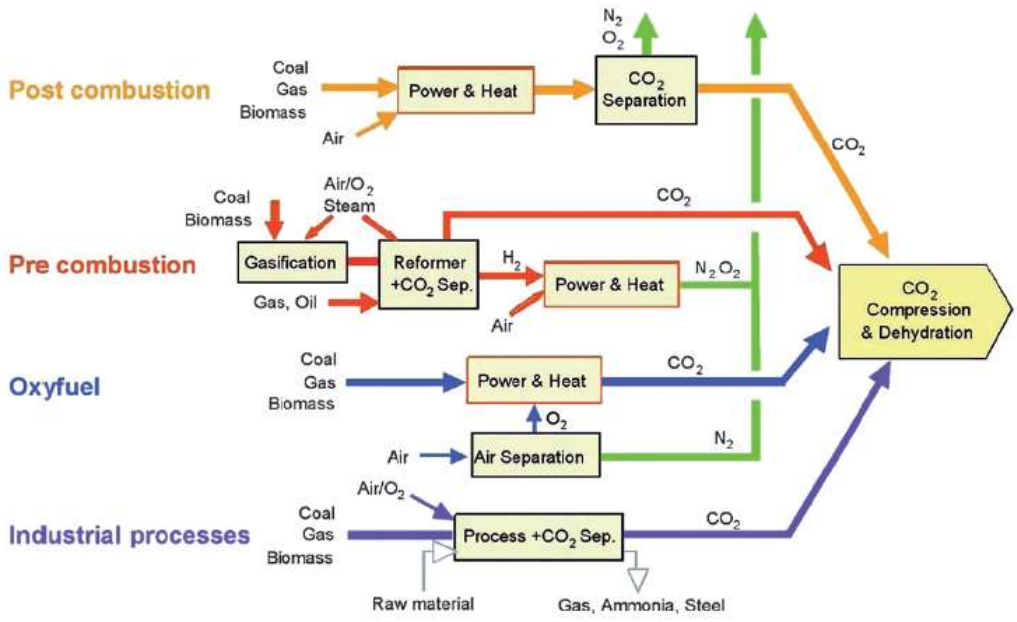

Figure 1: A schematic diagram of the processes which take place during individual combustion processes [34]

2.2 CO_2 capturing process by absorption

2.2.1 Chemical absorption

Absorption can be described as the separation of a gaseous component from a stream of gas employing a liquid. When two phases come into contact, absorption occurs from the

gas phase into the liquid phase. During absorption the liquid is sometimes referred to as either a solvent or absorbent. Absorption properties which need to be considered, include the solubility of the gas in the absorbent as well as the reactivity between the gas and absorbent. CO_2 is acidic in nature and necessitates an alkaline absorbent. An alkaline solution enables neutralization between an acid and base. Flue gas streams comprised of low to moderate partial pressures of $CO_{2,}$ are favourable conditions during the post combustion processes [35]. Chemical absorption processes which consume aqueous amines represent a technological approach to eliminate the presence of acid gases within a flue gas stream. This can be achieved by introducing amine based solvents. During the chemical absorption process, a reversible reaction occurs resulting in a weakly bound intermediate. Applying heat or pressure could result in a reversible reaction. The down side to these processes is the amount of energy consumed with sorbent regeneration, the loss of amines during evaporation as well as thermal and chemical degradation of amines, caused by the addition of oxygen [36]. Industrial processes such as the sweetening of natural gas, the hydrogen and ammonia production, makes use of chemical absorption employing amines. The IGCC process employs physical solvents such as Selexol and Rectisol amongst others [37,38].

2.2.2.1 Amine and Ammonia absorption

The natural gas industry uses absorption stripping equipment, employing amine solutions such as MEA, to absorb $CO_{2,}$ from flue gas streams. When the amine solution comes into contact with a stream of flue gas, CO_2 is removed. The absorbed CO_2 is then removed from the solvent by a counter flowing steam and the solvent is then passed through a regenerator unit. After water vapour has been condensed, the remaining stream of highly concentrated CO_2 may then be compressed for either storage

or commercial utilization. The amine solution can be recovered in an absorption column [39]. MEA is one of the oldest employed solvents and is still very popular presently. It is soluble in water giving various concentrations, reducing any concerns of solubility to arise. This characteristic confirms MEA's capacity to carry CO_2. MEA can be considered as a relatively cheap amine in comparison to others. It is made up of ammonia and ethylene oxide that are themselves cheap chemicals. The disadvantages however of using MEA are the enormous amounts of energy required, high equipment corrosion rate and amine degradation by SO_2, NO_2, HCl and HF. This can take place via three routes- carbamate polymerisation, oxidative degradation and thermal degradation [40, 41]. The aqua ammonia process is envisaged to replace the MEA process, to facilitate the capturing of acidic gases. The replacement of amine solvents, by the aqueous ammonia process, is a projected method to capture acidic gases- SOx, NO_x and CO_2 as well as HF and HCl from flue gas streams. The aqueous ammonia process is considered as a means to eliminate equipment corrosion and solvent degradation, affected by sulphur dioxide and oxygen in flue gas streams [42]. There are two variations for sequestration of CO_2 using aqueous ammonia. One is called a chilled ammonia process in which CO_2 is absorbed at low temperatures (2-10 °C) and the second absorbs CO_2 at ambient temperatures of between (25-40 °C) [43].

SO_x and NO_x react with ammonia to form by-products which can be marketed as fertilizers for crops. By-products of the aqueous ammonia process are ammonium bicarbonate, ammonium sulphate and ammonium nitrate. These by-products can however be commercialized [44]. The benefits of the aqueous ammonia process are their operating temperatures, which are lower than that of MEA. This leads to less evaporation of ammonia and thus its release into the atmosphere. The process enables a high CO_2 loading capacity. Ammonia's reaction conditions allow for a wider operating

range due to their fast kinetics. Both amine (MEA) and aqueous ammonia are liquid solvents but aqueous ammonia however is less expensive than MEA. This feature will consequently reduce the make-up costs of chemicals during the sequestration process [45]. The difference in the CO_2 removal efficiency of ammonia absorbent and CO_2 loading capacity compared to MEA's are 99% (1.20g CO_2/g NH_3) and for ammonia and 94% (0.409g CO_2/g MEA) [46].

2.2.2 Physical absorption

Physical solvents, physically dissolve acid gases and do not react with the solute, unlike chemical solvents. The physical absorption process obeys Henry's law, where the gas captured by the absorbent is dependent upon the partial pressure of the gas and the temperature of the absorbent. Solvents which do not react through chemical reactions can be referred to as physical solvents. During operation, physical solvents depend on their ability to dissolve various gases [47] [48]. Physical solvents can be used to remove H_2S, contaminants in the amine scrubbing process and CO_2. The removal of large quantities of CO_2 using physical solvents can occur when the concentrations and partial pressures of acidic gases are sufficiently high. These conditions have economic benefits for regeneration because it consumes much less energy and enables high acid gas loading in the solvent, than for chemical solvents. Commercial processes that employ physical solvents are the Selexol and Rectisol processes respectively. They have been employed in precombustion sequestration of CO_2, during precombustion application within the integrated gasification combined cycle (IGCC) process as well as syngas clean up [38]. The Fluor process (propylene carbonate) and Purisol (n-methyl-2-pyrollidone) may also be used to sequester CO_2 [46].

2.1.1.1 Selexol and Rectisol process

Selexol is a commercialized technique that has been in operation for decades. The process employs liquid glycol solvents such as dimethyl ether of poly (ethylene glycol) (DMPEG) for the selective removal and recovery of CO_2 and H_2S from natural gas processes. Selexol's approximate temperature and pressures at which operation takes place are 30 atm and 313 K (40°C) [46]. H_2S can be converted to elemental sulphur through a Claus process, in addition to the compression of pure CO_2 streams, which can either be sequestered in deep geologic formations or applied to the enhanced oil recovery [38]. Rectisol, another well-known physical solvent can be characterized by the implementation of low temperature methanol (chilled methanol) to remove CO_2. The process is primarily applied to treat synthesis gas and hydrogen gas streams to remove impurities. The temperature and pressures at which Rectisol is carried out are between 30-80 atm and 213-263 K [47].

2.3 CO_2 capturing process by adsorption

Adsorption can be described as the attachment of a gas or liquid, onto a solid surface, by means of a physical process. Adsorption behaviour can be influenced by surface chemistry and the porosity of an adsorbent [49].

The selectivity and adsorption capacity of an adsorbent should be highly selective towards CO_2. It should endure thermal and chemical stability, along with periodic adsorption- desorption cycles, which should remain stable throughout the capture process. The process by which adsorption takes place can affect the energy potential of a plant. It can reduce the cost of equipment as well as the amount of adsorbent material consumed, when separation and capturing occurs. The commercialization and success of

adsorption, a technique employed to sequester CO_2 depends on the characteristics mentioned above. However, research and development of new adsorbent materials, to effectively capture $CO_{2,}$ will increase the competitiveness of adsorption separation techniques. An adsorbent can be differentiated into two categories, namely: chemical and physical adsorbents. Adsorbents that can be employed to capture CO_2 are porous materials (zeolites, molecular sieves and activated carbon), porous silica, metal organic frameworks, activated alumina as well as metal oxides [50].

One important characteristic of a CO_2 adsorbent is its adsorption capacity, which is represented in the form of adsorption isotherms which are graphs that depict the adsorption process.

$$\text{Adsorbate} + \text{Adsorbent} \rightleftharpoons \text{Adsorption}$$

Scheme 2: Adsorption isotherms

Equilibrium arises when the amount of adsorbate adsorbed and the amount of adsorbate in solution are in contact long enough. This relationship is described by adsorption isotherms [51].

2.3.1 Chemical adsorption

Chemisorption is a subgroup of adsorption that is directed through chemical reactions taking place at an exposed surface. Adsorbents reacting via chemical reactions are typically metal compounds which may also be categorised into two groups; metal oxides and metal salts that can be used in adsorption processes [50].

2.3.2 Physical adsorption

Physisorption is a subgroup of adsorption in which the electronic structure of an atom or molecule are not affected by the adsorption process. The more well-known physisorbents are inorganic porous materials, zeolites, hydrotalcites and activated carbon. The size and volume of pores, within porous structures, are important features to note, during physical adsorption. Pore sizes between 2-50nm are considered mesoporous. Microporosity can be described as having pore sizes of 2nm and macropore materials having a pore size larger than 50nm [52].

2.4 Supports for CO_2 adsorption

Adsorbents for CO_2 capture consist of a scaffold to which functional groups are attached by different techniques. Several possibilities exist for the support and amine based functionalization (or amination). Although there are several publications on CO_2 adsorption, reviewed amongst others by Olajire [42], Samanta *et al.* [3] and Wang *et al.* [53], there is insufficient detailed comparative reviews for the solid amine sorbents.

2.4.1 Zeolite-Based Sorbents

The porous crystalline aminosilicate consists of an array of TO_4 tetrahedra, where T is either an aluminium or silicon atom. Aluminium atoms result in negative charges on the molecule that can be balanced by cations which are exchangeable within the pore spaces. These unique properties allow for the adsorption of a variety of gas molecules, including acidic CO_2. To date there are approximately 170 unique zeolites (molecular sieve topologies) which have been indexed by the international zeolite association.

Spectroscopic studies have shown that physisorption is the dominant process on specific zeolites (X) and (Y), when CO_2 is adsorbed. Whereas, chemisorption forms carbonate and carboxylate and with only a portion of CO_2 being adsorbed [54]. Zeolite CO_2 adsorption is influenced by the aluminium content which classifies the number of charge balancing cations within the structure and the type of moiety. The porosity of a zeolite's framework is one of its important features. Their pore structure variations are an indication of the diverse electric field properties which results in the different adsorptivities. When developing practical adsorbents with good adsorption properties, the structure of the pores and chemical composition should be carefully studied to ensure favourable results [55]. Zeolites possess ordered microporous crystals with a negatively charged structural framework and exchangeable cations that influence their ability to adsorb CO_2. At mild operating temperatures, zeolites exhibit high adsorption capacities. However, it would be more efficient if it could operate at higher temperatures [56, 57]. Superior adsorption capacities of CO_2 over gases like CO, CH_4, N_2, O_2, and H_2 by zeolites, are affected by van der Walls interaction between the CO_2 molecule and the adsorbent surface as well as by the pole-pole and pole-ion interactions between CO_2 molecules quadrupole and the polar and ionic sites of the adsorbent surface [58]. Water is a component found within flue gases, and it has the potential to compete with adsorption sites of zeolites. The effect of water on the absorptivity of the adsorbent is dependent on the CO_2 concentration found within the feed. The strong polarity of water decreases the electric field strength. The relation of CO_2 quadruple moment and the field gradient, influences the adsorption energy of CO_2 [59]. Chatti *et al.* synthesized adsorbents functionalized with various amines on synthetic zeolite 13X. They compared the findings of three techniques and determined a good correlation between amine loadings. CO_2 adsorption capacity for unmodified zeolite 13X was 16.01

mg/g. Zeolite modified with monoethanol amine was 19.98 mg/g and 22.78 mg/g for isopropanol amine, respectively [60]. Zeolites display good regenerability compared to other inorganic adsorbents (hydrotalcites and metal oxides), their regeneration can be performed through temperature swing adsorption (TSA) or pressure swing adsorption (PSA) [51].

2.4.2 Amine-Functionalized Activated Carbon Sorbents

Activated carbon is predicted to be a strong candidate, among solid sorbent supports, for CO_2 sequestration. This is emphasized by the lack of a moisture removal step and it exhibits a high CO_2 adsorption capacity at ambient temperatures and pressures. The acidic nature of CO_2 (weak Lewis acid) facilitates the insertion of Lewis bases onto the surfaces of the activated carbon supports enhancing the capture performance of CO_2. Well-known methods to prepare activated carbon with an enhanced basic property are through neutralization of the acid functional groups or complete removal thereof in addition to replacing the acidic functionalities with basic functional groups. The introduction of nitrogen containing functional groups onto the carbon surface can improve the CO_2 adsorption capacity for activated carbons. They can be introduced, either through reactions with nitrogen containing reagents or by activation with nitrogen precursors. Ammonia, a functional group containing one nitrogen can increase the basicity of the carbon surface. The reaction of ammonia with the surface, at elevated temperatures, causes ammonia to decompose to form free radicals such as nitrogen, atomic hydrogen, NH and NH_2 [61, 62].

Activated carbons have oxygen containing functional groups that are responsible for their acidic nature. The oxygenated groups are usually found at the edges of basal

planes or the outer surfaces, and contribute to the chemical nature of the support. The concentration of oxygen at the carbon surface is relatively high and influences the adsorption capacity. A few of the oxygen functional groups found on the surface of carbon include phenols, ethers, carboxylic acids, carbonyls and quinones to name a few. These surface oxygenated functional groups can be categorised with relation to their chemical character; being either basic, neutral or acidic. Thus phenolic hydroxyl, carboxylic acids and lactones are the suggested sources of surface acidity. To activate the support surface by introducing acidic oxygen functional groups, aqueous oxidants and gases can be employed (Fig 2) [63].

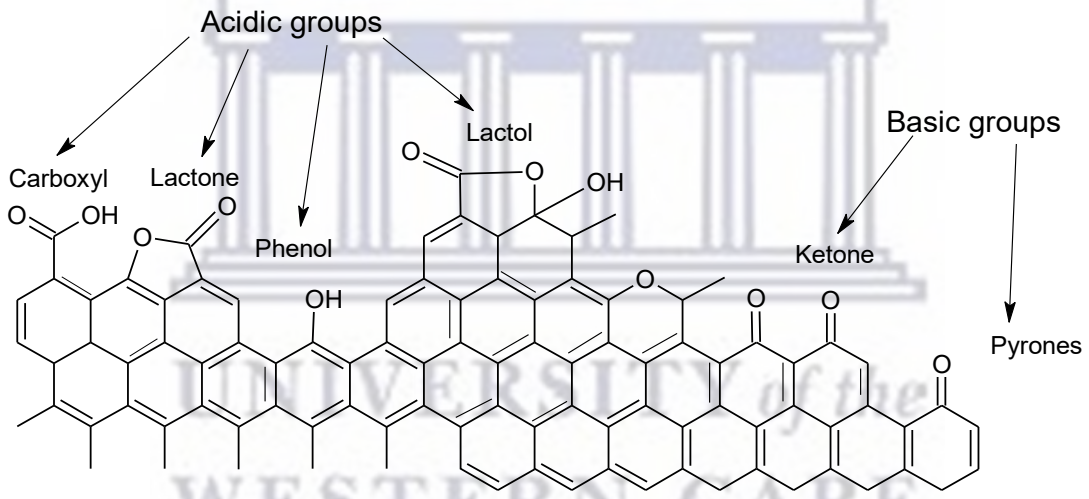

Figure 2: Basic and acidic functional groups on the carbon basal planes [61]

The basic character of an activated carbon support can firstly arise from surface functionalities that react with protons and secondly the delocalised electrons of carbon aromatic rings able to attract protons [61]. A fundamental property which activated carbon holds is in the delocalization of electrons of graphene layers. The electrons of these layers can act as Lewis bases. Leon *et al.* were able to show the adsorption of protons from a solution by oxygen-free carbons. The basic sites on the basal plane of

the carbon crystallites are positioned in electron rich areas and can be considered as a Lewis acid type within the carbon structure [64]. Reacting the activated carbon support with nitrogen containing functional groups can enhance the adsorption of CO_2. Nitrogen's basic character has the ability to improve the interaction between acidic molecules and the surface of carbon which include; dipole–dipole, H-bonding and covalent bonding [65].

2.4.3 Ordered mesoporous silica

According to IUPAC nomenclature, mesoporous materials can be defined as materials comprised of pores with a diameter range of 2–50 nm. The structural properties of mesoporous materials allow for their extensive application in areas such as catalysis, drug delivery control, biosensors, biofuel, sorption and membrane separation [66]. Ordered mesoporous silica has attracted a great deal of interest in recent years due to their ordered porosity and high internal surface area. OMSs are synthesized when silica is introduced at the beginning. Its abundance in the earth's crust, thermal stability and chemical inertness contribute to its affordability [67]. Since the discovery of mesoporous silica, surfactant template methods can lead to a wide range of compositions. The manipulation of hydrogen-bonding structure-directing functions of electrostatic and van der Waals interactions, associated with amphiphilic molecules, have been developed. Mesoporous silica materials can be synthesized under conditions where the silica surfactant self assembles at the same time as the condensation of the inorganic species. Amphiphilic polymers with large molecular weights have been predicted to be able to increase the dimensions of pore structures resulting from inorganic-organic composites. Zhao *et al.* reported the difference in the silica walls of

MCM-41 and SBA-15. They reported the difference when using amphiphilic block copolymers as organic structure-directing agents for SBA-15 and conventional cationic surfactants for MCM-41. It was concluded that SBA-15 possesses thicker walls because of the employment of the amphiphilic block copolymers, contributing to its superior hydrothermal stability [68]. MCM-41 and SBA-15 are members of a wide selection of mesoporous materials. MCM-41 was first patented in 1969 [69] and a lack of sufficient analytical tools limited its applicability. It was not until researchers at the Mobil Corporation, in 1992, unravelled the potential of the material by incorporating cationic surfactants under basic conditions to synthesize OMS materials. The material was named Mobil crystalline of materials (MCM-X) commonly known as MCM-41/ MCM-48 [70]. MCM-41 is a member of the M41S family and displays narrow pore size distribution as well as containing hexagonal arrays of non-intersecting channels. SBA-X was initiated by Stucky in 1998, where X represents a specific pore structure and surfactant. It now forms part of the Santa Barbara Amorphous family of materials. Zhao *et al.* in 1998 synthesized SBA-15, possessing hexagonally ordered cylindrical pores employing a triblock copolymer (P123) as a structure directing agent and TEOS as the silica source [68].

Lui *et al.* studied the direct incorporation of tetraethylenepentamine (TEPA) onto as-synthesized SBA-15, without removing the organic templates. They investigated SBA-15as-*x* absorbents and the effects TEPA loading had on their CO_2 adsorption capacity and amine efficiencies. It was found that there was a direct correlation between TEPA loading and CO_2 adsorption capacity and amine efficiency. They deduced that high amine density of TEPA affected the CO_2 adsorption capacity. It is indicative that densely anchored aminosilanes would be more effective as an adsorption site than those isolated on bare silica supports. The CO_2 adsorption capacity of TEPA-SBA-15 was 4.6

mmol g^{-1}. Another component other than high adsorption capacity of CO_2, under moist conditions, are their cyclic adsorption-desorption stability during long-term operations. These factors would determine the practical application of an adsorbent in an industrial plant. In their study into the effect of water vapour in the flue gas it was found that it resulted in the increase of the CO_2 adsorption capacity of TEPA-SBA-15. An increase from 0 to 10.6% (water vapour content) increased the CO_2 adsorption capacity from 4.6 to 5.0 mmol g^{-1}. This could be associated with the relatively hydrophobic surface property of TEPA-SBA- 15 adsorbents compared to pristine SBA-15. However, when the water vapour content was further increased from 10.6 to 14.1% the CO_2 adsorption capacity decreased slightly from 5.0 to 4.9 mmol g^{-1}. This could be linked to the competitive nature at the adsorption sites between CO_2 and H_2O [71]. Yue *et al.* reported the CO_2 adsorption of as-synthesized MCM-41 (AM) with TEPA. They investigated the difference in the amount and type of surfactant employed on four different samples of as-synthesized MCM-4. Amongst the four, MCM-41 (AM) was found to be the most competitive. It was hypothesized that the as-synthesized MCM-41's distribution of surfactant micelles occluded within the pores which differs from that of as-synthesized SBA-15. This is attributed by the use of cetyltrimethylammonium bromide (CTAB, ionic surfactant) during the MCM-41 synthesis. Ionic surfactants commonly have a stronger interaction with silica than amphiphilic block copolymers during SBA-15 synthesis. However, it was noted that less space between the silica wall and the template remains. This is not seen with SBA-15. The variation between the adsorption capacities between MCM (AM) and the other samples, loaded with equal amounts of TEPA was studied. The differences in the adsorption capacities were assigned to the distribution of amines on the porous support. There is a direct relation between the maximum amount of amine loaded which is due to good dispersion and

distribution of the guest species as well as the accessibility of the CO_2 adsorbate. This results in an increase of the final adsorption. MCM (AM) exhibits an adsorption capacity of 24, 120, 167, 211, and 221 $mg.g^{-1}$ when it is modified with TEPA of 10, 30, 40, 50, and 60 wt%, respectively. After loading with TEPA to 40 wt%, the MCM-AM sample possesses a CO_2 adsorption capacity (167 $mg.g^{-1}$) which is higher than that of pure TEPA (151 $mg.g^{-1}$) [72-73].

2.4.4 Graphene oxide sorbent

Graphene, a lamellar compound consisting of tightly packed carbon atoms that are sp^2 hybridized and with a high surface area. The single atom two dimensional structure has a honeycomb framework. Graphite is made up of individual graphene sheets that are held together by weak van der Waals forces [74]. Graphene oxide and graphite oxide display similar chemical characteristics (surface functional groups) but have different structures. The exact structure of GO remains elusive and has continued to be a debatable topic over the years. It is primarily based on the fact that GO is amorphous and contains a non-stoichiometric atomic structure [22]. GO can be described as having a monolayer coverage resulting from the exfoliation of graphite oxide layers (sheets) and exhibit an electrically insulating character [74]. Synthesis of GO has been reported through many methods such as the Brodie method, who synthesized the first graphene oxide material in the 18^{th} century. A century later, Hummer improved upon the Brodie method by using concentrated sulphuric acid in addition to nitric acid and potassium permanganate. More recently the acclaimed 'Modified Hummer's method' was devised. Staudenmaier's methodology uses fuming nitric acid and a $KClO_3$ oxidant and the Tour

method incorporates concentrated phosphoric acid with $KMnO_4$. Both the Brodie and Staudenmaier synthesis produces ClO_2 gas which is extremely toxic [75] (Table 1).

Table 1: Oxidation methods of graphite to graphite oxide [76]

	Brodie	**Staudenmaier**	**Hummers**	**Modified Hummers**	
Year	1859	1898	1958	1999	2004
Oxidants	$KClO_3$, HNO_3	$KClO_3$ (or $NaClO_3$), HNO_3, H_2SO_4	$NaNO_3$, $KMnO_4$, H_2SO_4	pre-ox: $K_2S_2O_8$, P_2O_5, H_2SO_4 ox: $KMnO_4$, H_2SO_4	$NaNO_3$, $KMnO_4$, H_2SO_4
C:O ratio	2.16	N/A	2.25	1.3	1.8
	2.28	1.85	2.17		
Reaction time	3–4 days 10h	1–2 days 10 days	≈2h	6h pre-ox+2h ox	≈5 days
Intersheet spacing [A°]	5.95	6.23	6.67	6.9	8.3

2.5 Graphite and Graphene

Graphite, originates from the Greek word "graphe-in" which means to write. It is an allotrope of carbon with low density and important economic benefits due to its wide availability. It has attracted much interest within the sphere of chemistry, physics and engineering. Graphite has a lamellar structure that possesses rare electronic and mechanical properties and is made up of isolated layers of carbon atoms, referred to as graphene sheets. Its unique structural characteristics display high specific surface areas. These morphological properties have led to its attraction and use in the storage of energy as well as commercial applicability [77].

Graphene is considered to possess a honeycomb like structure with two dimensional sheets (2D). Graphene sheets can be accumulated through stacking to form graphite, a three dimensional (3D) structure and when rolled, forms nanotubes, a one dimensional structure (1D) as well as zero dimensional (OD) structure, fullerene (Fig 3) [78].

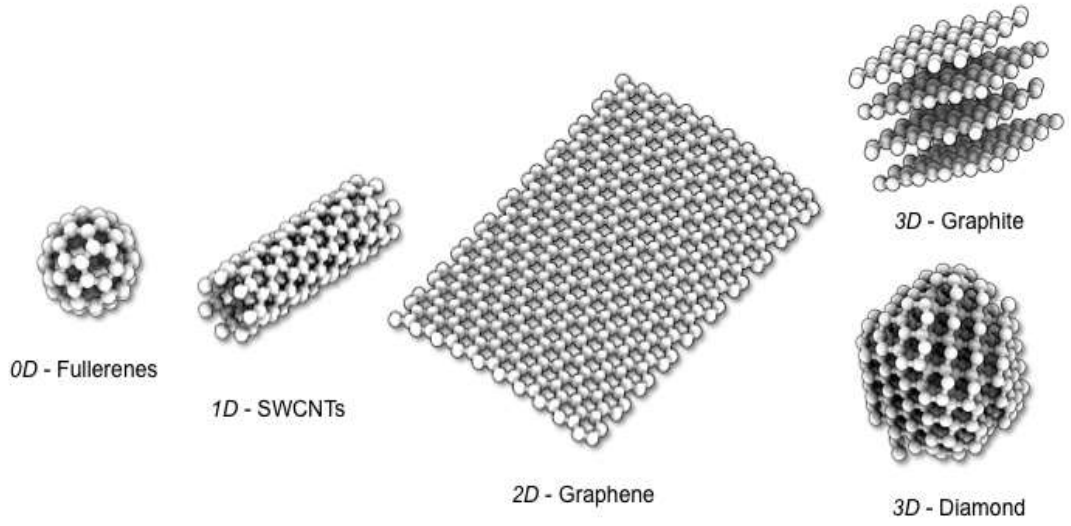

Figure 3: Different structural carbon models [79]

2.6 Overview of Graphene oxide (GO)

This subsection gives a general idea of graphene oxide, previously referred to as graphitic acid. It is a carbonaceous, amorphous material that is strongly hygroscopic and has been defined as a non-stoichiometric compound [80]. It has a wrinkled-like character containing oxygenated functional groups on its basal planes and periphery. Due to its high polarity, GO is hydrophilic and forms a stable colloidal suspension when mixed with water [81]. The dimensions of the carbon sheets include a thickness of approximately 1nm and its lateral dimensions fluctuate between several microns and a few nanometres. GO was first synthesized in the 1800's and subsequently gained popularity within the scientific community mainly due to it being thought of as a

precursor to graphene. GO can be prepared through the exfoliation and heating of graphite oxide [82].

2.7 Synthesis of Graphene oxide

The first synthesis of graphene oxide dates back to 1840 when Schafhaeutl, a German scientist reported the exfoliation of graphite with strong acids, as well as intercalation which is the addition of a molecule between the carbon lamellae. Nearly 20 years later in 1859, B.C. Brodie, a British chemist continued investigating the formation and structure of graphite. This involved the addition of potassium chlorate to a solution of graphite as well as fuming nitric acid. Brodie's method was enhanced by L. Staudenmaier 40 years later. His improved technique was to add the potassium chlorate in several aliquots throughout the reaction process. Sulphuric acid was also added to increase acidity. Staudenmaier's method varied in that the addition of solvents was conducted stepwise as supposed to a one pot reaction. Twenty years following the Brodie and Staudenmaier discovery, Hummers and Offeman further improved upon the method to oxidize graphite by incorporating potassium permanganate and concentrated sulphuric acid. The aforementioned methods are the primary synthesis to produce graphene oxide [77].

2.8 Structural features of Graphene oxide

To date, there is no unambiguous suggested structure defining graphene oxide which is attributed to the complexity of the material. GO's atomic structure continues to be questioned [83]. Its structure has been extensively studied over many decades by making use of various physicochemical and chemical techniques and a number of

structural models have been suggested [84]. The first proposed model of GO was postulated by Hofmann and Holst in which they suggested that the carbon atoms of the hexagonal planes were bound to oxygen atoms through epoxy linking with a molecular formula- C_2O [22]. Ruess's model described the GO structure as having a wrinkled sheet of carbons that include trans linked cyclohexane chairs with the fourth valence carbon atoms bound to axial OH group and an ether oxygen placed in 1,3 positions. His model was the first to recognize the hydrogen content [84]. Later, these postulated models were revisited and revised by Scholz and Boehm, who suggested a model that substitutes the epoxide and ether functional groups with a quinoidal structure with corrugated layers of carbon atoms [85]. Subsequently, Mermoux *et al.* favoured Ruess's model by suggesting a similar structure to that of CF [poly (carbon monofluoride)]. Further, Nakajima *et al*. suggested a model contrary to this, which includes stage 2 type $(C_2F)n$ through the fluorination of GO. However, all the previously mentioned models were rejected by Lerf and co-workers. Their assertion was based on the research conducted using NMR studies which suggested that the flat aromatic regions of GO layers are distributed randomly with unoxidized benzene rings as well as wrinkled regions of alicyclic six-membered rings [86]. The distance between its exfoliated layers permits ions to intercalate with ease. The presence of C-OH groups has been confirmed by NMR studies conducted by Mermoux *et al.* [87] and He *et al.* [88]. The strong oxidizing properties of GO are said to be attributed by epoxide groups. Research by Lerf *et al.* [89] and He *et al.* [88] described a situation in which GO has two regions that can be separated into aromatic areas with unoxidized benzene rings as well as areas in the structure which contain 6 membered aliphatic rings. The relation of these regions is relative to the extent of oxidation that actually occurs (Fig 4) [90].

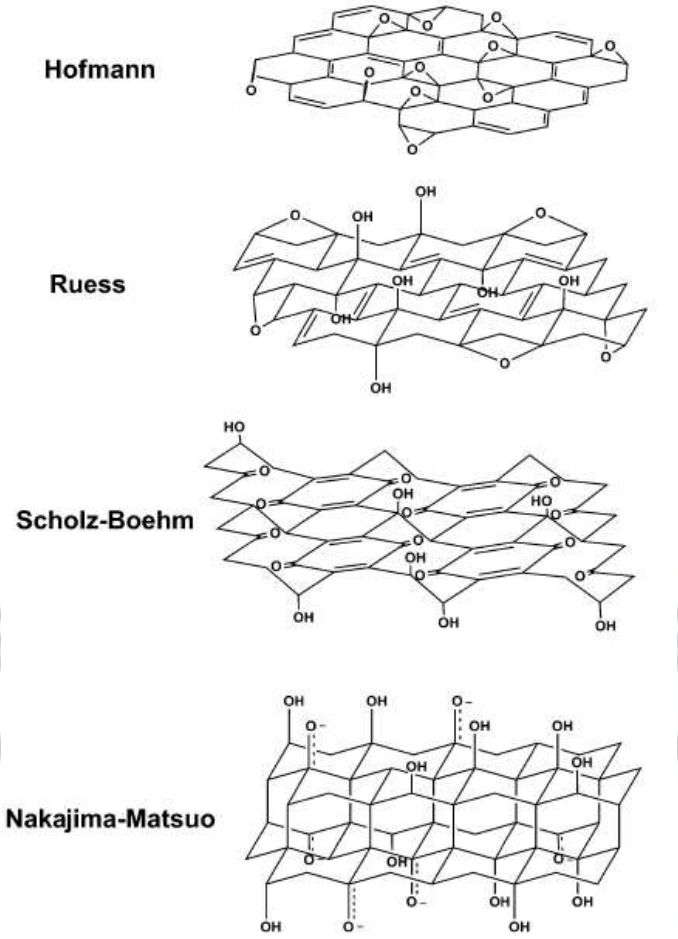

Figure 4: Structural models of graphene oxide [22]

2.9 Chemical reactivity and functionalization of GO

Chemical functionalization affects the performance of adsorption by modifying the surface of adsorbents. The attachment of functional groups increases the adsorption of CO_2. Functionalization with amine molecules enhances basicity for favourable adsorption of acidic CO_2. APTES has been used extensively to modify porous supports [57]. Chemical reactivity can either occur through reduction, which is the process of reducing GO to graphene or through oxidation, which oxidizes graphite to graphene oxide, and through exfoliation of the individual layers producing graphite oxide.

Graphene oxide has a chemical nature which is analogous to graphite oxide. However, their structural properties are very different from one another. Techniques used to modify layered materials can take place through various mechanical and thermal methods [91]. Organic molecules can be intercalated into the layered structure of the carbon material through covalent bonding which facilities selective adsorption. Aminosiloxanes can be grafted onto the surface of GO through silylation reactions forming Si-O-Si bonds. The facilitation of cyclic stability of amino functional groups is enhanced by these grafting techniques. Increase in exfoliation can be attributed to the intercalated organic molecules and can be corroborated by the increase in d-spacing, information obtained from FT-IR analysis. The reaction between APTES and GO has been investigated by Matsuo *et al*. [91]. Amine molecules promote an increase in the affinity for CO_2 and in turn the uptake of adsorbed CO_2 is enhanced [57]. GO ordered mesoporous silica has demonstrated significant adsorbent properties in addition to having an environmentally friendly nature and low cost. OMS have attracted a great deal of interest in recent years due to their ordered porosity and high internal surface area. Adsorbents based on inorganic supports, which incorporate basic organic groups, usually amines, is an important functionality of porous solid supports [92].

2.9.1 Functionalization by APTES

Adsorbents based on high surface area inorganic supports that incorporate basic organic groups, usually amines, are of particular interest to aid in the sequestration of CO_2. The interaction of acidic CO_2 and basic support surfaces forms bicarbonate and carbonate species, in the presence of water. The co-condensation of a silica precursor, typically TEOS, with APTES in the presence of a template results in 3-aminopropyl-

functionalized silica. These mesoporous substrates contain pores with large accessibility for derivatizing reagents and can facilitate fast gas diffusion to and from their surfaces [93]. Synthesizing organic/inorganic amine-tethered silica materials with high amine loadings, should demonstrate reversible binding of CO_2 after several cycles [94]. Chemical functionalization affects the performance of adsorption in which the attachment of functional groups increases the adsorption of CO_2. The first step when developing an efficient adsorption separation process, is discovering a suitable adsorbent. Hence, the importance of screening effective adsorbents onto which an amine is attached or immobilized [95] is a really vital first step in this process. Supports with well-developed structural integrity can influence the efficiency of amine functionalized CO_2 adsorbents. The characteristics of a suitable support, comprise of large pore size, high surface area and high pore volumes [53].

In this study, GO is used as the adsorbent. Graphene oxide has been functionalized with APTES, reported by Hong *et al.* The paper concluded that the adsorption uptake is attributed by an increase in basicity. Unfunctionalised GO had a low adsorption uptake of 0.074 mol/kg and GO-APTES illustrates an impressive increase to 1.16 mol/kg at a temperature of 30 °C and a pressure of ~1 atm [57]. Organic molecules can be intercalated into layered structures of carbon materials through covalent bonding, facilitating selective adsorption. Aminosiloxanes can be grafted onto the surface of GO through silylation reactions forming Si-O-Si bonds. Cyclic stability, of amino functional groups is enhanced by grafting techniques. An increase in exfoliation can be attributed to the intercalated organic molecules and can be corroborated by the increase in d-spacing obtained from FT-IR analysis [91]. The bifuntional nature of aminopropylalkoxysilanes offers the opportunity for its wide application due to their surface chemistry and when applied as a coupling agent displayed unique properties in

aqueous media. Amine groups bonded to the aminosilane can intra/intermolecularly functionalize as well as catalyse the reaction between the silane molecule and surface silanol group to produce siloxane bonds. APTES is one of the most commonly applied aminosilanes, the amine group, hydrogen bonds to the surface silanol group. It can polymerize in water and has the potential to provide many surface structural possibilities such as covalent attachment, self-assembly and multilayers. Grafting densities decrease when aminosilane layers covalently attach, as a result of vertically and horizontally positioned silane molecules. In order for APTES to form multilayers in organic solvents and hydrolyse ethoxy groups in silane layers, water needs to be present [96].

2.9.2 Functionalization by TRIS and Guanidine

Graphene oxide (GO) is a derivative of graphene and consists of oxygen functional groups on their basal planes and edges. The modification of GO's surface with amines or amine-containing molecules takes place through a nucleophilic substitution reaction [97]. Different surface treatments and functionalization techniques have been proposed for improving the dispersion and interface of GO [98]. TRIS, Guanidine and PEI are employed for sorbent functionalization. To the best of my knowledge no reports have been published on the use of GO functionalized with TRIS and Guanidine for CO_2 sequestration. However, amine functional groups have been impregnated and or grafted onto GO for various other applications. PEI has been functionalized with GO by Shin *et al.* and reported a CO_2 adsorption capacity of 32.89 $mg.g^{-1}$ which demonstrated and proved that the CO_2 adsorption capacity increased with increasing PEI content. In this

research report the authors investigated the CO_2 adsorption capacity of GO modified with OMS and then functionalized PEI [99].

Amines grafted onto mesoporous silicas have proven to be capable of capturing CO_2. Mesoporous silicas, grafted with amines-TRIS have been investigated by Bhagiyalakshmi *et al.* The CO_2 adsorption of TRIS was studied at 25, 50 and 75 ºC and mesoporous silica grafted with TRIS presented a maximum of 7% CO_2 adsorption. They concluded that branched chain amine (TRIS) exhibited superior activity over straight chain aminosilanes when grafted on mesoporous silicas [100]. Yue *et al.* investigated the hydroxyl groups of the Pluronic P123 template and how they enhance the CO_2 adsorption capacity when modified with amine functional groups. They reported a CO_2 adsorption capacity of 173mg.g^{-1} for the mesoporous silica–amine composite directly related to a specific interaction between Pluronic P123 with the amine [73]. Sui *et al.* developed a facile method synthesizing GO and PEI for gas and dye adsorption. PEI has a high amine density and its primary amine sites at the chain ends are more easily accessible. PEI, has over the past few years been recognized as a versatile building block for adsorbents [101]. Wang *et al.* studied the effects PEI has on the CO_2 adsorption of mesoporous materials. Their objective was to develop high-selectivity CO_2 sorbents by increasing the amount of polymer and improving the mass transfer in the sorption/desorption processes. The objective of their work was to identify the interactions between CO_2-philic polymer PEI and SBA-15 and to gain insight into the CO_2 sorption-desorption mechanism and the nature of sorbed CO_2 species on the nanoporous PEI/SBA-15 sorbent [102].

A novel graphene oxide-ordered mesoporous silica material with two-dimensional mesoporous structures via sol-gel and self-assembly methods was successfully synthesized by Wang *et al.* The adsorbents demonstrated an ability to remove toxic

waste from waste water. The as prepared GO sheets exhibited two-dimensional and honeycomb-like mesostructures exhibiting a high surface area of 872.9 m^2/g, uniform pore size 6.3 nm, and large pore volume (1.28 cm^3/g) [20]. Yang *et al.* synthesized two dimensional sandwich-like graphene based mesoporous silica (GM-silica) sheets. The mesoporous silica shell was embedded within a fully separated graphene sheet which possessed a high surface area, mesoporous structure, high monodispersity and high aspect ratio. These properties facilitate guest ion diffusion in many diffusion-controlled systems and make allowance for GM-silica sheets to be employed as a universal template for the creation of various functional sheets, such as graphene-based mesoporous carbon in which graphene is individually dispersed. The synthesis of GM-silica sheets included the use of cationic surfactant, CTAB, employed to electrostatically adsorb and self-assemble onto the surface of negatively charged GO, in alkaline solution. During this process mesoporous silica surrounds the surface of single-layered GO. The use of cationic surfactants eliminates aggregation problems between GO and inorganic materials and provides the molecular template for controlled nucleation and growth of mesoporous silica on the surface of graphene oxide sheets [19].

2.10 Adsorption of CO_2 on chemically modified GO

GO is a carbonaceous material with a lamellar structure, containing covalently attached oxygen functional groups. The structure displays randomly distributed sp^2 aromatic carbon atoms and sp^3 aliphatic carbon atoms (Fig 5) [97].

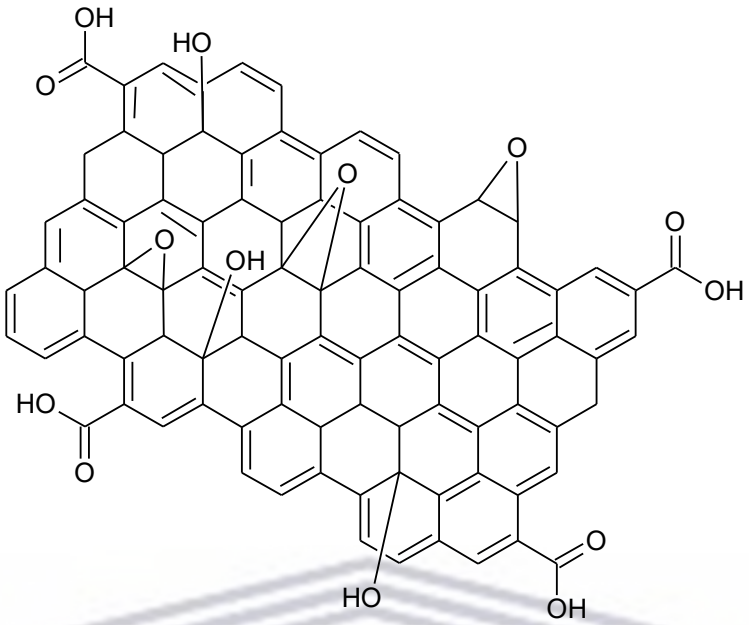

Figure 5: Structure of Graphene Oxide [103]

Organic functional groups can be further transformed onto oxygenated groups found on the basal planes and periphery of the carbon material. This can be achieved with silylating reagents as well as ordered mesoporous silica. They act as intercalating species which react through covalent bonds and self-assembly. Silylation can be described as the reaction between a silane coupling reagent and an oxide, producing a covalently attached organic functional species on the surface of a solid support. Functionalization through the modification of carbonaceous supports, influences the chemical and physical properties of carbon nanomaterials [104]. CO_2 and amine functional groups share a weak chemical interaction between the basicity of amine groups and slight acidity of CO_2. The chemical reaction between amines and CO_2 can take place through a two-step zwitterion reaction producing carbamates and bicarbonates [105].

Chapter 3

Materials and Methodology

3.1 Materials

Chemical	**Supplier**
Graphite	Sigma Aldrich
Potassium permanganate	Sigma Aldrich
Sodium nitrate	Sigma Aldrich
Sulphuric acid	Sigma Aldrich
Hydrochloric acid 99.9%	Sigma Aldrich
Hydrogen peroxide	Sigma Aldrich
Toluene 99.9%	Sigma Aldrich
Aminopropyltriethoxysilane (APTES)	Sigma Aldrich
Chloropropyltriethoxysilane (CPTES)	Sigma Aldrich
Tris (2-aminoethyl) amine 96%	Sigma Aldrich
Guanidine hydrochloride 98 %	Sigma Aldrich
$K_2S_2O_8$	Sigma Aldrich
P_2O_8	Sigma Aldrich
Phosphoric acid (H_3PO_4)	Sigma Aldrich
TEOS 99.9%	Sigma Aldrich
P123 (Pluronic acid polymer)	Sigma Aldrich
PEI	Sigma Aldrich
CTAB	Sigma Aldrich
Ethanol 99.9%	Sigma- Aldrich
Methanol 99.9%	Sigma- Aldrich
Anhydrous acetonitrile 98%	Kimix

3.2 Methodology

3.2.1 Synthesis of graphene oxide (GO)

GO was prepared using more than one method to modify and optimize the exfoliation of GO.

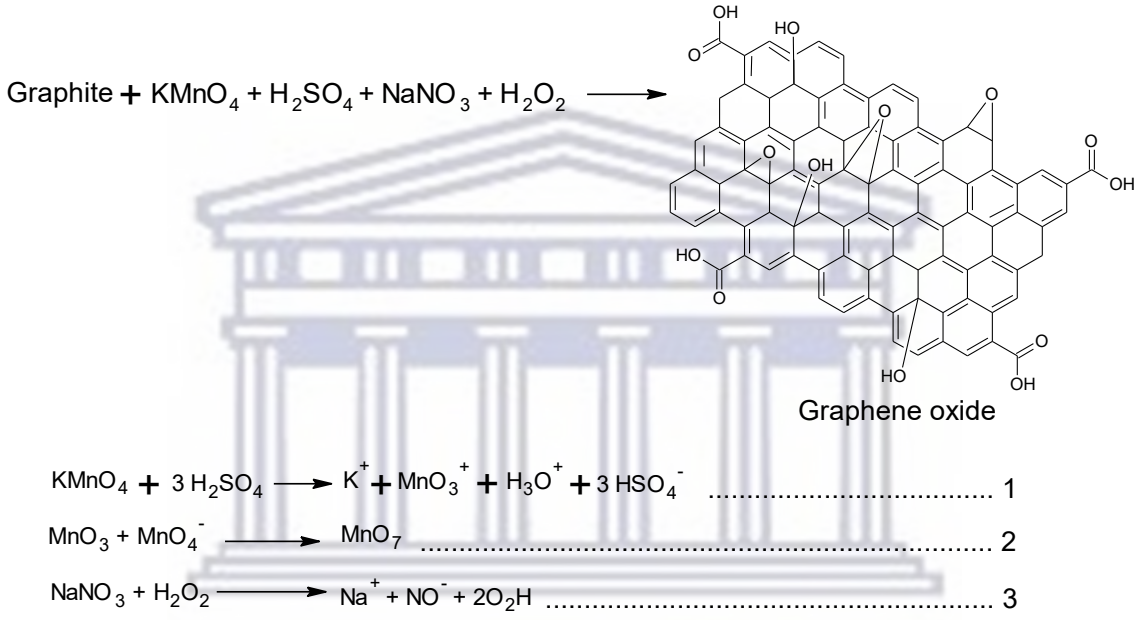

Scheme 3: Reaction equations for the synthesis of GO

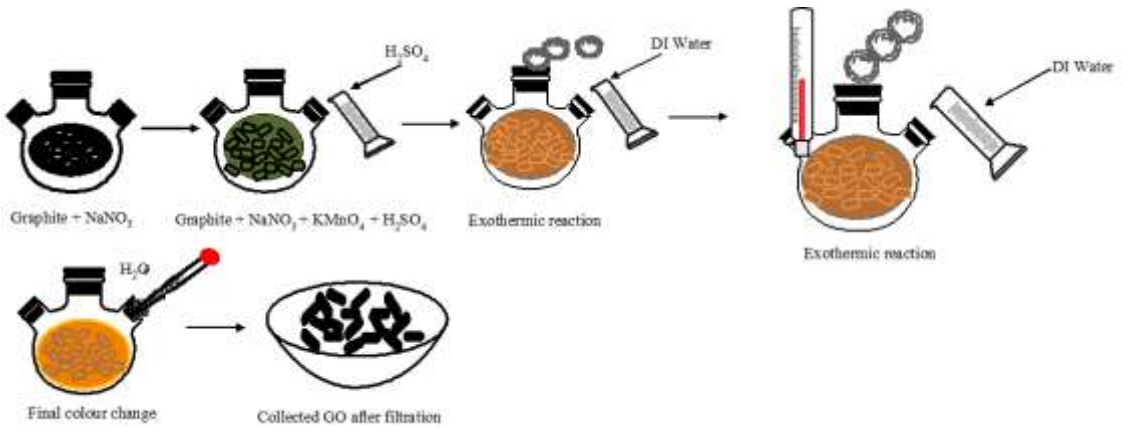

Scheme 4: Reaction steps for the synthesis of GO

3.2.1.1 Method 1

Graphite powder was oxidized to graphene oxide by employing a modified Hummers method [106]. Scheme 3 shows the reaction of the synthesis of GO and scheme 4 shows synthetic route of GO. Approximately, 1g of graphite powder and 1g of $NaNO_3$ were placed together in a 500 ml round bottom flask. 70 ml of H_2SO_4 was added to the round bottom flask (containing $NaNO_3$ and graphite) and magnetically stirred for 15 minutes in an ice bath. The temperature was kept below 5 ºC. 5g of $KMnO_4$ was slowly added over a period of one hour while the temperature was kept below 5 ºC. Once all the $KMnO_4$ was added, the solution was stirred for an additional hour. The colour of the solution changed from grey to dark green. This was followed by the gradual addition of 46 ml of deionized (DI) water to the solution with the temperature maintained below 90 ºC. Upon the addition of DI water, the colour of the solution changed from dark green to dark brown. The solution was left to stir for another 30 minutes. Subsequently, 5.5 ml of the oxidizing agent H_2O_2 was added followed by 140 ml of DI water. The colour of the solution changed from a dark brown solution to a yellow, brown (mustard) colour. The reaction was left to stir for an additional hour to afford a homogeneous suspension. The prepared GO was filtered and washed through centrifugation with 30% HCl solution. Hereafter the GO solution was centrifuged 3 times with 30% HCl and washed 8 times with DI water to produce a pH of between 6-7. The GO solution was filtered with a 45 micrometre membrane filter. The filtered material was left to dry under air and then placed in a vacuum oven at 60 ºC (Scheme 5).

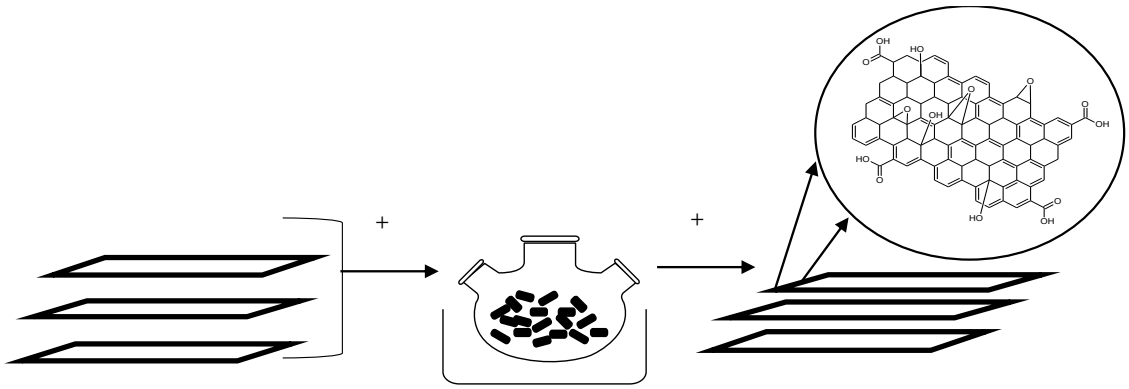

Scheme 5: Synthetic route of GO using method 1

3.2.1.2 Method 2

In this case GO was synthesised by a modified Hummers method [107] (Scheme 6). 1.5g of graphite was introduced into a 500ml round bottom flask with 75ml of H_2SO_4 and magnetically stirred for 15-30 minutes in an ice bath. 4.5g of $KMnO_4$ was gradually added over a period of 30-45 minutes, while the temperature of the solution was kept at below 10ºC. The solution was left to stir for an hour and the colour of the solution became dark green

The solution was then stirred at 35 ºC for 2 hours. 75ml of DI water was gradually added, a spontaneous exothermic reaction took place raising the temperature to between 100-110 ºC. The colour of the solution changed from dark green to a chocolate brown. 7.5ml of H_2O_2 was added followed by an additional 100 ml of DI water during which process the colour of the mixture changed from brown to a yellowish colour. After a further addition of 150 ml of deionized water, the solution became yellow (not a bright yellow but mustard yellow). The solution was left to stir for 45 minutes. The suspension was centrifuged at 4000 rpm for 30 minutes by washing with 30% HCl and then DI

water, until the pH of the solution was 6-7. The mixture was then filtered and dried in a vacuum oven at 60 ºC.

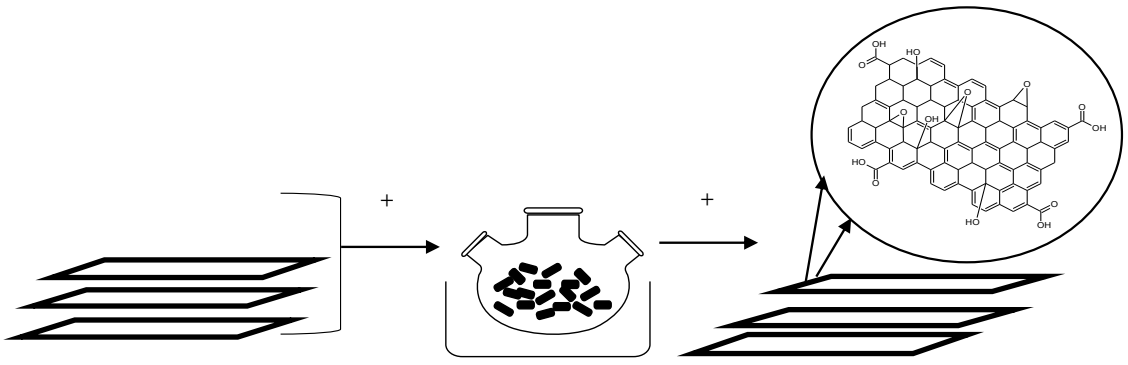

Scheme 6: Synthetic route of GO using method 2

3.2.2 Functionalization of graphene oxide

GO was modified with three functionalities, i.e. APTES, TRIS and Guanidine which was conducted via the grafting of alkoxy groups through silylation reactions.

3.2.2.1 Functionalization of GO with APTES

The as-synthesized GO was functionalized as follows with APTES. 0.2g of as-synthesized GO was dispersed in 200ml of DI water and sonicated for an hour. This was followed by the drop-wise addition of 2ml of APTES to the solution, followed by further sonication for an additional hour. The solution was heated under reflux under nitrogen at 110 ºC for 24 hours. The solution was then washed several times with DI water and the precipitate was obtained after centrifuging at 8000 rpm for 10 minutes and dried in a vacuum oven at 60 ºC (Scheme 7).

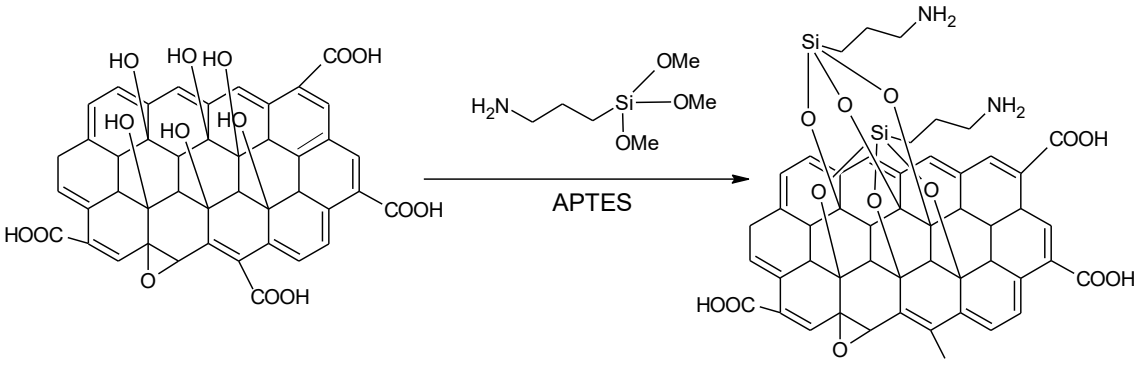

Scheme 7: Functionalization of GO with APTES

3.2.2.2 Functionalization of GO with TRIS

0.2 g of as-synthesized GO was dispersed in 10 ml of dry toluene in a 50 mL round bottom flask and the solution was sonicated for 2-3 hours. Since the GO solution did not homogeneously disperse in the solvent, 15ml of ethanol was added to the round bottom flask to assist in the process of creating a homogenous solution. The ethanol/ toluene GO solution was sonicated for an additional 2 hours. 1ml of CPS was added drop wise to the round bottom flask. The reaction was heated under reflux for 24 hours at 110 ºC under nitrogen. The solid GO/CPS was then filtered, washed with toluene and left to air dry before being placed in a vacuum oven at 60 ^{o}C.

The functionalized GO/CPS solution was re-dispersed in 10 ml of toluene. To the mixture, 2 ml of TRIS was added drop wise and the solution was left to reflux for 24 hours at 110 ^{o}C under nitrogen (Scheme 8).

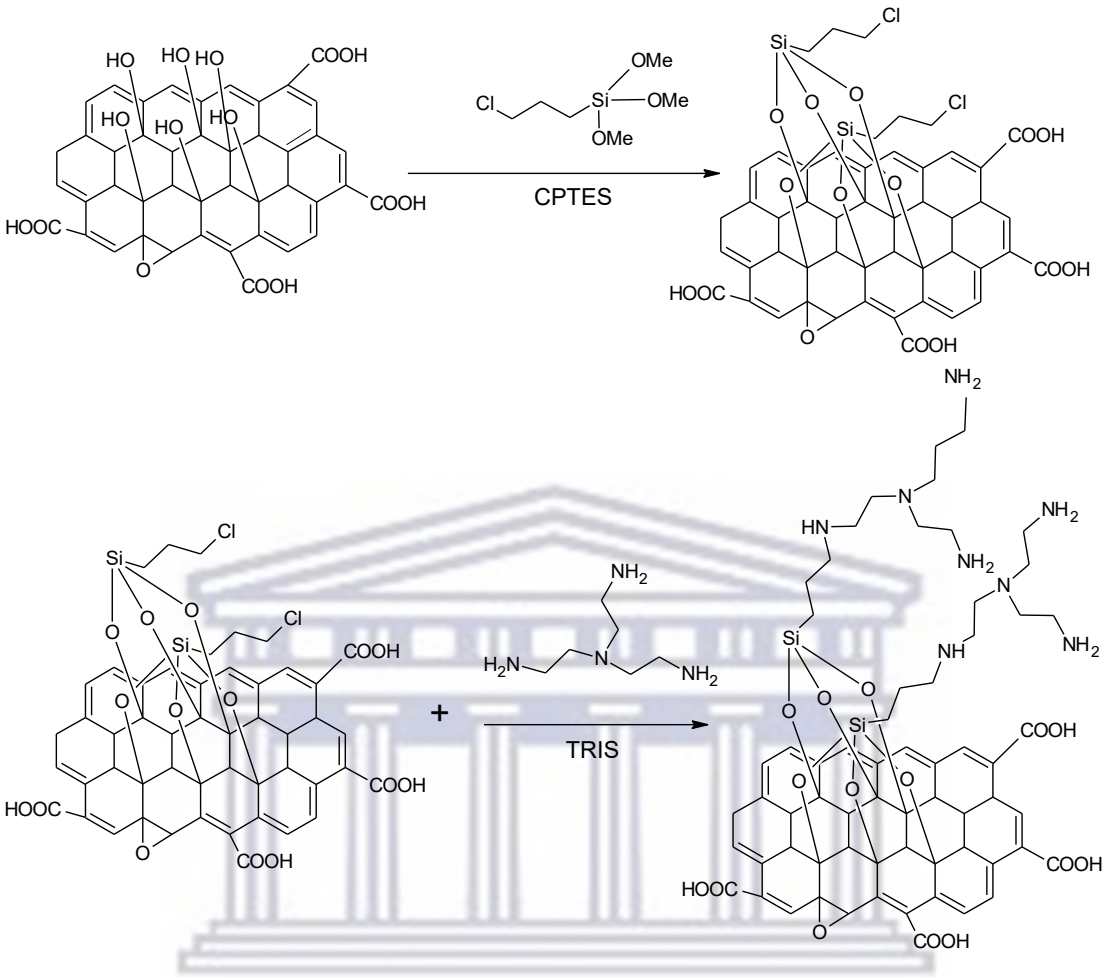

Scheme 8: Functionalization of GO with TRIS

3.2.2.3 Functionalization of GO with Guanidine

The as-synthesized GO was functionalized with Guanidine as follows. 0.2 g of as-synthesized GO was dispersed in 10 ml of dry toluene and the solution was sonicated for 2-3 hours. 1ml of CPS was added to the reaction mixture which was then heated under reflux under nitrogen at 70 ºC for 24 hours. The solid products were collected and filtered while being thoroughly washed with toluene and subsequently dried under vacuum at 60 ºC. 0.1669 g of the GO/CPS and 0.6656 g of KI were added to a solution containing 0.0941g of Guanidine and 0.6084 g of K_2CO_3 in 40 ml of acetonitrile. The reaction mixtures were left

to stir under reflux under nitrogen at 82 ºC for 5 hours. The obtained solids were thoroughly washed with DI water and absolute ethanol, approximately 60ml. The solid was then collected, air dried and placed in a vacuum oven 60 ºC (Scheme 9).

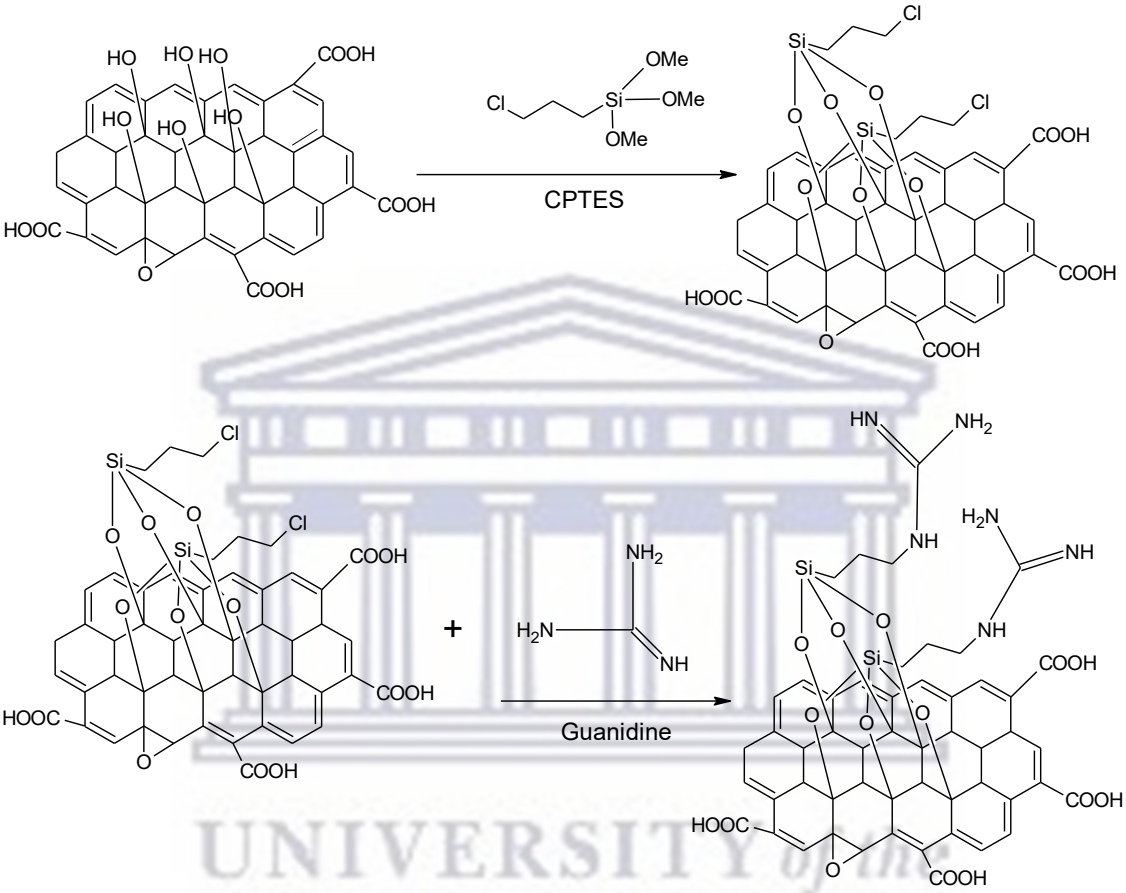

Scheme 9: Functionalization of GO with Guanidine

3.2.3 Self-assembly of GO

GO was modified via the self-assembly of ordered mesoporous silica (OMS) incorporating surfactants i.e. CTAB and P123 into the GO layers followed by the functionalization with PEI.

3.2.3.1 Self-assembly of GO with (P123)

As- synthesized GO was functionalized with P123 as follows. Initially, 1.8 ml of H_2SO_4 and 1.4g of P123 were dissolved in 30 ml of DI water with vigorous stirring at 40 ^oC to form a homogeneous solution. Then 60 mg of GO was added and homogeneously suspended under sonication followed by the drop wise addition of 2.3 ml of TEOS over a period of 15 minutes. The reaction was left to stir at 40 ºC overnight under nitrogen. The resulting black mixture was transferred into a Teflon lined autoclave and heated to 100ºC for 24 hours and then cooled to room temperature. The products were further purified with DI water and ethanol and dried in air before being placed in a vacuum oven at 70 ^oC for 3 hours. Finally, the powder was placed in a tube furnace at 550 ^oC for 5 h under a flow of nitrogen at a low flow rate to remove the template, P123 and form GO-OMS (Fig 6).

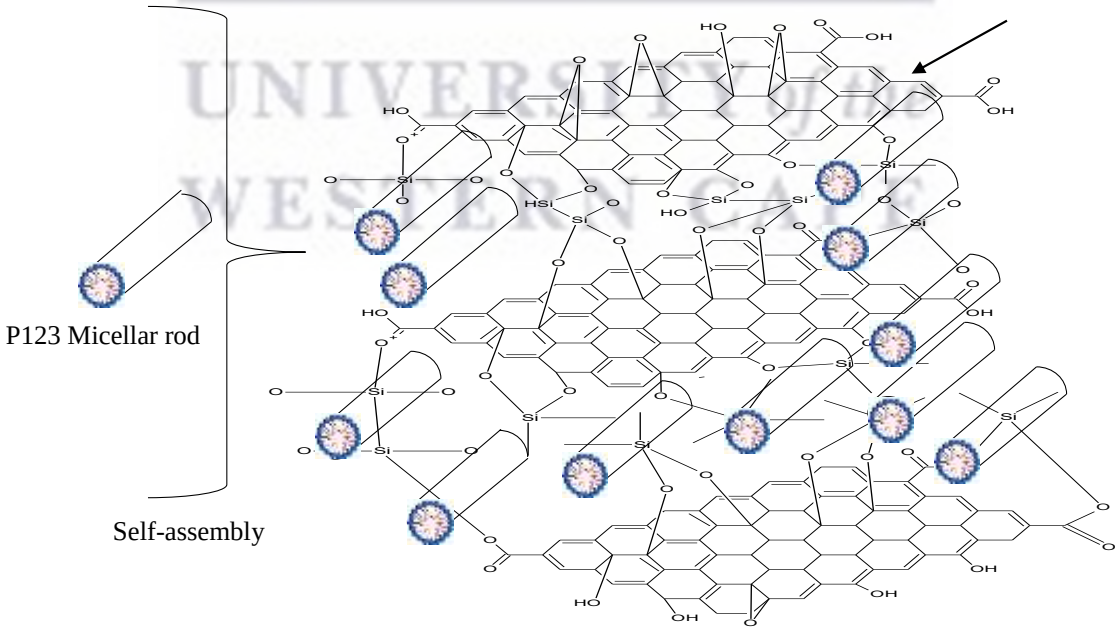

Figure 6: Synthetic route for GO-P123

3.2.3.2 Functionalization of GO- (P123) with PEI

As- synthesized GO- P123 was functionalized with PEI as follows. Initially, 0.27g of PEI was dispersed in 3ml of methanol and 0.3g of GO-P123 was slowly added with continuous stirring until the solution became homogenous. The solution was then sonicated for 30 minutes. The solution was left to stir overnight for the solvent to evaporate. The resulting solid product was left to air dry and then placed in a vacuum oven at 60°C.

3.2.3.3 Self-assembly of GO with (CTAB)

The as-synthesized GO was functionalized with CTAB as follows. 60mg of As-synthesized GO, 80mg of NaOH and 2.0g of CTAB were suspended in a round bottom flask containing 100 ml of DI water. The reaction was left to sonicate for a couple of hours to create a homogeneous suspension. The solution was magnetically stirred for 2 hours at 40 °C under nitrogen and followed by the drop-wise addition of 2ml of TEOS over a period of 15 minutes. The reaction was left to stir overnight while being heated under nitrogen at 40 °C. The product was filtered, washed with warm ethanol and left to air dry. After two days the product was placed in a tube furnace at 550 °C under inert conditions for 5 hours.

3.2.3.4 Functionalization of GO (CTAB) with PEI

As- synthesized GO- CTAB was functionalized with PEI as follows. Initially, 0.25g of PEI was dispersed in 3ml of methanol and 0.3g of GO-CTAB was slowly added with continuous stirring, until the solution became homogenous. The solution was then sonicated for 30 minutes and placed in a rotary evaporator at 70 °C to evaporate the solvent. The final product was left to air dry and then placed in a vacuum oven at 60 °C.

Chapter 4

RESULTS AND DISCUSSION: CHARACTERIZATION

4.1 Fourier-Transform Infrared Spectroscopy (FT-IR)

Fourier transform infrared spectrometry is an analytical method employed to study the absorption spectra which arise from the molecular vibrations of a sample. The spectroscopic technique can identify specific functional groups in a molecule from the rotation, vibration and asymmetric molecular stretching of chemical bonds. Infrared radiation of a wide range of frequencies is passed through a sample with some of the frequencies being absorbed and the rest being transmitted. A detector analyses the frequencies that have been transmitted which in turn gives information about the frequencies which have been absorbed. A spectrum is created representing the wavenumber vs. transmittance. Absorption bands are located in the mid- infrared range between 400-4000 cm^{-1}. Every sample has its own distinct arrangement of atoms and therefore no two compounds will have identical infrared spectra [108-110].

4.1.1 Sample preparation

Two FT-IR instruments were employed to analyse the as synthesized materials; Perkin Elmer UATR 2, where 2.0mg of the as synthesized material to be ground into a fine powder with a mortar and pestle and transferred onto a crystal diamond surface. A pressure arm was used to increase the contact between the solid material and diamond so as to allow the radiation to pass through.

The second instrument was a Perkin Elmer spectrum two. The sample was mixed with KBr and ground to a fine powder using a mortar and pestle. A hand press was used to

apply high pressure to the KBr/sample powder mixture to produce a high quality KBr disk. Both instruments had a scanning range between 400- 4000 cm^{-1}.

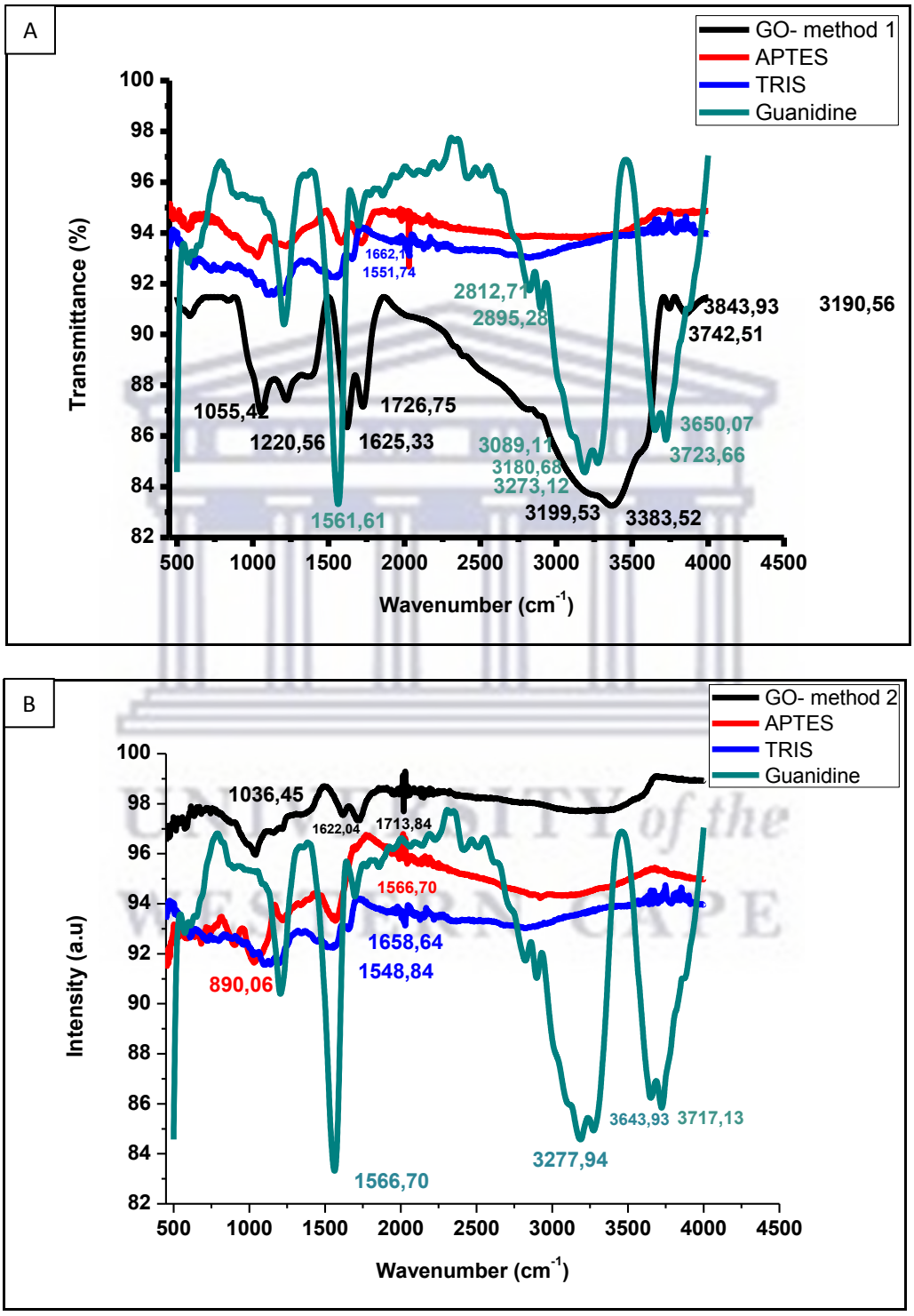

Figure 7: FT-IR spectra for GO (methods 1 and 2)-APTES, TRIS, Guanidine

The FT-IR spectra of Figure 7 (a) and (b) display similar peaks. FT-IR spectra for GO displays a broad band between 3000 and 3600 cm^{-1} representing the hydroxyl group (-OH). The absorption bands at 1051 cm^{-1} corresponds to an alkoxy group (C-O), 1218 cm^{-1} corresponds to the epoxy groups (C-O), 1619 cm^{-1} corresponds to aromatic groups (C=C) and 1728 cm^{-1} corresponds to carboxyl group (C=O). The appearance of the oxygenated functional groups confirms that graphite was successfully oxidized to GO and is consistent with literature [111]. GO-APTES displays an absorption peak at 1017 cm^{-1} attributed to Si-O. Peaks at 2933 and 2871 cm^{-1} correspond to CH_2 bending vibrations. The absorption peaks at 917 and 766 cm^{-1} correspond to Si-CH_3. Characteristic peaks at 1470 and 1444 cm^{-1} are associated with (-NH) and (-NH_2). All of the aforementioned absorption bands prove that APTES was successfully grafted onto GO [56]. Upon grafting with TRIS, GO was modified and corresponding peaks at 1130 cm^{-1} can be attributed to C-N. Peaks at 1569 and 1657 cm^{-1} show asymmetric and symmetric bending of primary amines. All of the aforementioned absorption bands prove that TRIS was successfully grafted onto GO [100]. Upon grafting with guanidine, absorption bands at 1211 cm^{-1} can be attributed to C-N absorption band. Peaks at 3183, 3275, 3651 and 3719 cm^{-1} are attributed to N-H stretching. Guanidine typically absorbs between 1561 and 1698 cm^{-1} which may be attributed to C=N stretching bands. Guanidine usually absorbs in the 1500-1689 cm^{-1} range because of C=N stretching, N-H and NH_2 deformations. Bellamy quoted a higher region of 1590-1718 cm^{-1} for the C=N stretch absorption of guanidine [112]. The appearance of the above mentioned peaks confirmed that guanidine was successfully grafted onto GO.

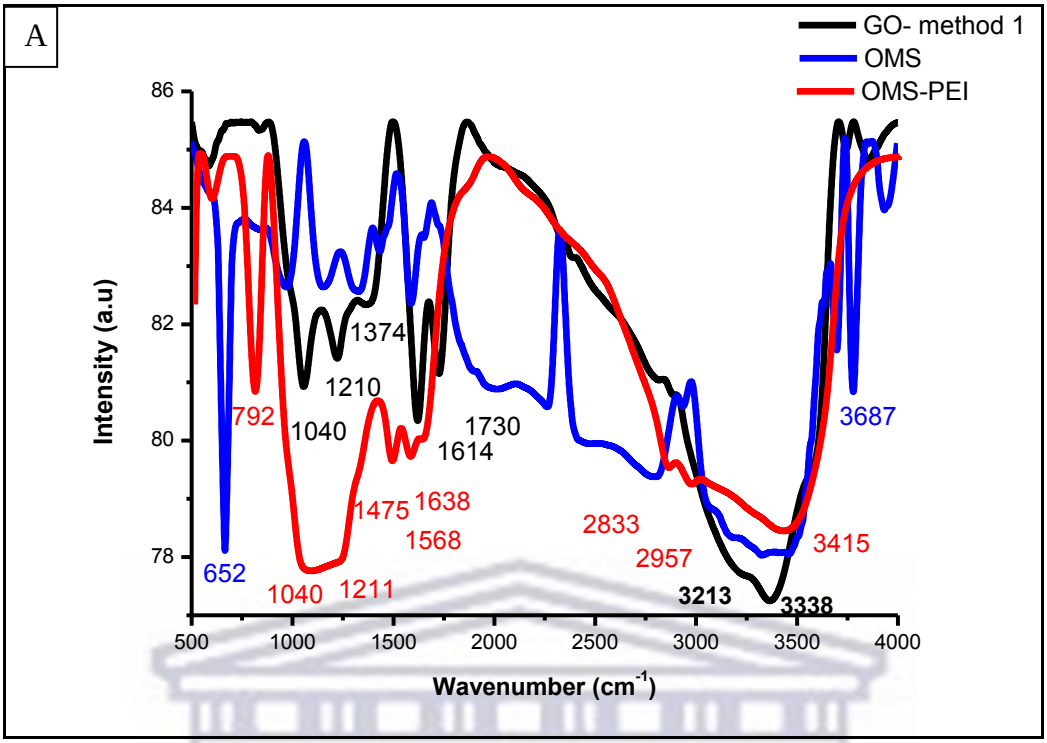

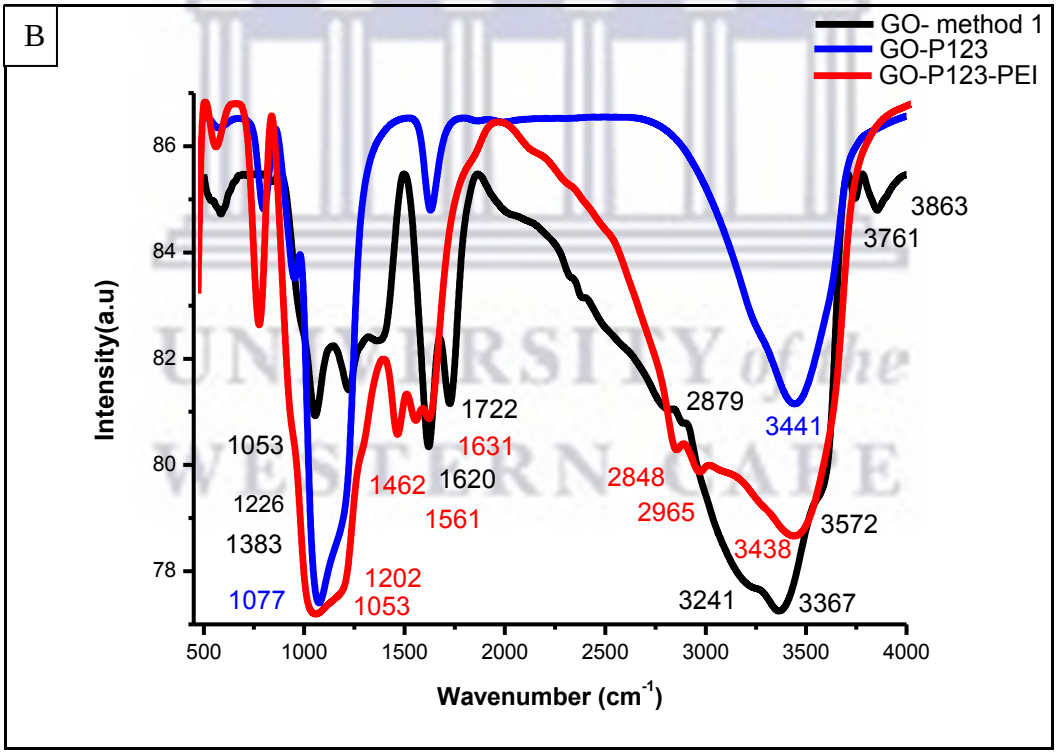

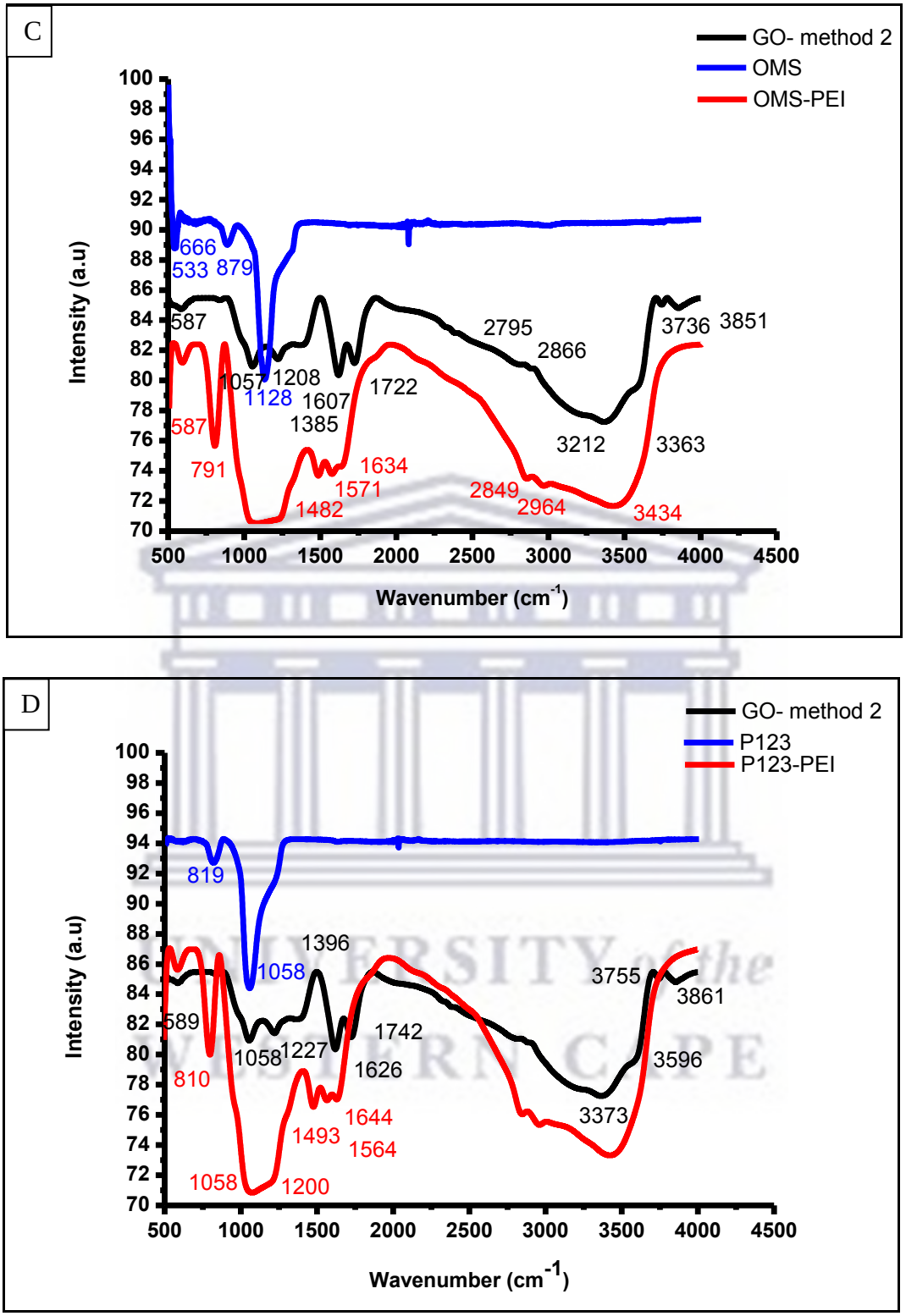

Figure 8: FT-IR spectra for GO (method 1 and 2), GO-CTAB/P123 and GO-CTAB/P123-PEI

The FT-IR spectra of Figure 8 (a), (b), (c) and (d) display similar peaks. FT-IR spectra of the GO (method 1 and 2), GO-CTAB, GO-P123 and GO-CTAB-PEI, GO-P123-PEI samples. GO shows transmittance bands at 1040, 1210, 1614 and 1730 cm^{-1}. The peak at 1070 cm^{-1} arises from the C-O stretch of epoxy groups. The band at 1640 cm^{-1} corresponds to the vibrational mode of ketone groups. The band at 1735 cm^{-1} is associated with stretching of the C=O bond in carbonyl and carboxyl groups. C-OH functional groups are also observed at 1224 cm^{-1}. Absorption bands at 954 cm^{-1} correspond to the bending of Si–OH groups on GO-CTAB and 1040 cm^{-1} which is due to the asymmetric stretching of Si-O-Si bonds on GO-CTAB-PEI. A broad OH peak of GO is detected in the range observed at 3000-3500 cm^{-1}, which suggests the presence of abundant– OH groups on the surface walls of G-silica and G-silica-PEI. The appearance of the –OH functional groups on silica walls can interact with $–NH_2$ functional groups in PEI via hydrogen bonds to form strong adhesion PEI-silica interfaces, which will be favourable for the CO_2 capture of G-silica-PEI enabling excellent cycle performance. The linking of PEI to GO- CTAB and P123 through formation of an amide bond shows two peaks at 2833 and 2957 cm^{-1}. These two bands are due to the symmetric and asymmetric stretching modes of methylene groups of PEI molecules. The peak at 1731 cm^{-1} for GO is attributed to the C=O of COOH. This infers that most carbonyl moieties might convert into amides, which results in the appearance of a new band at 1638 cm^{-1}. In addition, new bands at 1475 cm^{-1} (C−N stretching vibration) and 1568 cm^{-1} (N-H bending vibration) appear in GO-CTAB/P123-PEI, also reflecting the introduction of PEI [113].

4.2 X-ray Diffraction (X-ray)

X-ray diffraction enables the characterization of crystalline features of materials. X-rays are generated from high energy electrons striking an anode in a vacuum. An incident beam of X-ray radiation passes through the crystalline material and is diffracted in various directions by either constructive or destructive interference. Analysis of an XRD spectrum allows one to identify an unknown material's crystal structure. Every solid crystalline material has its own x-ray powder diffraction pattern and the orientation of a single crystal can be determined. XRD can be used to study the arrangement of atoms in the crystalline state, the angles of incident x-ray beams as well as the interatomic distances. The inter planar lattice spacing can be measured using Braggs equation when constructive interference occurs, $2d \sin\theta = n\lambda$ [114] [115]

Where d = interplanar spacing

$\theta =$ angle between the lattice plane of both the incident and diffracted x-ray beam

$\lambda =$ wavelength of the x-rays

n = order of Bragg reflection

4.2.1 Sample preparation

The prepared samples were transferred from the sample container straight into the instrument. XRD was performed on a Bruker AXS, D8 Advance. Measurements was performed with a ϑ-ϑ scan, in locked coupled mode using a Cu-Kα radiation ($\lambda K\alpha_1$=1.5406Å) tube and a LynxEye PSD detector. A V20 variable slit, tube voltage at 40kV and tube current at 40mA was employed. The diffraction data was recorded in the 2θ range between 2- 60° at a scan rate of 0.5 sec/step.

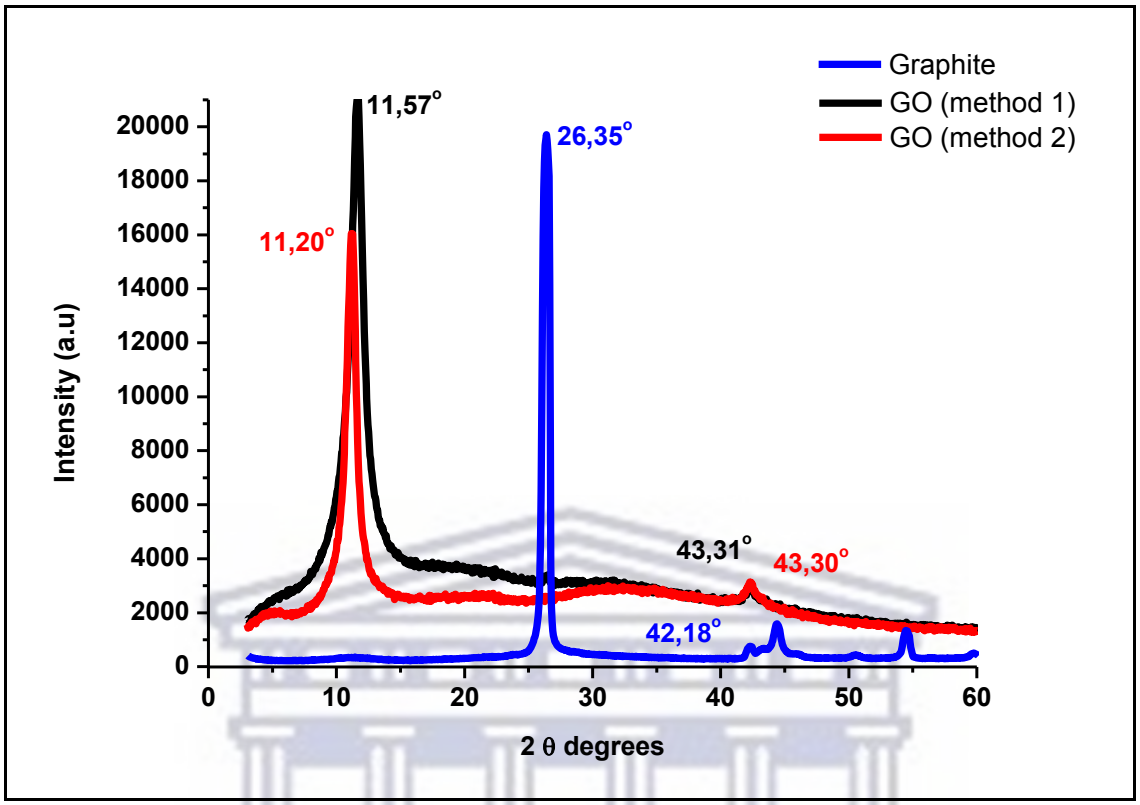

Figure 9: XRD patterns of Graphite and GO (method 1 and 2)

The XRD spectra of Figure 9 displays a sharp (002) peak centred at 2θ =26.35° attributed to graphite and corresponds to the crystalline graphite. This indicates that the interlayer distance of graphite (d-spacing) was about 3.38 Å. The calculation was performed using Bragg's law. Oxidation caused a shift of the GO parent peaks (method 1 and method 2) with a diffraction peak of 11.57° and 11.20° and an interlayer distance of 7.64 Å and 7.90 Å. This is a result of the insertion of oxygen containing functional groups as well as water molecules, which increases the interplanar spacing. The peaks of GO (method 1 and 2) have also been slightly broadened which indicates that the structure of oxygenated graphite has an amorphous structure. [95]

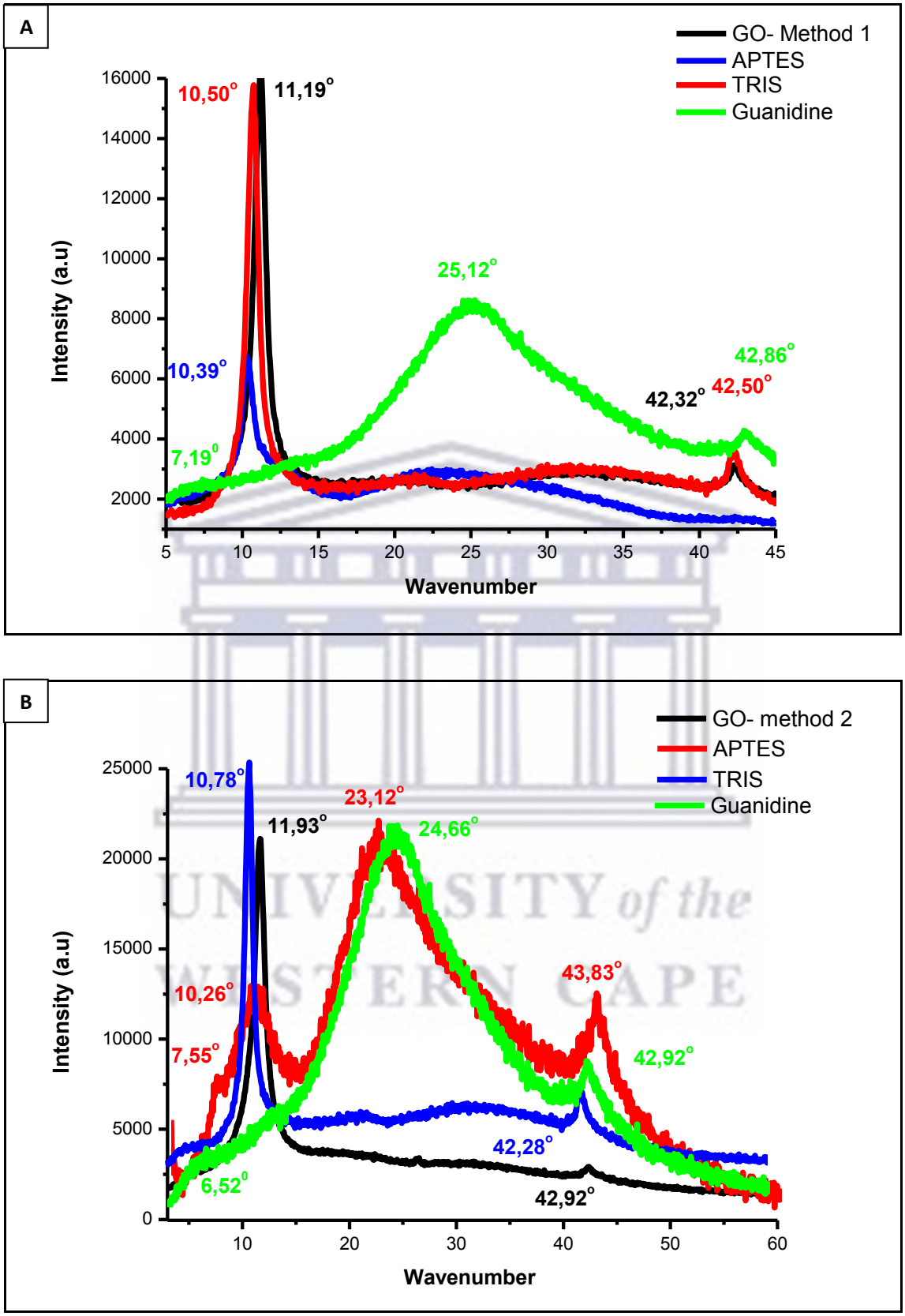

Figure 10: XRD patterns of GO (method 1 and 2) -APTES, TRIS, Guanidine

The XRD spectra for Figure 10 (a) - method 1 display peaks for amine functionalized GO (APTES, TRIS and Guanidine), one of which (Guanidine) was not that well resolved, indicating a lower degree of ordering. The broadness of the peak and weak intensity could imply the presence of highly disordered and randomly arranged guanidine [116]. APTES and TRIS exhibited sharp well-ordered peaks. GO-APTES exhibited a diffraction peak at about 10.39° and an interlayer distance of 8.51 Å. GO-TRIS exhibited a sharp diffraction peak at 10.50° with an interlayer distance of 8.41 Å. The amine-modified graphite oxide materials showed a slight shift from the parent GO and the observed increase in the interlayer distance was attributed to amine molecules being covalently attached onto the GO surface. The increase in the interlayer distance is confirmation of the aminosilanes (APTE and TRIS) being functionalized onto GO sheets. GO-Guanidine exhibited a lower intensity, with a diffraction peak at 7.19° and an interlayer distance of 12.29 Å. The broad diffraction peak could be attributed to the disordered stacking structure. The contribution of guanidine, found at the basal plane of GO could have contributed to the higher interlayer distance as compared to GO-APTES and GO-TRIS. While no shift in d-spacing to lower angles was observed, this could be an indication that the grafting step did not cause any structural changes [117]. It has been reported that the diffraction peaks in XRD patterns become weak or even disappear if GO is cross-linked at either edge or side of the sheets leading to its regular stacks being destroyed [101]. The XRD spectra in Figure 10 (b) - method 2 displays three peaks for amine functionalized GO (APTES, TRIS and Guanidine) two of which (TRIS and Guanidine) were not well resolved, indicating a lower degree of ordering. TRIS exhibited a sharp diffraction peak at 10.78° with an interlayer distance of 8.20Å. APTES displayed two peaks in the lower angle region, corresponding to a slightly diminished diffraction peak at 7.55° and broad diffraction peak at 10.26° with interlayer

distances of 1.71 Å and 8.62 Å respectively. The resulting large interlayer distance of GO-APTES can attributed to the presence of the functional groups between the layered structures causing successful intercalation of aminosilanes. Guanidine exhibited a shift in d-spacing to lower angles with a peak at 2θ =6.52° with a corresponding d-spacing of 13.55 Å and an additional broader peak at 24.66° with a d-spacing of 3.61 Å [118].

The XRD spectra of Figures 11(a), (b), (c) and (d) display essentially similar peaks with variations in their intensities. GO-1-CTAB and GO-1-CTAB-PEI display broad peaks at 2θ =11.89° and 2θ =12.17° which may be due to the presence of residual oxygen and hydrogen indicating incomplete reactions between CTAB and GO [119]. The broadened diffraction peak at 24.30° for GO-CTAB sheets reveals an amorphous structure. GO's presence within the structure has an influence on the self-assembly of the impregnation of CTAB into the sheets of GO [120].

The structure of GO, before and after the functionalization with PEI was characterized and the results are compared for both methods 1 and 2 silylated with CTAB and P123. The diffraction patterns of GO diminished when mesoporous silica self assembles onto the surface. The diffraction patterns of GO-1-P123 and GO-1-P123-PEI are similar indicating that the structure of GO-P123 was preserved upon functionalization with PEI, however, the intensity of the diffraction peaks compared to that of the parent GO, decreased. This could possibly be attributed to pore filling by PEI. These peaks indicate ordered two-dimensional hexagonal mesostructures. GO's presence within the structure has an influence on the self-assembly of the tri-block copolymer (P123) [121].

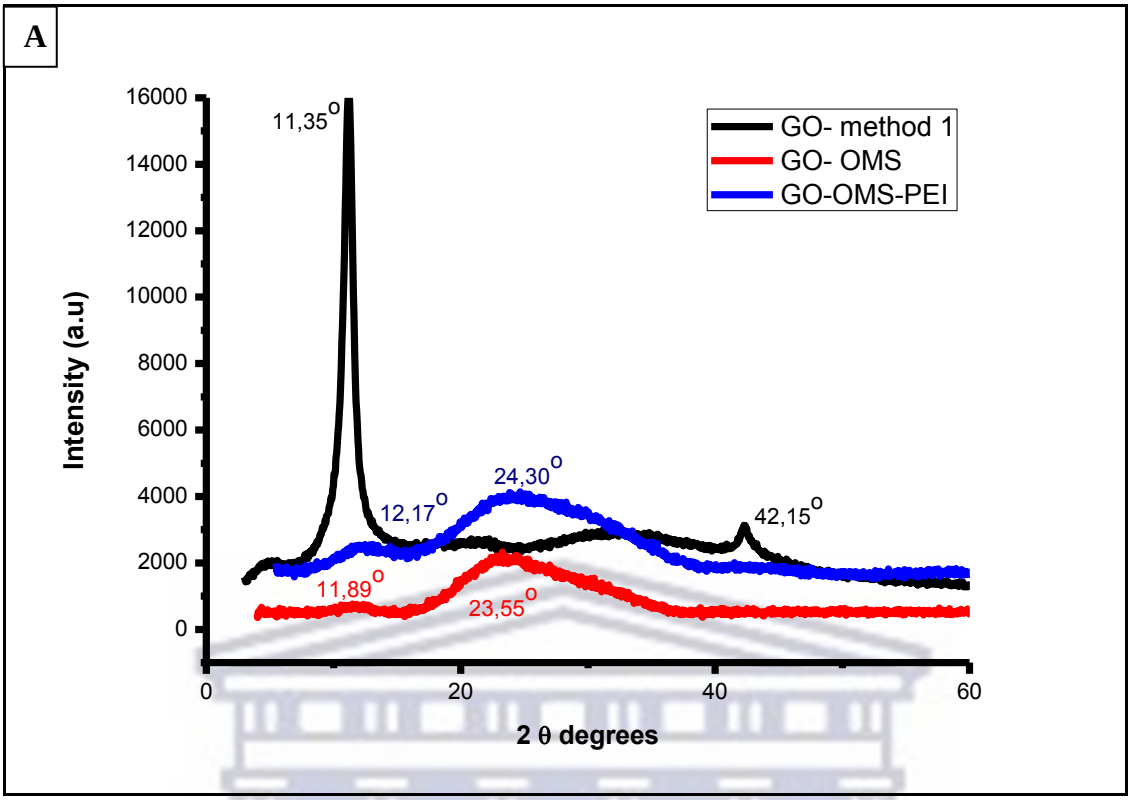

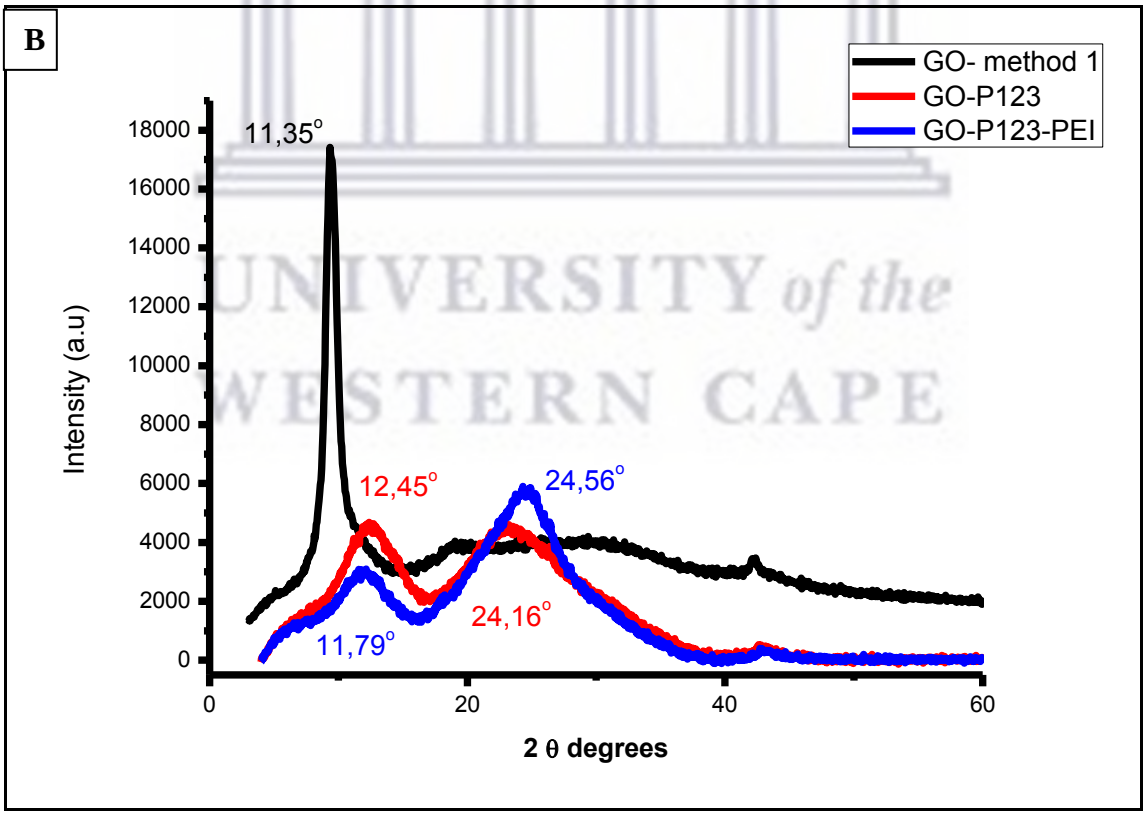

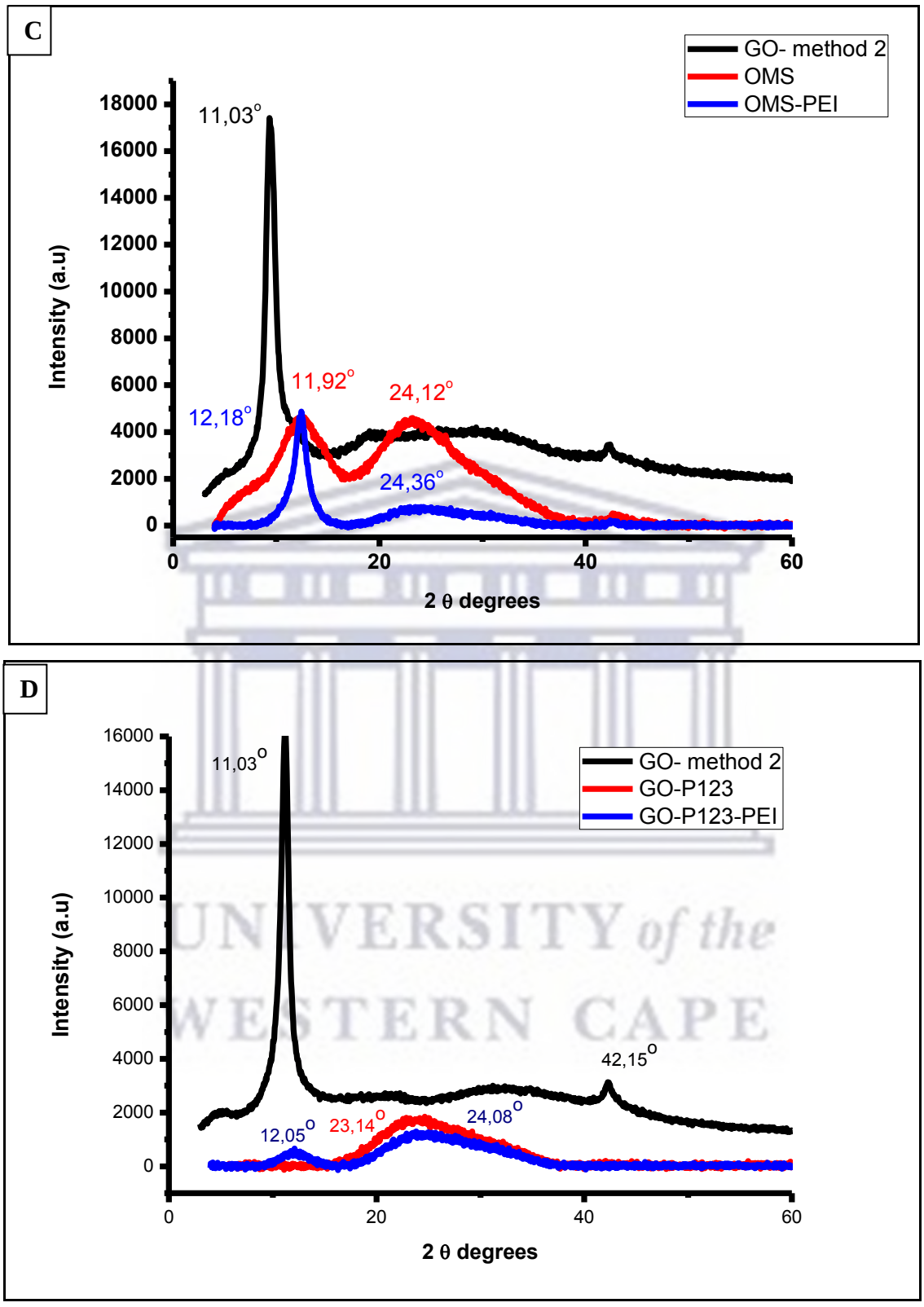

Figure 11: XRD spectra for GO (method 1 and 2), GO-CTAB/P123 and GO-CTAB/P123-PEI

4.3 High Resolution Scanning Electron Microscope (HR-SEM)

SEM is used to study the morphology of materials. SEM produces images through an electron beam that is focused into an extremely fine probe, which scans across the surface of the materials. SEM utilizes electrons which are created through the heating of a cathode filament. The electron beam irradiates electrons by scanning the sample in a raster like motion [122]. When the electron beam comes into contact with the sample, backscattering and secondary electrons are emitted. Secondary electrons possess a low energy and can therefore be used to examine the topography of the sample. Backscattered electrons possess a higher energy than secondary electrons and can be referred to as the electrons that are 'scattered backward' and discharged from the sample.

Samples which are not conductive need to be coated with a thin metal film over the surface of the sample including the employment of vacuum evaporation using inert gases to heat and vaporize the sample. Typically, noble metals such as gold (Au) or Palladium (Pd) or a combination of both as well as Platinum (Pt) are used due to their stability. The irradiated electrons derived from secondary and backscattered electrons are detected and recorded as a signal [123]. EDS is used in combination with SEM and is limited to only providing atomic information and not molecular evidence [124].

4.3.1 Sample preparation

The samples were prepared by sticking the powered samples on an aluminium stub, using a carbon adhesive. The samples are not electrically conductive therefore a plasma sputter coating was employed, using a Quorum 150 TES machine. A mixture of 60%

gold and 40% palladium was sputtered on the stub for 30 seconds to render them conductive. In addition, argon gas was purged through the system. The stubs were then removed from the machine and loaded into the spectrometer. The analysis was conducted using a Carl Zeiss Auriga field emission gun (FEG) SEM, operated at 5 keV. The EDX spectra were collected at 20keV using a silicon solid-state drift detector.

The morphology of the samples was studied using SEM. Figures 12A and 12B shows the SEM images of GO (method 1 and 2). The individual exfoliated layers can be seen with smooth wave-like edges. The exfoliation of the layers is an identification that graphite was oxidized to GO. The EDX spectrum indicates the composition of the individual elements within synthesized GO [125].

Figure 13 shows the SEM image of GO-APTES displaying a wrinkled like surface structure. However, the exfoliation of the layers observed after silyation is very similar to GO [22]. The EDX spectrum confirms the silyation of GO, indicating a high silicon (Si) and nitrogen (N_2) weight percent [126]. The relatively smoother surface of GO exfoliated sheets (Figures 12 A and B) with respect to GO-APTES images suggests that APTES molecules have been successfully functionalized onto the GO surface [91].

Figure 14 shows the SEM image of GO-OMS (CTAB). It can be deduced that the surfactant (CTAB) is concentrated on the surface of GO and displays a coating of the mesoporous silica on the sheets of GO. The EDX micrographs illustrates a high weight percent for Si, C and O content which could be an indication that graphene remains in the graphene mesoporous silica sheets [19].

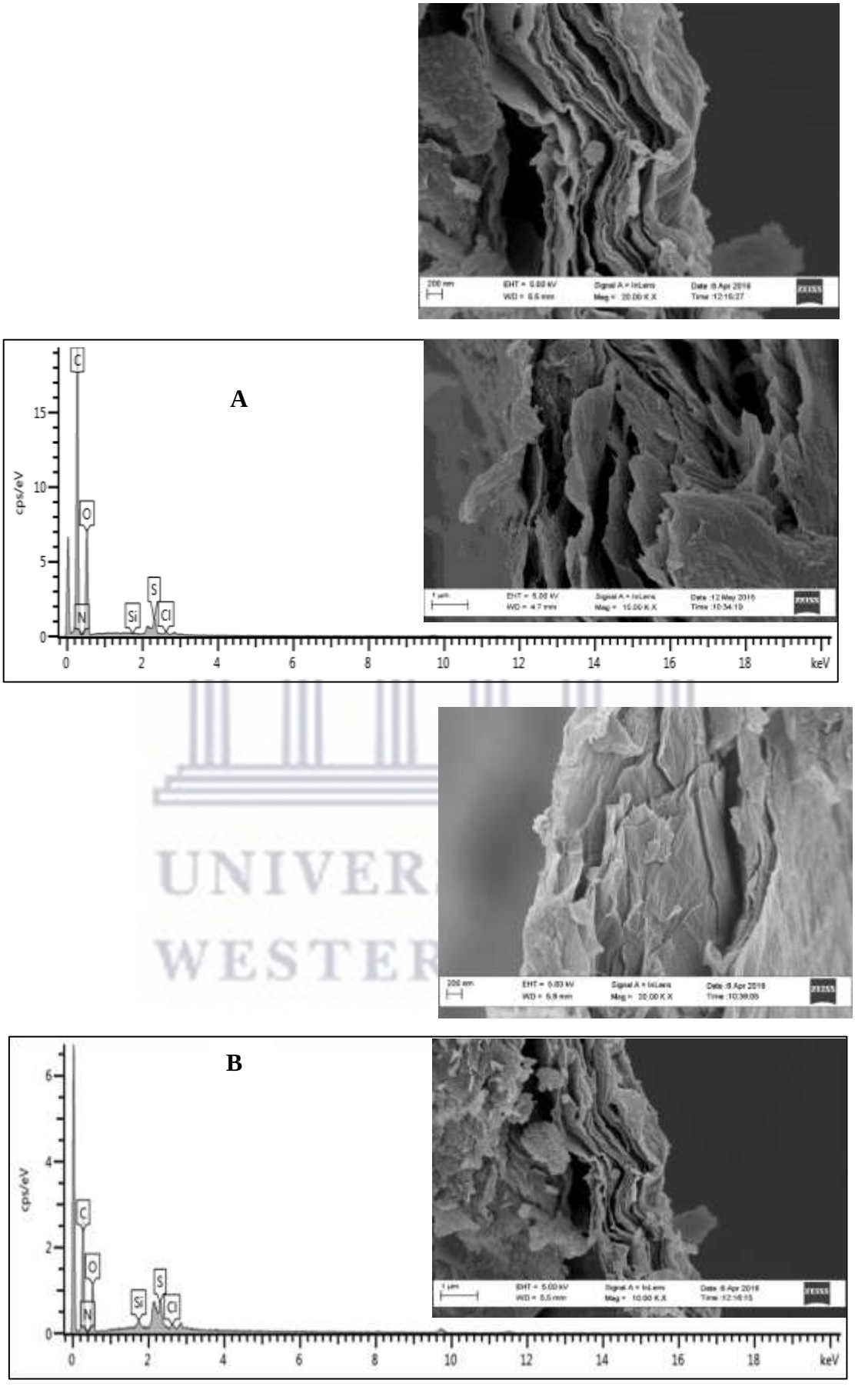

Figure 12: Scanning electron micrograph and EDX of GO method 1 (A) and 2 (B)

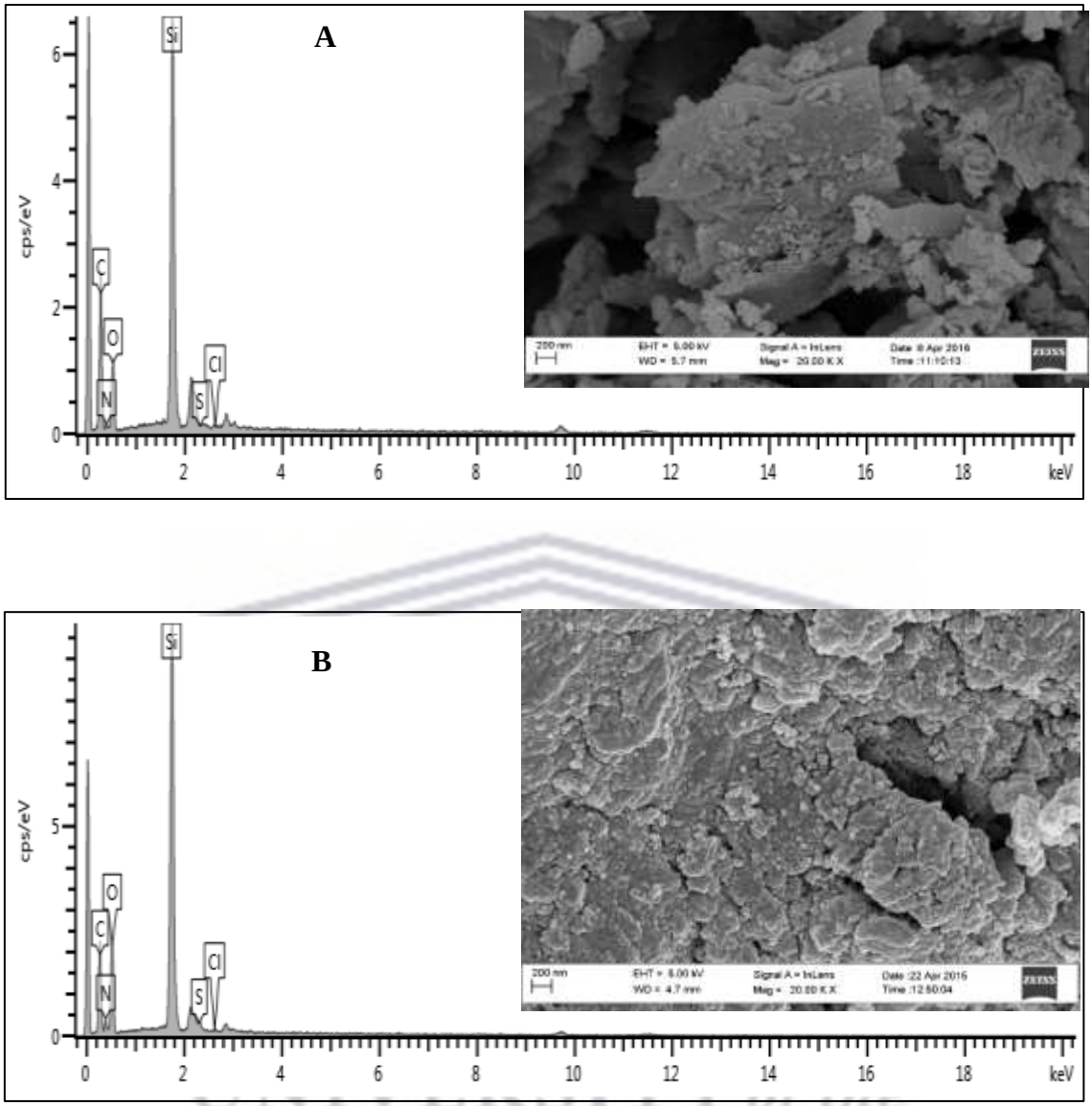

Figure 13: Scanning electron micrograph and EDX of GO-APTES [method 1 (A) and method 2 (B)]

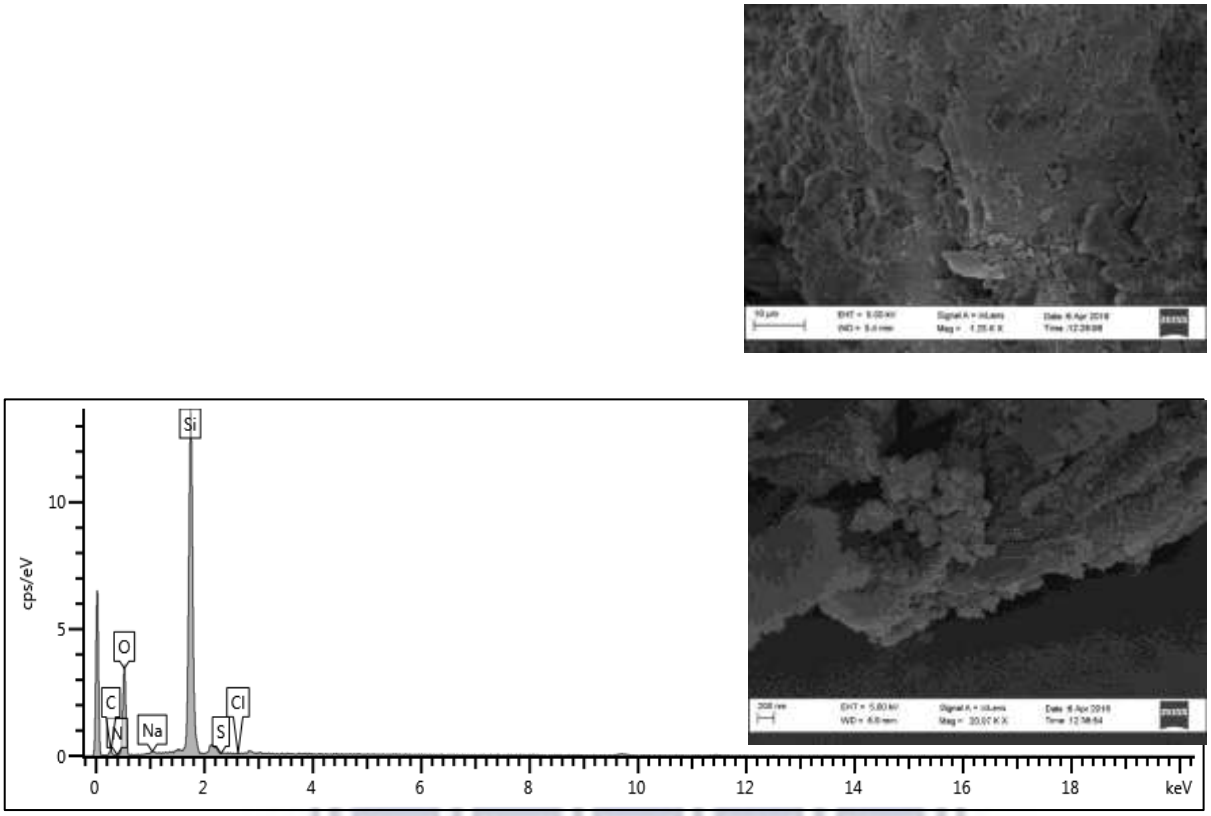

Figure 14: Scanning electron micrograph and EDX of GO- Method 1- CTAB

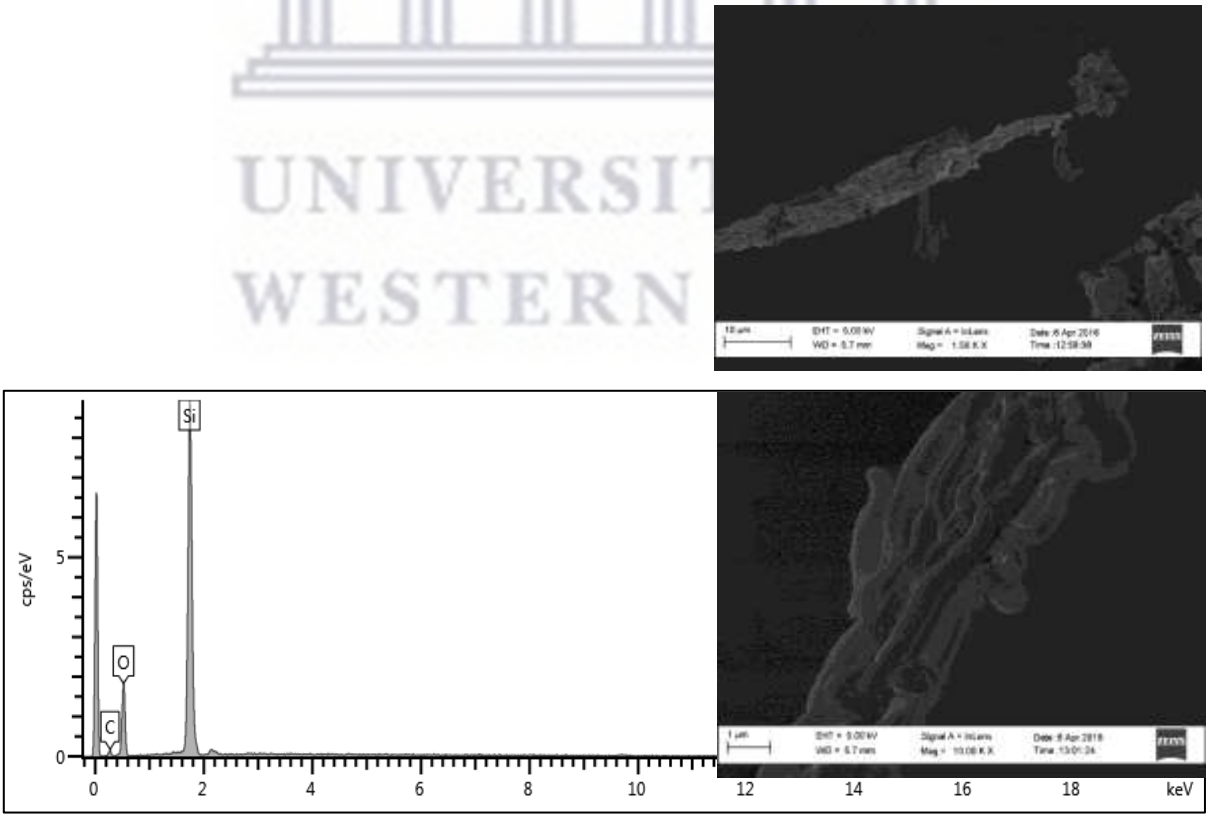

Figure 15: Scanning electron micrographs and EDX of GO-Method 1- P123

Figure 15 illustrates the SEM and EDX images of GO-Method1-P123 and were employed to visually examine the morphology of GO-OMS (P123). It displayed a spherical like morphology which is consistent for polymer based surfactants (P123) concentrated on the surface of the GO sheets. The EDX micrographs displays the Si, C and O content, the high Si weight percentage [20].

4.4 Transmission Electron Microscope (TEM)

A light microscope emits light and the light emanating from the instrument contains a specific wavelength. TEM functions in a similar manner, except that instead of the instrument emitting light, electrons are irradiated from an electron gun. The resolution of a TEM is almost 100 times greater than that of a light microscope. This feature enables lighter atoms, which scatter electrons less effectively, to be detected. Therefore, it is an important imaging tool utilized in material science and catalysis. Subsequently electrons from the electron gun in a TEM contain a significant amount of energy interacting with the atoms of the specimen. These electrons are transmitted right through the specimen creating an image which can be analysed. TEM provides useful information regarding the morphology which encompasses the arrangement of particles in atomic diameters as well as shape and size. Crystallography can also be attained from electrons which have been diffracted due to the order and arrangement of atoms [127].

4.4.1 Sample preparation

An adequate amount of sample, approximately 1mg, was placed in a vial and diluted with approximately 2-3mL ethanol. The samples were then sonicated for approximately 5 minutes to create a homogenous dispersion and then dispersed with a micropipette

onto a carbon coated copper grid. The grid was placed under a light for the ethanol to air dry and evaporate. Lastly, the carbon coated copper grid sample was placed on a sample holder for analysis conducted using a FEI Technai $G^2$20 Field Emission Gun (FEG)-TEM operated at 200kV, coupled with Electron Dispersive X-ray spectroscopy (EDAX SiLi detector) for elemental analysis.

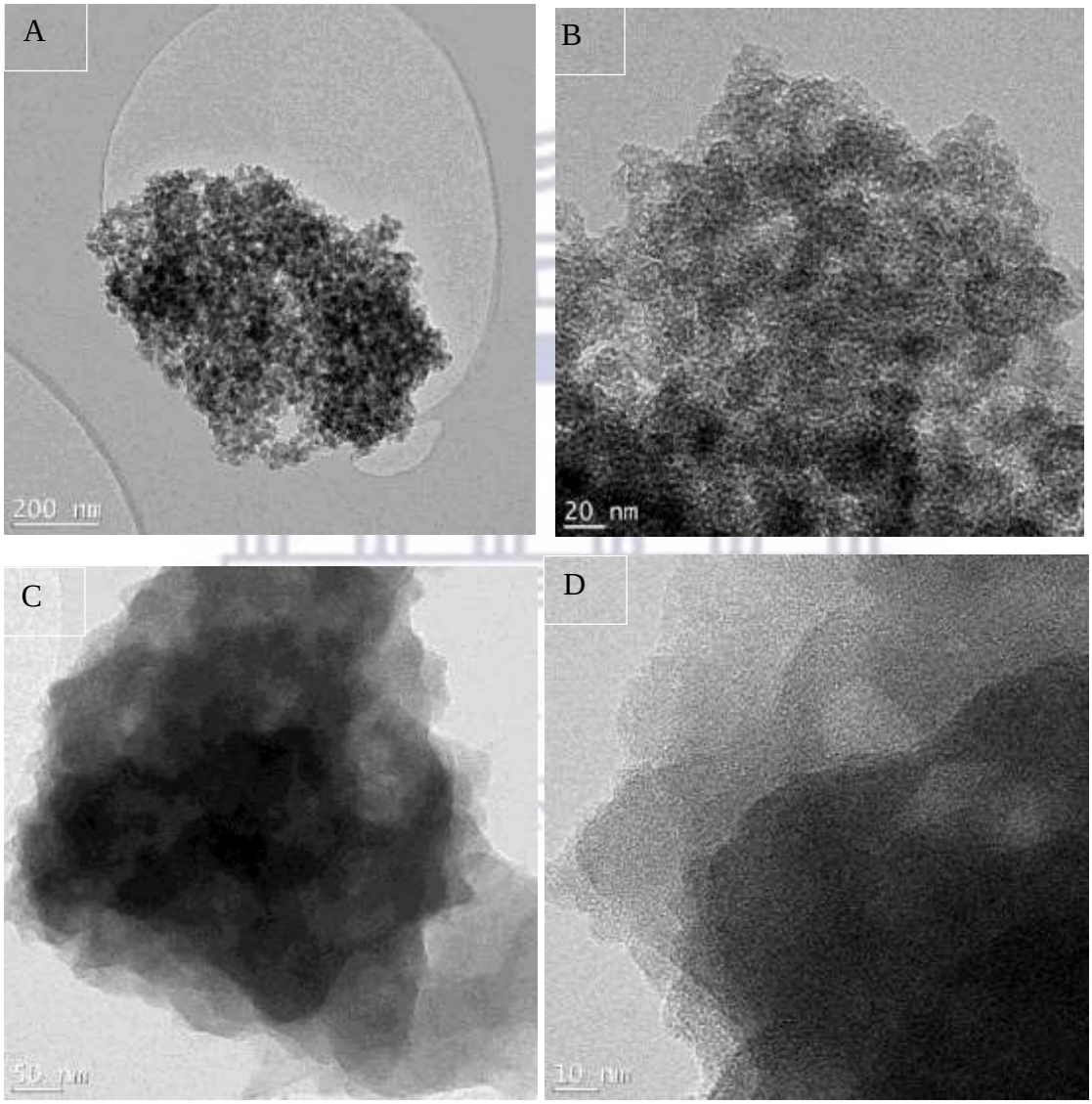

Figure 16: TEM micrograph of GO-CTAB [method 1 (A) and method 2 (B)] and TEM micrograph of GO-CTAB-PEI [method 1 (C) and method 2 (D)]

Figure 16(A and B) indicates the TEM micrograph of GO- CTAB, the mesoporous silica structure. The image reveals the stable morphology of the mesoporous silica structure after calcination. The TEM micrograph of GO- CTAB-PEI Figure 16(C and D) [24] indicates the existence of micro pores which can serve as channels for the diffusion of gas [16].

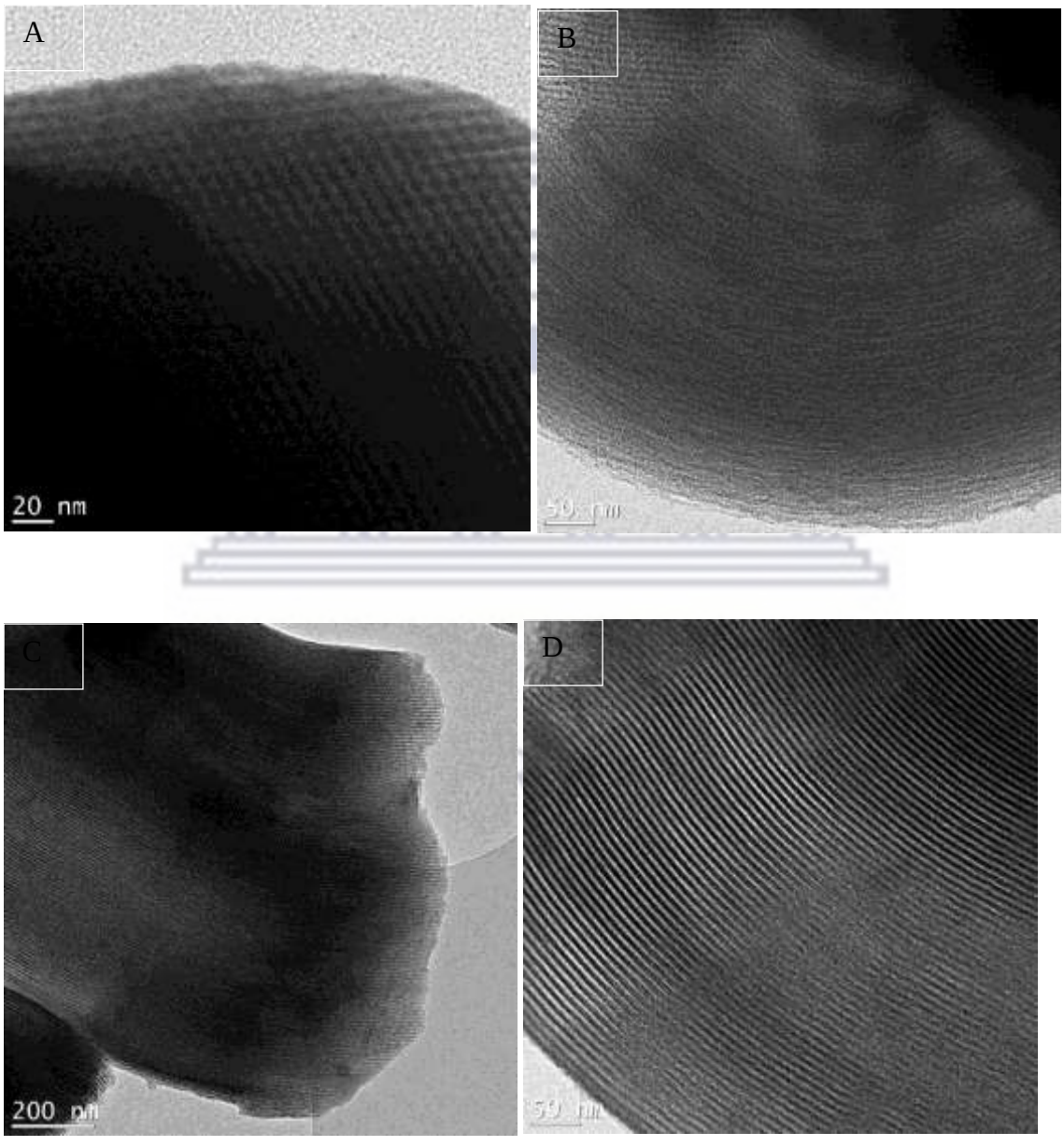

C **D**

Figure 17: TEM micrograph of GO-P123 [method 1 (A) and method 2 (B)] and TEM micrograph of GO-P123-PEI [method 1 (C) and method 2 (D)]

The images in Figure 17 reveal that both GO-P123 and GO-P123-PEI retained ordered channels which is a characteristic of ordered mesoporous structure. It is also associated with the stability of the morphology after heat treatment at high temperatures [15].

4.5 Nitrogen Physisorption

Nitrogen physisorption is a technique used to characterize the textural properties of mesoporous materials such as their porosity and specific surface areas. During the analysis, an inert gas, usually nitrogen is adsorbed onto the surface of the material. The relationship between the amount of gas adsorbed per unit mass of solid and the equilibrium pressure and known temperature, is characterised as the adsorption isotherm. There are many recorded adsorption isotherms for various gas-solid systems and each have their own unique characteristic shape. The shapes of the isotherms provide important information about the pore structure of the adsorbent material. The five types are classified as type I, II, III, IV and V (Figure 18) [128].

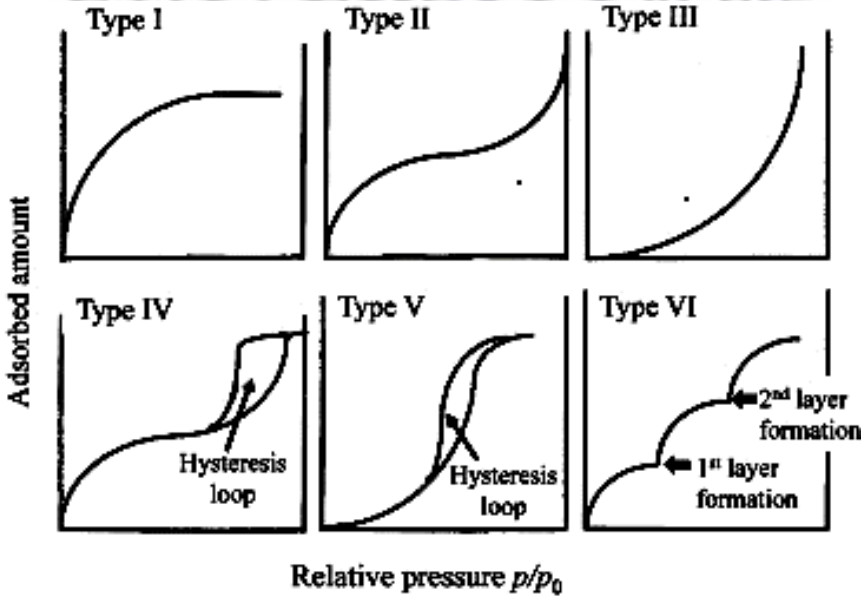

Figure 18: Adsorption isotherms [129]

Brunauer-Emmett-Teller (BET) is considered to be one of the most commonly implemented techniques used to determine specific surface areas of porous solid materials. The adsorption theory is based upon a monolayer-multilayer adsorption model. The determination of pore size distribution employed the Barrett, Joyner and Halenda (BJH) methods. Porous solids can be categorised into their individual classes depending on the size of their pores [130]. Macropores are greater than (>50 nm), mesopores are between (2 nm and 50 nm) and micropores are less than (<2 nm). Specific surface area can be calculated using the BET method where α is the surface area, assuming nm has monolayer coverage with known molecular area and when nitrogen (N_2) is employed, δ (N_2) = 0.162 nm^2, assuming a nitrogen monolayer that is completed with a close packed liquid like structure. Before analysis, samples are degassed to remove all volatile physisorbed molecules as well as any impurities [131].

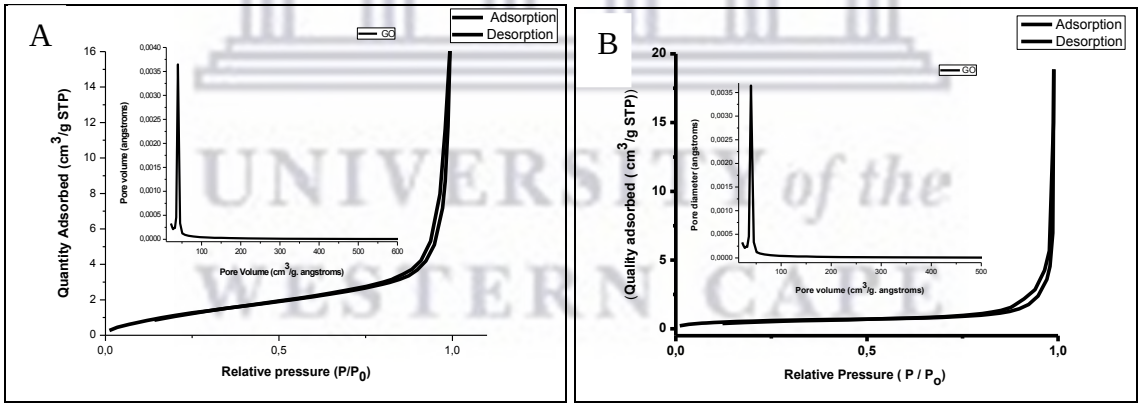

Figure 19: Nitrogen adsorption-desorption isotherms and corresponding pore size distributions of GO [method 1 (A) and method 2 (B)]

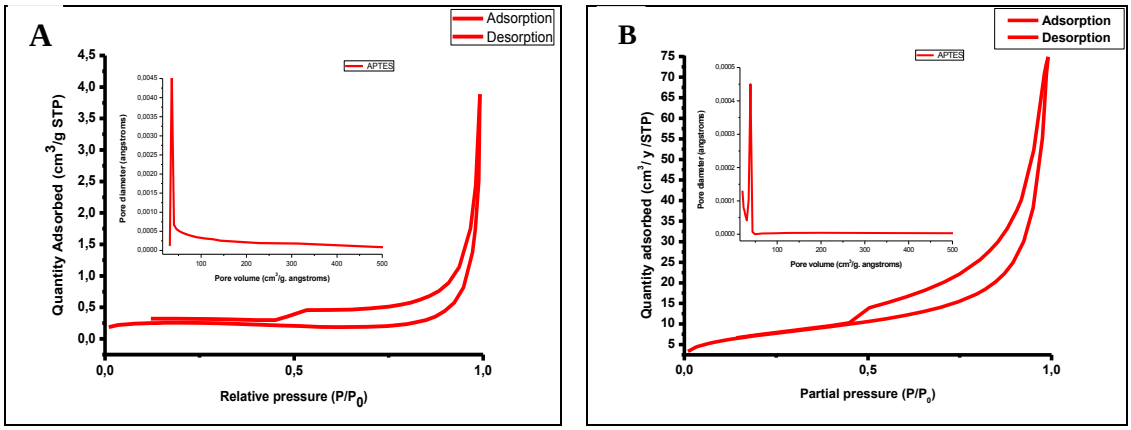

Figure 20: Nitrogen adsorption-desorption isotherms and corresponding pore size distributions of APTES [method 1 (A) and method 2 (B)]

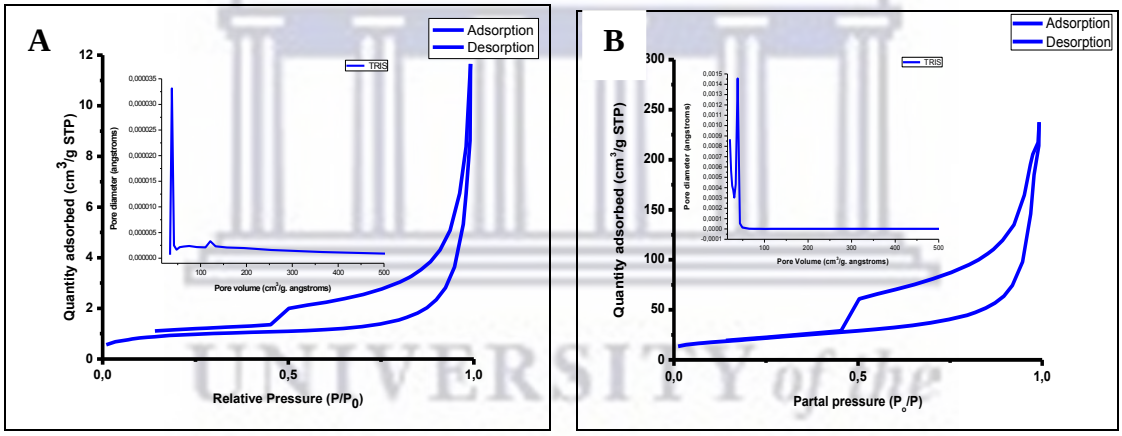

Figure 21: Nitrogen adsorption-desorption isotherms and corresponding pore size distributions of TRIS [method 1 (A) and method 2 (B)]

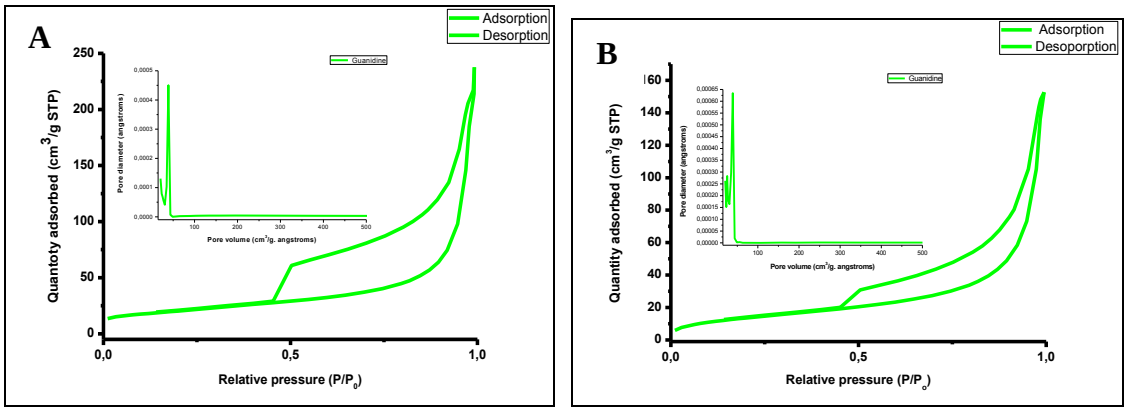

Figure 22: Nitrogen adsorption-desorption isotherms and corresponding pore size distributions of Guanidine [method 1 (a) and method 2 (b)]

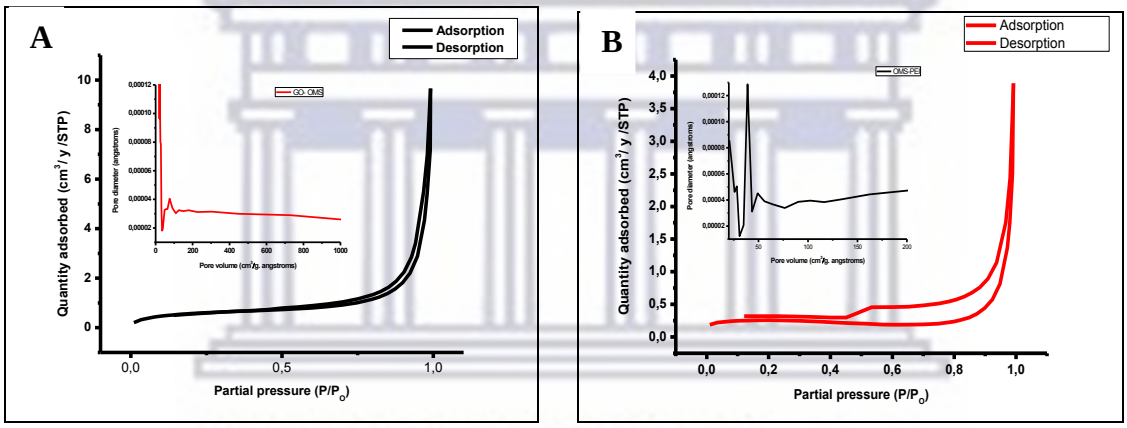

Figure 23: Nitrogen adsorption-desorption isotherms and corresponding pore size distributions of Method 1 [GO-CTAB (A) and GO-CTAB-PEI (B)]

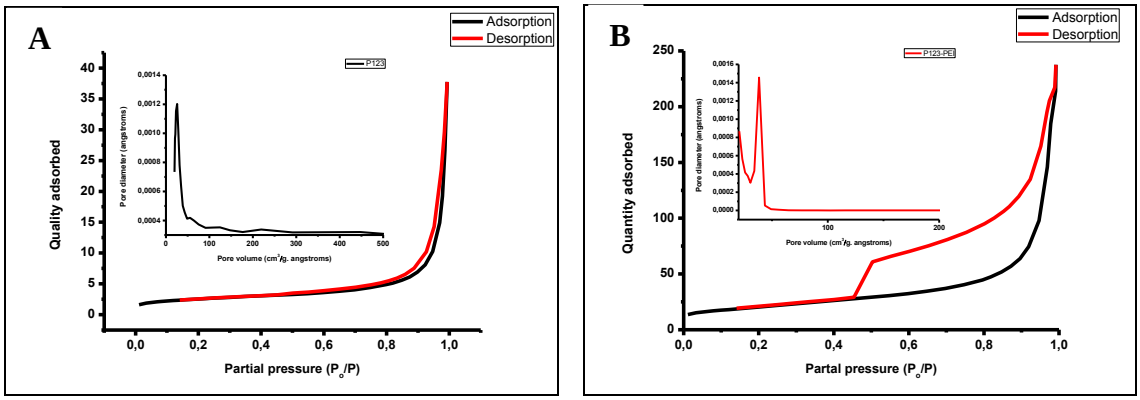

Figure 24: Nitrogen adsorption-desorption isotherms and corresponding pore size distributions of Method 1 [GO-P123 (A) and GO-P123-PEI (B)]

Figures 19-22 display the adsorption-desorption isotherms of GO and its functionalized derivatives for method 1 and 2. Figures 19-22 display type IV isotherms which are typically characteristic of the adsorption behaviour for none rigid slit-shaped pores of aggregated powders. Figures 19 and 20 display type 3 hysteresis loops and Figures 21 and 22 display type 4 hysteresis loops [132]. These hysteresis loops are usually found on solids consisting of aggregates or agglomerates of particles with uniform size and/or shape. Hysteresis can be attributed to the difference in adsorption and desorption behaviour. Hysteresis illustrates monolayer/multilayer coverage that is coupled to micropores and mesopores according to the IUPAC [133]. The BET surface area of GO (method 1), APTES, TRIS and Guanidine were 29.56, 14.46, 4.53 and 5.70 m^2/g respectively. The surface areas are very low compared to typical activated carbons and graphite sheets which have surface areas with values between 100–1000 m^2/g and 700–1500 m^2/g. The low surface areas for this study can be attributed to the fact that the GO employed in this study was just GO powder and that it was not treated by any exfoliation such as thermal expansion. This was observed for GO (method 2), APTES, TRIS and Guanidine as well. The BET surface areas were 25.39, 12.88, 4.36 and 5.09 m^2/g, respectively. The decrease in surface area from parent GO to the functionalized derivatives could be due to the blocking of fine pores (capillaries) of the parent support GO or due to poor loading of alkyl chains introduced onto the surface GO layers through Si-O bonding. The increased surface area of GO-1-APTES and GO-2-APTES compared to GO-1-TRIS and GO-2-TRIS may be caused by the breaking of sp_2 hybridized structures enabling widened interlayers during surface modification. This can be corroborated with the XRD patterns (Figure 10) which display a higher interlayer distance for APTES and Guanidine, for both methods 1 and 2.

N_2 adsorption/desorption isotherms of PEI/G-silica sheets show small hysteresis loops visible for GO-CTAB and GO-P123 (Figure 23a and Figure 24a). The small hysteresis between the adsorption and desorption branches suggests a uniform pore size which could suggest no pore-blocking during desorption. The adsorption/desorption isotherms for G-silica PEI (Figure 23b and Figure 24b) exhibit a type IV nitrogen adsorption branch associated with a well-defined capillary condensation step, characteristic of uniform mesopores. A well-defined hysteresis loop indicates the existence of an ordered mesopores in the framework [19]. The BET surface areas were 8454, 5137, 7235 and 4937 m^2/g for GO-CTAB, GO-CTAB-PEI, GO -P123 and GO-P123-PEI, respectively. The lower surface areas can be attributed to, as mentioned earlier, the GO employed during this study which could have had an impact on the G-silica composites.

The pore size distributions were determined by the Barrett-Joyner-Halenda (BJH) method from the adsorption branch of the isotherm. The pore size and pore volumes for of GO method 1 and 2 and its functionalized derivatives can be found in Table 2. The pore volume decreased from 0.16 cm^3/g for GO-1 to 0.029, 0.015 and 0.024 cm^3/g for GO-1-APTES, GO-1-TRIS and GO-1-Guanidine respectively and can be seen for GO-2, GO-2-APTES, GO-2-TRIS and GO-2-Guanidine as well and referred to in Table 2. The reduction in pore volume suggests that the organic material was successfully grafted inside the pores of GO. The PSD of APTES, TRIS and Guanidine was narrow. This could indicate that the aminosilanes were evenly distributed on the pore walls. The pore volumes decreased from 0.11, 0.02, 0.008, 0.14 cm^3/g for GO-2, APTES, TRIS and guanidine respectively. The considerable decrease in pore volume for GO-TRIS could be attributed to insufficient absorption of N_2 onto the parent GO, due to the organic material grafted onto the surface as well as inside the pores [134].

Table 2: BET surface area of the as-synthesized GO and its derivatives

	Surface area (m^2/g)	Pore size (nm)	Pore volume (cm^3/g)
GO- Method 1	29,56	1.64	0.1949
GO-APTES	14.46	0.92	0.1290
GO- TRIS	8.53	0.66	0.0851
GO- Guanidine	10.70	0.76	0.0975
GO- Method 2	27.79	1.23	0.1817
GO-APTES	12.88	0.91	0.1153
GO- TRIS	8.36	0.58	0.0784
GO- Guanidine	10.09	0.70	0.0950
GO-1- CTAB	84.54	3.98	0.3691
GO-1- CTAB-PEI	51.37	2.60	0.3072
GO-1- P123	72.35	3.01	0.3101
GO-1- P123- PEI	49.37	2.24	0.2982

Chapter 5

CO_2 ADSORPTION STUDIES

INTRODUCTION

This chapter describes CO_2 adsorption studies performed on graphene oxide and amine-functionalized GO conducted by thermogravimetric analysis. GO and the modified GO supports were evaluated through the adsorption capacity of CO_2. The adsorption capacity of the materials was optimized by changing the experimental conditions presented in Table 3. The adsorption-desorption recycling application was conducted via a three cycle process lasting 8 hours. This represented successful regeneration of adsorbents. The duration of one adsorption-desorption cycle was approximately 1.5 hours. N_2 gas was used as a carrier gas to sweep away the CO_2 that was physically adsorbed by the adsorbent. N_2 was chosen because it is an inert gas and will not react with the adsorbent. On the desorption step, thermal decomposition of surface carbonates occurred. Carbon dioxide when passing through water reacts to form surface carbonate salts enabling an easier and faster reaction. The bonding between CO_2 and the adsorbents occurs via ionic bonding which is a relatively weak bond and hence can easily be broken during the desorption process.

Table 3: Experimental condition for CO_2 adsorption

Entry	Purge gas	Temperature (°C)	Period (min)	Gas flow (ml/min)
1	Nitrogen	40 to 200	16	50
2	Nitrogen	200 (isotherm)	120	
3	Nitrogen	200 to 40	16	
4	CO_2	40	60	10
5	Nitrogen	40 to 200	16	50

The adsorption capacity was calculated according to the equations 1 and 2

$$CO_2 \text{ adsorption capacity in mg/g} = \frac{We\ (mg) - Wi\ (mg)}{Wi\ (mg)} \quad (1)$$

$$CO_2 \text{ adsorption capacity in mmol/g} = \frac{We\ (mg) - Wi\ (mg)}{Wi\ (g) Mm\ CO_2} \quad (2)$$

W_e and W_i are the amounts of adsorbent in mg before and after adsorption respectively, and Mm is the molar weight (g/mol) of the CO_2 molecule.

5.1 Adsorption capacity of synthesized GO by different methods

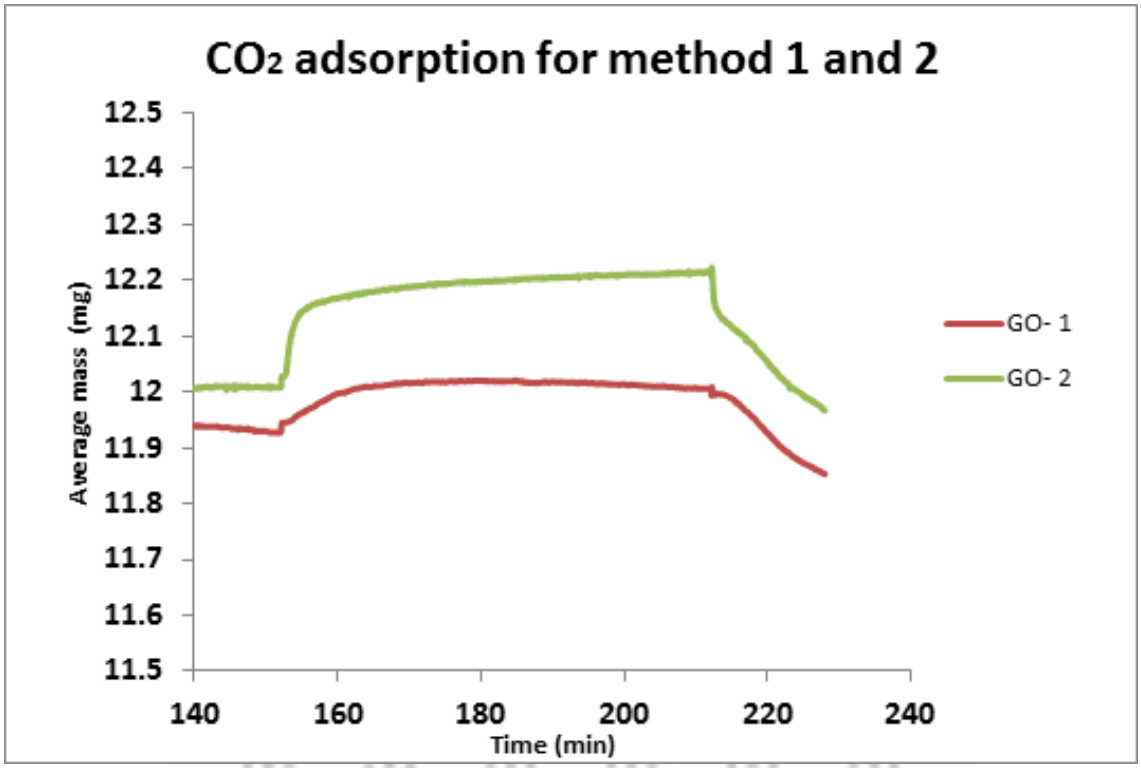

Figure 25: CO_2 adsorption of synthesized GO via two methods

The CO_2 adsorption capacity of GO was measured by the changes in weight, in relation to changes in time. Figure 25 displays the CO_2 adsorption isotherms for GO employing different synthesis methods. The thermal analysis was conducted for 4 hours. Thermal treatment step was necessary to remove moisture from the samples. Method 1 (support) shows the highest adsorption capacity of 0.070 mg/g compared to method 2 with a CO_2 adsorption of 0.067 mg/g. The adsorption of CO_2 in the support materials was sharp, followed by a quick desorption, with a high flow rate of nitrogen. CO_2 interacted with available adsorption sites of GO without compromising the sorption in the pore channels. In light of the easy sorption of CO_2 in GO, it could be concluded that GO supports are relatively weak adsorbents. The difference in the synthetic approaches are described in Chapter 3. The addition of $NaNO_3$ in method 1 was found to have slightly

increased the interlayer distance of GO i.e. more oxygen containing functional groups were introduced in the GO structure, influencing the degree of oxidation. The addition of H_2O_2 was employed to remove manganese salts and to break manganese ester bonds which are formed during the oxidation process [135]. It is presumed that strong oxidizing agents could influence the formation of carboxylic acids at the edges of GO sheets as well as the sonication process which cause defects in the GO structure increasing the interlayer spaces [136]. Furthermore, the differences in synthetic methods influenced the adsorption capacity of CO_2. Table 4 displays a summary of the adsorption capacity for GO.

In conclusion the addition of $NaNO_3$ proved to increase the adsorption capacity of GO-1, which was evident in the sorption studies performed. It could be concluded that GO supports are relatively weak adsorbents and this was corroborated by studies conducted by Hong *et al.,* who reported a CO_2 adsorption capacity of 0.074 mol/kg for GO, conducted in two different research investigations [137,138].

Table 4: Adsorption capacity of GO

	As-synthesized compounds	**CO_2 adsorption capacity (mg)**	**CO_2 adsorption capacity (mmol/g)**
1	Method 1- GO support	12.029	0.070
2	Method 2- GO support	11.928	0.067

5.2 Adsorption capacity of functionalized GO

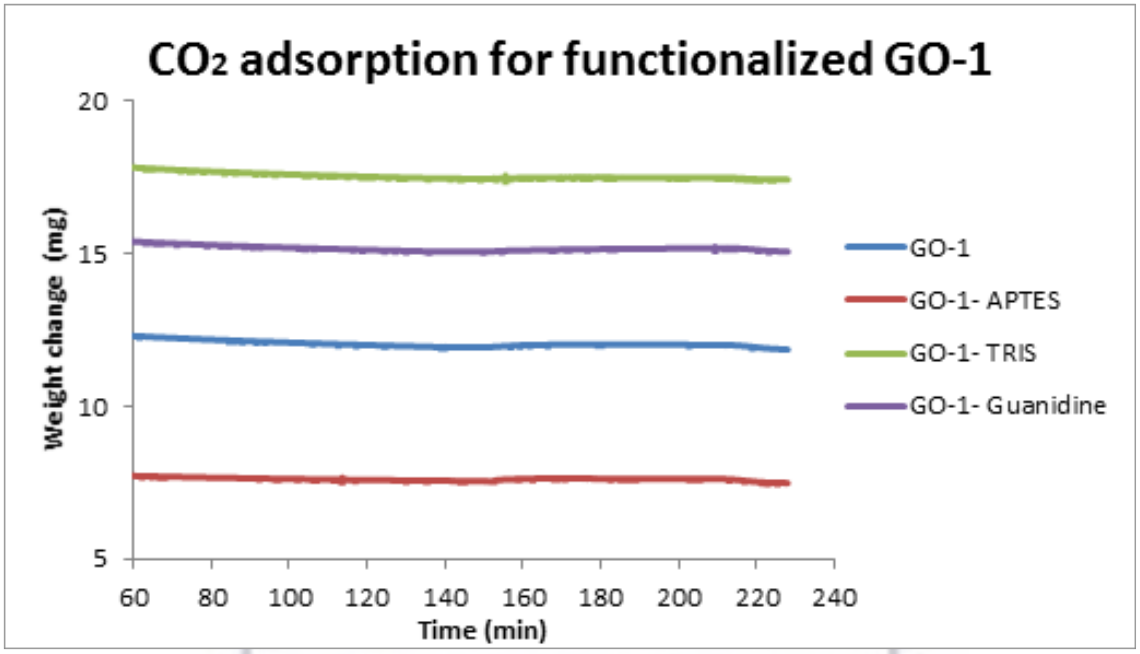

Figure 26: Adsorption capacity for the functionalized GO- method 1

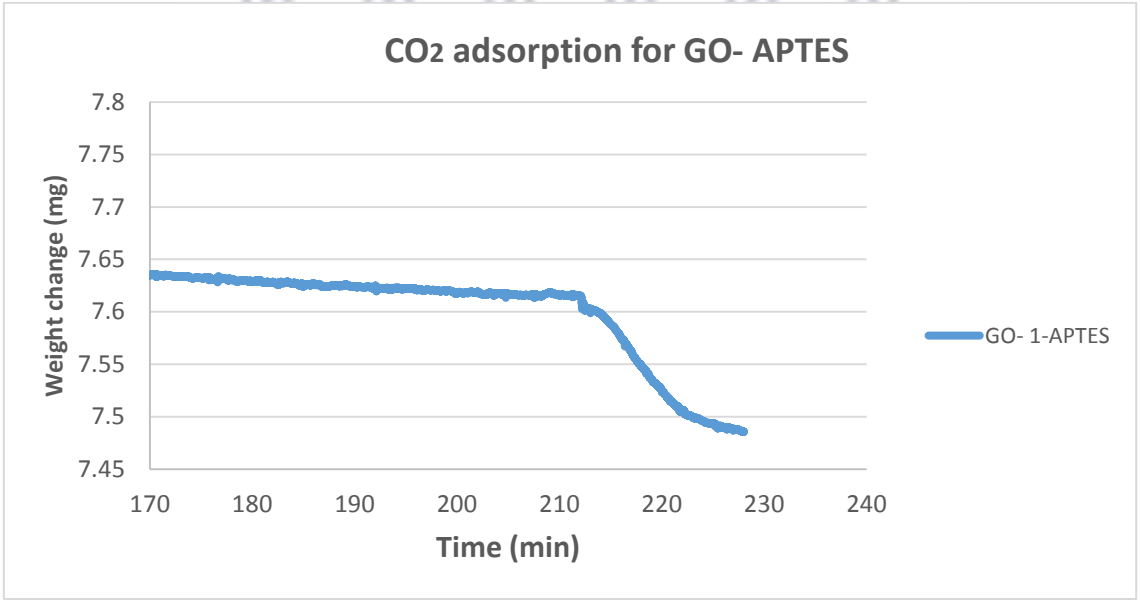

Figure 27: Adsorption capacity for the functionalized GO-APTES

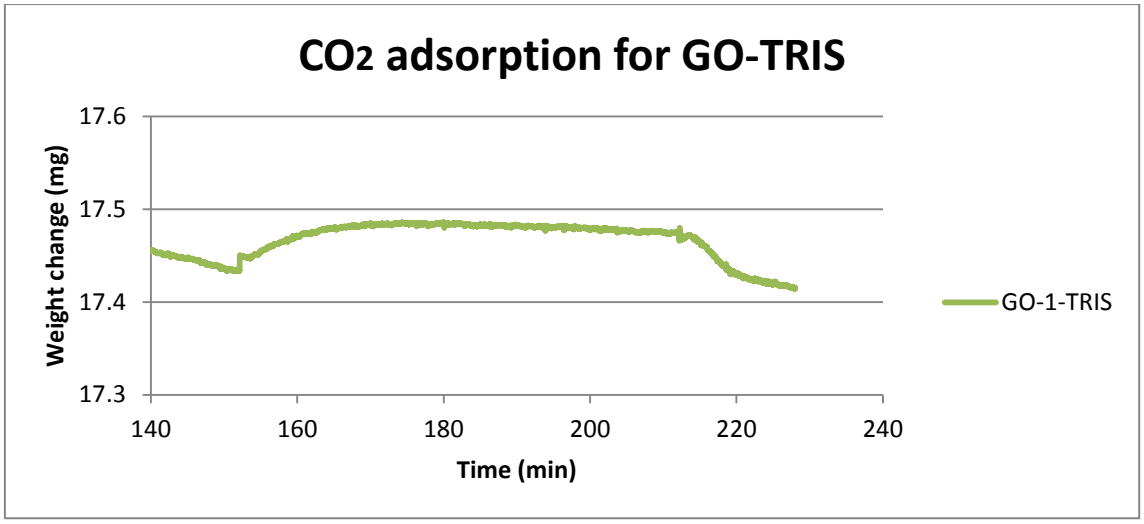

Figure 28: Adsorption capacity for the functionalized GO-TRIS

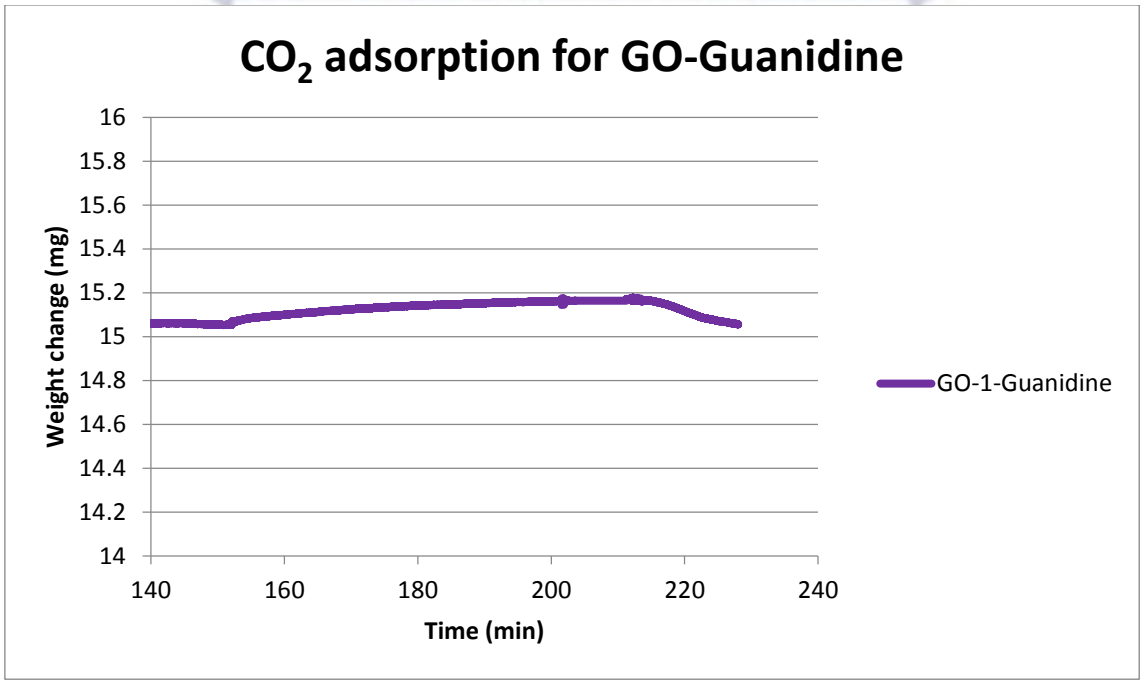

Figure 29: Adsorption capacity for the functionalized GO-Guanidine

Figure 26 displays the CO_2 adsorption uptake for as-synthesized GO functionalized with various aminosilanes. The thermogram graphs displayed are for 4 hours. The adsorption capacities of as-synthesized functionalized materials were determined from the change in mass during the adsorption step. The results of GO-method 1 and its functionalized derivatives are shown in Figure 26 and the expanded individual graphs are shown from Figures 27-29. The four TGA curves indicated in Figure 26 indicate the compounds start to lose weight upon heating under N_2 atmosphere below 100°C. The isothermal step (200 °C) ensured that physisorbed water was removed. The weight loss observed as the temperature ramp increased was due to the decomposition of the grafted organic molecules. As the temperature increases GO is unstable and exhibits decomposition behaviour because of labile oxygen containing functional moieties such as epoxy, hydroxyl, and carboxyl. For functionalized GO, labile O-containing functional groups are converted to other functional groups such as Si–O–Si/Si–O–C bands for APTES, TRIS and Guanidine due to partial chemical reduction [139]. The functionalized GO results indicate the compounds have better thermal stability in comparison with the parent GO. Table 5 displays a summary of the adsorption capacities for as-synthesized functionalized GO.

APTES linker is a widely used grafting agent and has been reported in literature. Hong *et al.* reported CO_2 adsorption capacity for APTES-GO to be 1.16 mol/kg [56] and 1.64 mol/kg [138]. APTES and Guanidine functionalized supports have a slightly higher adsorption capacity in comparison to TRIS functionalized sorbent. The adsorption capacities were found to be 0.9760, 0.1386 and 0.5781 mg/g for APTES, TRIS and Guanidine, respectively. Enhanced adsorption capacity could be attributed to the number of amine groups available on the surface and inside the pores, providing more adsorption sites for CO_2 to interact [140]. This was confirmed by the pore volume,

Table 2, for the respective aminosilanes. The pore volume for APTES, TRIS and Guanidine were 0.129041, 0.085131 and 0.097492 cm^3/g respectively. The facilitation of gas diffusion proves that functionalization with amine groups increases the CO_2 uptake [91]. However, GO- TRIS and GO-Guanidine adsorption capacity in comparison to GO-APTES showed a decrease in adsorption capacity. Zhao *et al.* postulated that amines with shorter chain lengths intercalate the GO layers with less difficulty than its longer chain counterparts. The latter could be due to the long amine chains that block the interlayers, preventing further intercalation of GO and thus reducing the amount of oxygen containing groups reacting with aminosilane. One of the other reasons could be attributed to the difference in adsorption energies for CO_2 by amine groups with longer chains. CO_2 adsorption capacity of aminated GO can be increased through the introduction of more basic nitrogen functionalities into the GO surface and interlamination. If the oxidation ratio of graphite is increased, the amount of amine groups introduced could grow [95].

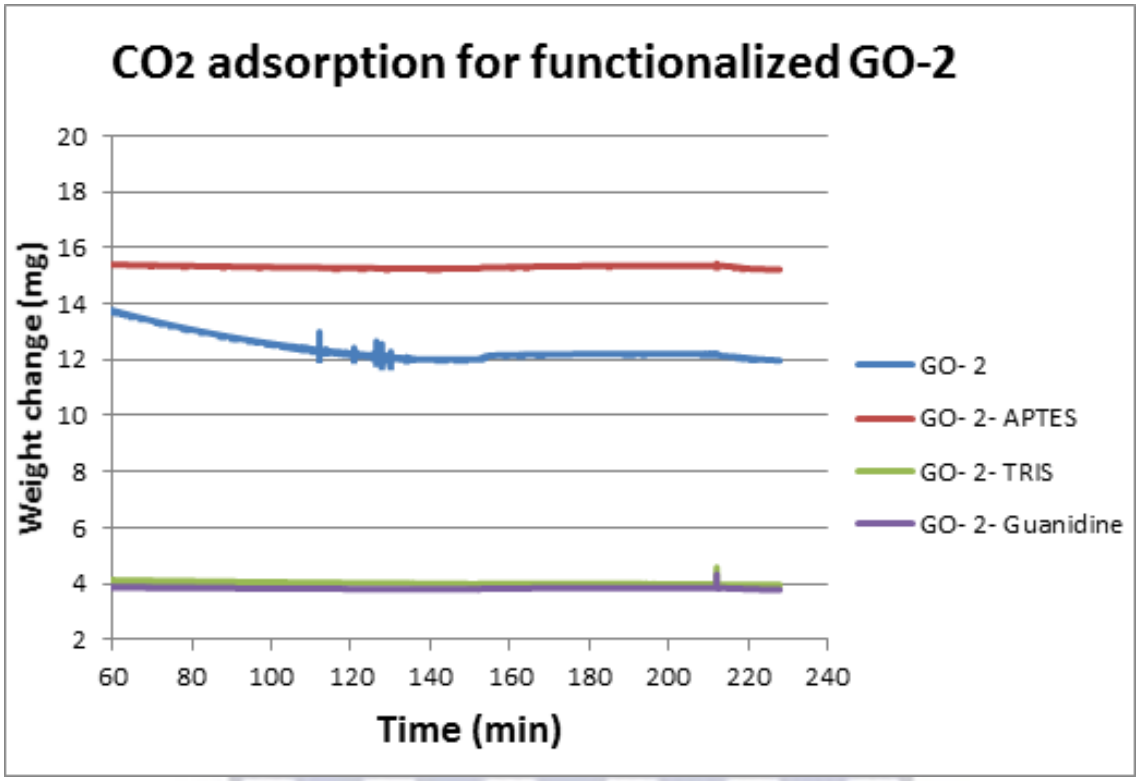

Figure 30: Adsorption capacity for functionalized GO-method 2

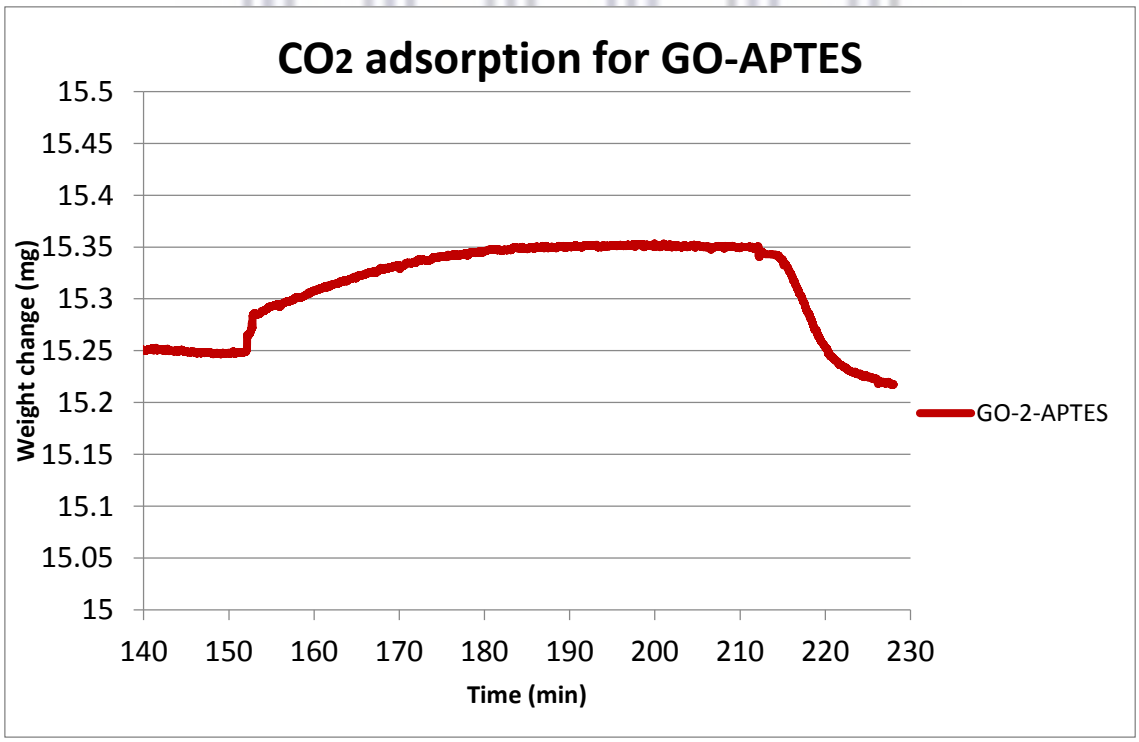

Figure 31: Adsorption capacity for functionalized GO-APTES

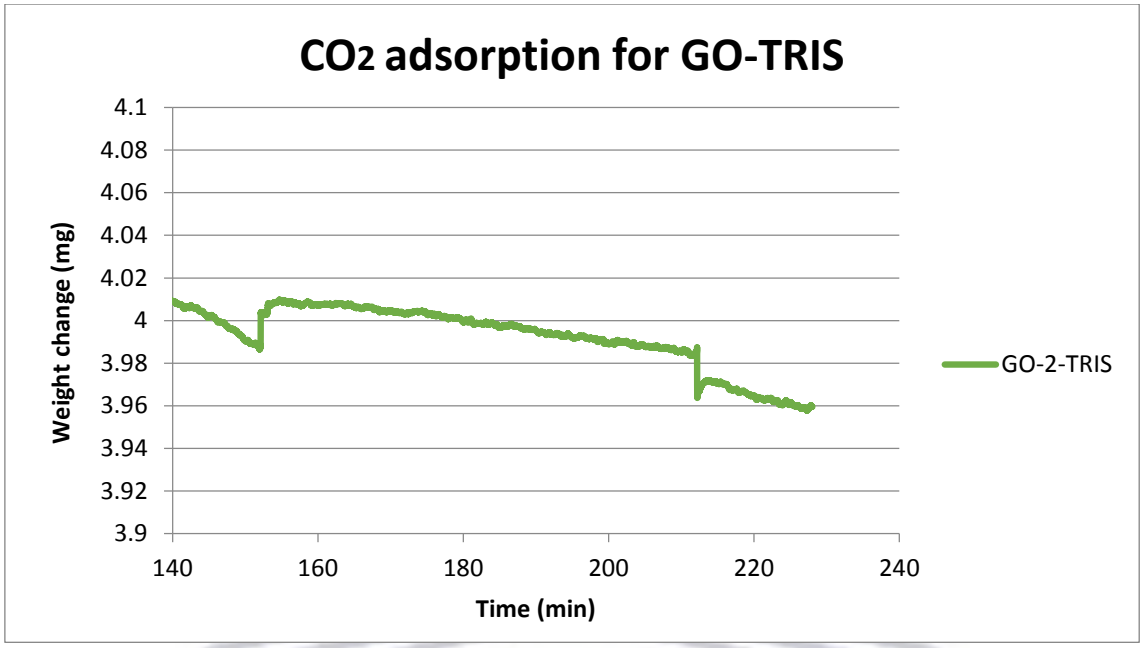

Figure 32: Adsorption capacity for functionalized GO-TRIS

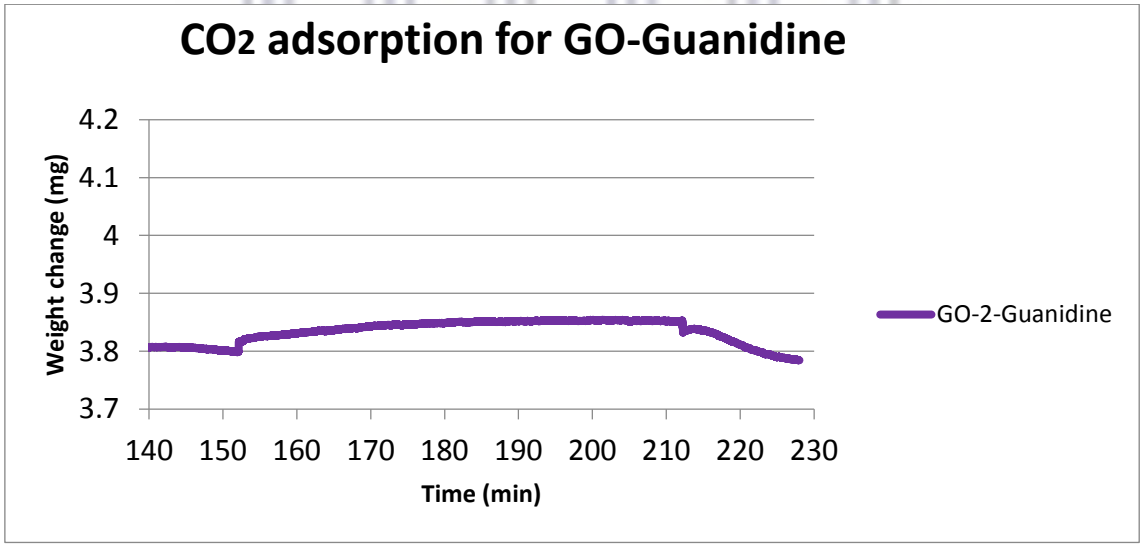

Figure 33: Adsorption capacity for functionalized GO- Guanidine

Figure 30 and the expanded individual graphs are shown in Figures 31-33 representing the adsorption-desorption isotherms of the aminosilanes functionalized onto GO-2. The isothermal treatment step is necessary to remove moisture from the samples. Silanol groups attached to APTES react with the OH groups on the GO surface. GO-2 functionalized with APTES, TRIS and guanidine have lower adsorption capacities as compared to GO-1. The adsorption capacities were 0.8245, 0.1223 and 0.4618 mg/g, respectively and can be seen in Table 5 and the respective pore volumes displayed in Table 2 were 0.1153, 0.0784 and 0.0950 cm^3/g for APTES, TRIS and Guanidine respectively. As mentioned previously, the removal of $NaNO_3$ could have influenced the amount of oxygen containing functional groups introduced in the GO layer. The reduced hydrophilic oxygen containing functional groups on the basal plane of GO sheets affect the functionalization of aminosilanes. Silylation reactions of GO have been investigated by Matsuo *et al..*, who found that the reaction between the hydroxyl groups of GO and the ethoxy groups of aminosilanes form Si–O bonding. Therefore, the number of silane reactions between aminosilanes and GO is directly proportional to the available oxygen sites on the GO surface structure. Specific precursors in the synthesis reaction can influence the amount of amine groups introduced into the GO structure which could also affect the ratio of oxidation [140]. Chemisorption of CO_2 on the amino sites of aminated GO seems to be the main adsorption mechanism. Primary and secondary amines readily react with CO_2 and form carbamates. GO-2 TRIS and Guanidine have slightly lower CO_2 adsorption capacities as compared to GO-2-APTES. This could be attributed to the length of the organic molecular aminosilane chains. Steric hindrance caused by longer amine chain lengths can negatively affect CO_2 adsorption [95]. The increase in CO_2 absorptivity is directly proportional to the active primary amine sites. The formation of carbamates is dependent on the grafting of

aminosilanes to GO carbonaceous materials. The lone pair of electrons on the –N atom of $–NH_2$ is involved in the interaction with CO_2 molecules. When NH_2 and CO_2 react, nucleophilic substitution occurs between the lone pairs and the –C atom, resulting in the formation of carbamates through carboxyl interactions. Hydrogen bonding takes place between the -H atom (from the carboxyl group) and surrounding amine groups generating chemisorption with CO_2. Typically, one mole of CO_2 should react with two moles of $–NH_2$ to produce a stable product. However, it needs to be mentioned that there is a lack of insight and comprehensive understanding between surface functional groups and the carbon surface due to their intricate behavioural properties [61].

Table 5: Adsorption capacities for functionalized GO

	As- synthesized compounds	**CO_2 adsorption capacity (mg)**	**CO_2 adsorption capacity (mmol/g)**
1	Method 1- GO (APTES)	16.539	0.9760
2	Method 1- GO (TRIS)	12.433	0.1386
3	Method 1- GO (Guanidine)	15.069	0.5781
4	Method 2- GO (APTES)	15.249	0.8245
5	Method 2- GO (TRIS)	10.987	0.1223
6	Method 2- GO (Guanidine)	11.798	0.4618

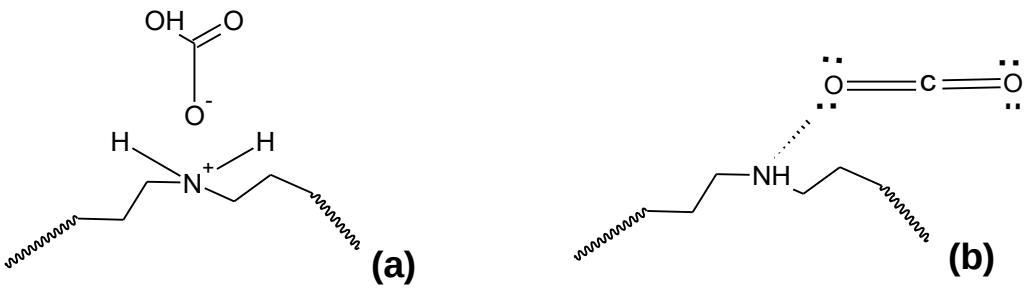

Figure 34: Wet adsorption (a) and Dry adsorption (b)

CO_2 adsorption processes can either take place under wet or dry adsorption conditions. Figure 34-a depicts adsorption which takes place with moisture (wet adsorption) and Figure 34-b is illustrative without moisture (dry adsorption). When water is included during the CO_2 adsorption uptake, CO_2 reacts with water to form carbonic acid. The carbonic acid protonates the amino group forming ammonium salts. This reaction takes place through ionic bonding which can be categorized as strong bonds. When CO_2 adsorption takes place without any moisture, the only possibility of bonding is through hydrogen bonding due to the C=O bond of CO_2 being polar. This is a relatively weak bond compared to ionic bonding in wet adsorption (Figure 34-b). In this study no moisture was introduced during the adsorption uptake and the lack of moisture could have contributed to the low CO_2 adsorption capacities for GO-supports and functionalized GO [141].

5.3 Adsorption of functionalized mesoporous GO

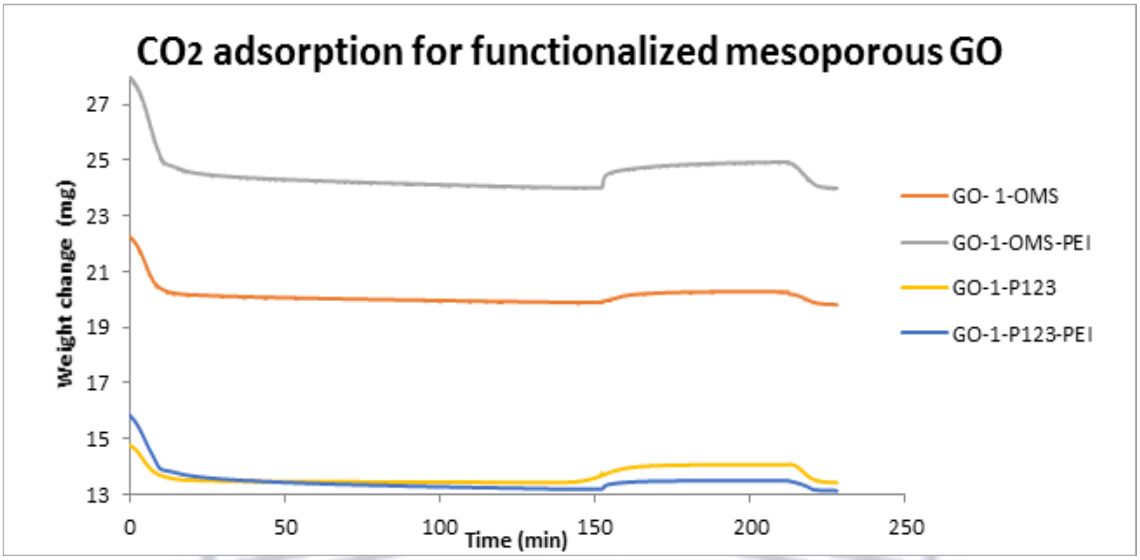

Figure 35: Adsorption of GO mesoporous/ mesoporous polymer

Figure 35 displays the CO_2 adsorption isotherms for GO siliceous materials (CTAB and P123) functionalized with PEI. Employing surfactants in a carbonaceous framework has the ability to solve the issue of hydrophobic/hydrophilic incompatibility problems, but also provides the molecular template for controlled nucleation and growth of nanostructured inorganics [142]. GO's rich intercalation chemistry enables the accommodation of inorganic and organic species into its interlayer space. This allows for the possible formation of a nanoporous material species into the interlayer space of GO by chemical methods. In this study we formed a nanoporous graphitic composite by incorporating active species, surfactant (CTAB) and a co- block polymer (P123) between the exfoliated GO layers. There exists two possibilities which dictate the interaction between GO, the co- block polymer and solvent. The block polymer could first form micelles and then adsorb on the GO sheet surface or the block copolymer chains adsorb onto the GO sheets and then aggregate together. GO consists of carbon atoms linked through sp_2 bonds and have an abundance of oxygen-containing functional

groups. P123 is comprised of poly(ethylene oxide) (PEO) which interact robustly with the oxygen-containing functional groups of GO. This inhibits the movement of the molecular chains which could lead to block copolymer phase separation. PEO contains a large number of OH groups which can be modified with various functional groups. The modification of GO-P123 can form multifunctional nanohybrid structures [21]. GO was fabricated with TEOS on the surface of GO with the aid of a cationic surfactant, CTAB. The GO-silica composites were functionalized with PEI [142]. The morphological studies via SEM (Figures 14 and 15) showed that GO-CTAB/P123 structures are characteristic of an ordered mesoporous structure. There are two types of polyethylenimine viz., linear and branched. Linear polyethylenimine contains only secondary amine groups, while branched polyethylenimine contains primary, secondary, and tertiary amine groups. In this study hyper branched PEI was employed [99]. PEI possesses a high amine density. The reaction between silica and PEI forms a silica/PEI composite and has the potential to exhibit good adsorption capacity for CO_2 [101]

PEI reacts through the silica layer. The OH functional groups in the silica walls interacts with $–NH_2$ functional groups in PEI via hydrogen bonds. These bonds form strong adhesion PEI-silica interfaces [101]. The primary and secondary amines of PEI can undergo a reversible reaction with CO_2 increasing the reaction selectivity [9]. The CO_2 adsorption for GO-CTAB/P123 and GO/Silica amine functionalized composites viz. GO-CTAB, GO-CTAB-PEI, GO-P123 and GO-P123-PEI were 0.45, 0.91, 0.39 and 0.45 mmol/g, respectively displayed in Table 6. It can be noted that the adsorption capacity of GO/silica increased on functionalization with an amine moiety.

Yang and co-workers studied the modification of GO-Silica PEI composites. The CO_2 adsorption capacity reported for PEI-GO/silica was 171 $mg.g^{-1}$ [99]. Research conducted by Sayari *et al.* discovered that primary amines grafted onto OMS exhibit

higher CO_2 adsorption capacities compared to secondary amines; and tertiary had almost no effect. These characteristics were interesting to note, because the basicities of secondary and tertiary amines are higher than that of the primary amines [143]. This could be a contributing factor to the higher adsorption capacity of GO-OMS- PEI compared to GO-P123-PEI.

Table 6: Adsorption capacity of mesoporous GO

	As- synthesized compounds	CO_2 adsorption capacity (mg/g)	CO_2 adsorption capacity (mmol/g)
1	Method 1- GO- P123	17.25	0.39
2	Method 1- GO-CTAB	19.88	0.45
3	Method 1- GO-P123-PEI	17.82	0.40
4	Method 1- GO- CTAB-PEI	40.04	0.91

5.4 Recycling of the adsorbents

The regenerability and stability of the adsorbents viz. GO-APTES, GO-CTAB-PEI and GO-P123-PEI, were the representative materials investigated. The recycling process was studied for three adsorption-desorption cycles (Figures 36-39) which indicated a slight decay of the adsorbent which could be coupled to a loss of material. The adsorption/ desorption cycles were repeated three times with no noticeable decrease in the adsorption capacity. The cyclic adsorption-desorption process also indicated that the above adsorbents have good durability [144]

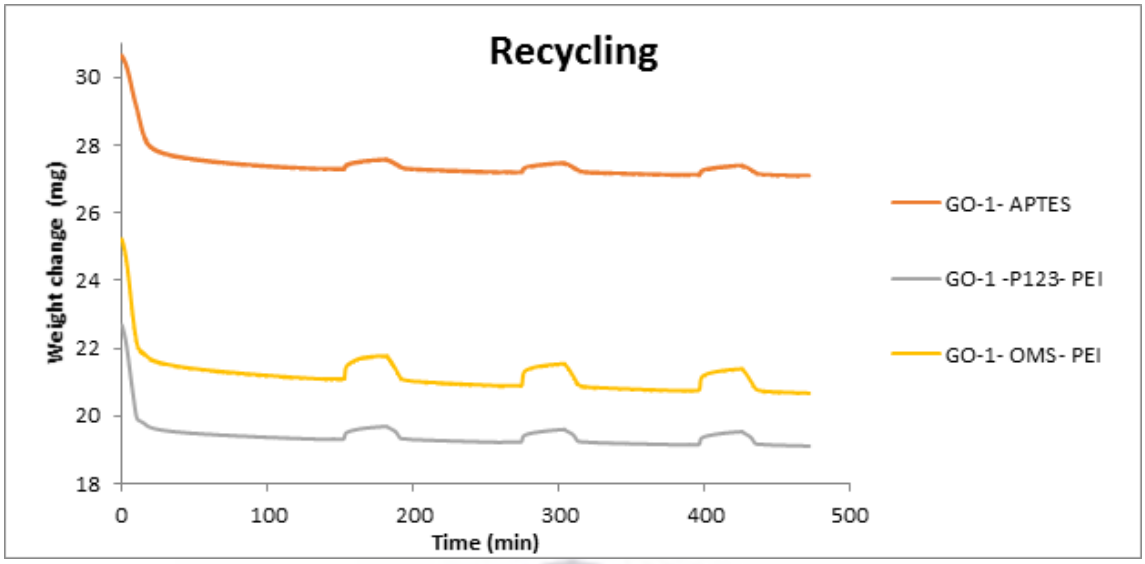

Figure 36: Cyclic adsorption/desorption of GO-APTES, GO-P123-PEI and GO-CTAB-P123

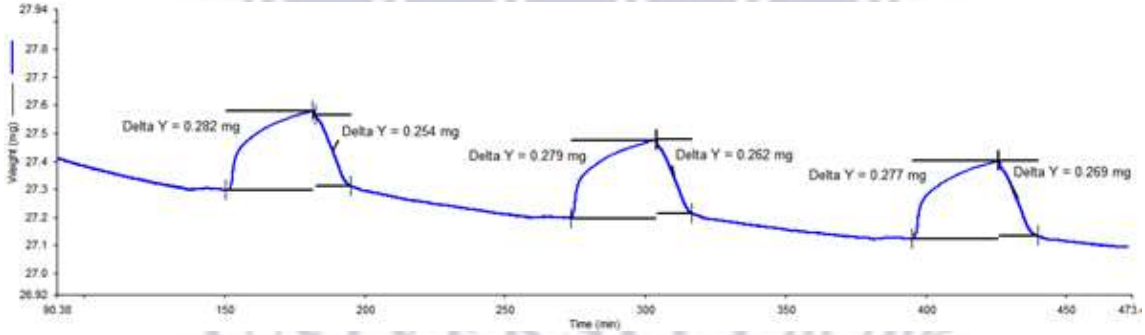

Figure 37: Displays the cyclic adsorption-desorption measurements of CO_2, observed for GO-APTES

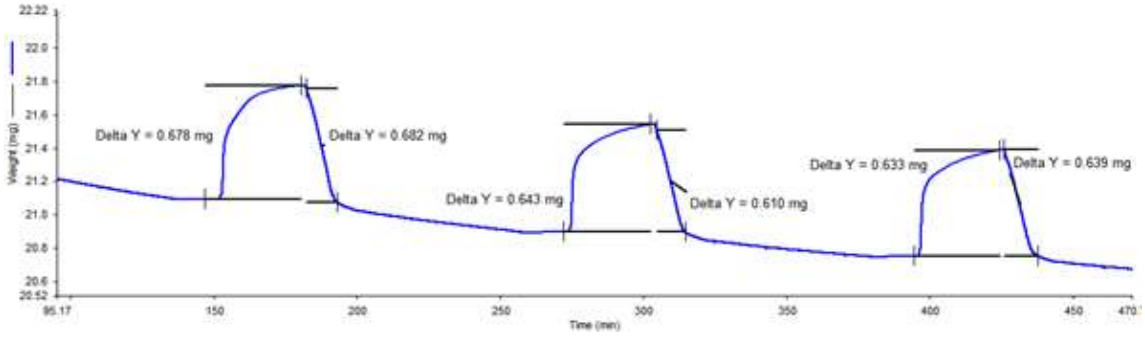

Figure 38: Displays the cyclic adsorption-desorption measurements of CO_2, observed for GO-CTAB-PEI

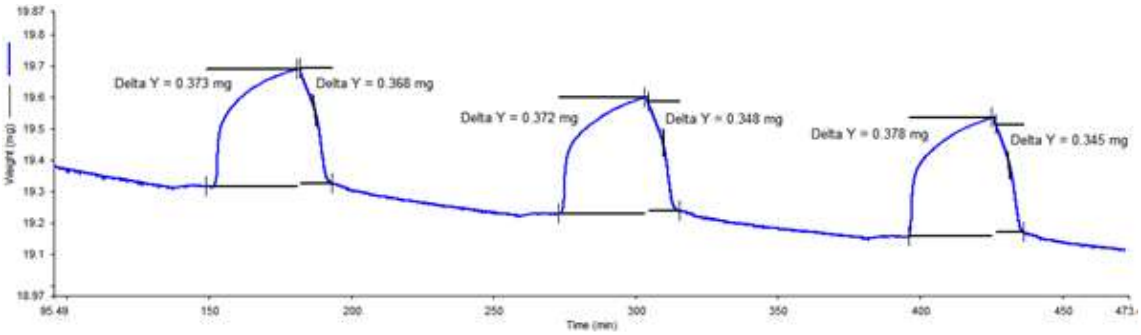

Figure 39: Displays the cyclic adsorption-desorption measurements of CO_2, observed for GO-P13-PEI

During all three adsorption/ desorption cycles for GO-APTES (Figure 36); the adsorption step is more than the desorption step. This could be attributed to pore blocking during gas diffusion of CO_2 in the porous material. This is seen for GO-CTAB-PEI and GO-P123-PEI. Results showed that the performance of adsorbents were stable, with only a slight decrease in capacity. The slight decrease could be attributed to some loss of PEI coated on the surface of GO [145]. In our study, the adsorption took place in the absence of any moisture, however it has been shown that the presence of water generally increases the CO_2 adsorption capacity of amines by allowing the formation of bicarbonates. In this case, only one amino group is necessary for every CO_2 molecule instead of two in the case of carbamate formation in the absence of water [146].

Chapter 6

6.1 Conclusion

In this study graphite was successfully oxidized to graphene oxide using two different synthetic routes. GO was successfully modified with three aminosilanes (APTES, TRIS and Guanidine) and to the best of our knowledge TRIS and Guanidine were employed for the first time to functionalize GO for CO_2 sequestration. The ordered mesoporous as-synthesized functionalized GO materials were characterized using XRD, FTIR, HRSEM, HRTEM, N_2 Physisorption (BET) and TGA. The BET surface area of GO-method 1 was 29.56 m^2/g and GO-method 2 was 27.79 m^2/g. The reduced surface area for method 2 could be attributed to the absence of $NaNO_3$ causing less oxidation, resulting in less oxygen containing functional groups and hence a lower surface area. Textural properties revealed that the functionalization process led to a decrease in specific area, pore volume and pore size, which was brought about by partial pore filling by organic molecules (aminosilanes). Powder XRD patterns showed that post modification of GO resulted in the structural integrity of the supports remaining unchanged, with a slight decrease in intensity of diffraction patterns. The total N_2 uptake was reduced but the isotherms still displayed type IV isotherms according to the IUPAC classification, owing to the mesoporous character of the GO modified with OMS. TG studies of APTES, TRIS and Guanidine functionalized by methods 1 and 2 and displayed weight loss attributed to the decomposition of organic molecules (APTES, TRIS and Guanidine) that were functionalized on the GO supports. FT-IR spectra confirmed the presence of hydroxyl groups (-OH), alkoxy groups (C-O), epoxy groups (C-O), aromatic groups (C=C) and carboxyl groups (C=O) for GO. It also confirmed the presence of C-H stretching vibrations of propyl chains of APTES and TRIS. The presence of asymmetric NH_2 stretching, symmetric NH_2 stretching and NH_2

deformation of hydrogen bonded amino groups as well as the C=N stretching vibration also confirmed the functionalization of APTES, TRIS and Guanidine on GO supports and was thus carried out successfully. In this work, PEI with high amine density has been chosen as the cross-linking agent to interact with GO-OMS sheets. The FT-IR spectra confirmed the presence of the stretching, bending and out of plane of Si—O bonds for PEI/GO-OMS and GO-OMS as well as the stretching vibration of amide groups suggesting that PEI was linked to GO. SEM and TEM results showed that GO-OMS exhibited a long range order mesoporous structure.

In summary, we have demonstrated an efficient amine-based solid adsorbent for CO_2 capture based on GO-APTES/TRIS/Guanidine as well as PEI/G-silica materials. The unique features of the as-synthesized functionalized materials proved to be favourable for CO_2 adsorption. Consequently, PEI/GO-silica materials exhibited a higher CO_2 adsorption compared to GO-APTES/TRIS/Guanidine. The three selected materials (GO-1-APTES, GO-CTAB,-PEI and GO-P123-PEI) employed to demonstrate regenerability exhibited good cycle stability. The results of this study shed light on the utility of graphene as a starting material to achieve promising adsorption functionality.

6.2 Recommendations and future work

Further studies would investigate the effect temperature and moisture has on the adsorption capacity of as-prepared solid sorbents. Changing synthetic parameters to establish the optimal condition for the synthetic process would form a focused part of this process as well. A real model comprising a CO_2 effluent gas generating entity with a higher concentration of CO_2 should be studied to determine the behaviour of solid sorbents under these very real conditions.

References

1. Gohar, L. & Shine, K. 2007, "Equivalent CO_2 and its use in understanding the climate effects of increased greenhouse gas concentrations", Weather, vol. 62, no. 11, pp. 307-311.
2. Rowland, F.S. 2000, "Atmospheric changes caused by human activities: From science to regulation", Ecology LQ, vol. 27, pp. 1261.
3. Samanta, A., Zhao, A., Shimizu, G.K., Sarkar, P. & Gupta, R. 2011, "Post-combustion CO_2 capture using solid sorbents: a review", Industrial & Engineering Chemistry Research, vol. 51, no. 4, pp. 1438-1463.
4. Urban Earth 2012, February 2012-last update, South African Carbon Snapshot. Available: http://www.climatefruitandwine.co.za/download/Urban%20Earth_SA%2^{o}Carbon%20Snapshot.pdf [2012, February].
5. IETA Climate Changes Market Solutions May 2015, South Africa.
6. Wackernagel, M. & Rees, W. 1998, Our ecological footprint: reducing human impact on the earth, New Society Publishers.
7. Lee, Z.H., Lee, K.T., Bhatia, S. & Mohamed, A.R. 2012, "Post-combustion carbon dioxide capture: Evolution towards utilization of nanomaterials", Renewable and Sustainable Energy Reviews, vol. 16, no. 5, pp. 2599-2609.
8. Sharma, B. & Sharma, D. 2008, "Impact of climate change on water resources and glacier melt and potential adaptations for Indian agriculture", New Dehli: International Water Management Institute
9. Adam, D. 2008, Climate change 'making seas more salty', Climate Change edn, The Guardian
10. Huddleston, N. & Moghari, F. 2012, Climate ChangeEvidence, Impacts, and Choices and answers to common questions about the science of climate change, The National Research Council of The National Academies.
11. Songolzadeh, M., Ravanchi, M.T. & Soleimani, M. 2012, "Carbon dioxide capture and storage: a general review on adsorbents", World Academy of Science, Engineering and Technology, vol. 70, pp. 225-232.
12. Songolzadeh, M., Soleimani, M., Takht Ravanchi, M. & Songolzadeh, R. 2014, "Carbon dioxide separation from flue gases: a technological review emphasizing reduction in greenhouse gas emissions", The Scientific World Journal, vol. 2014, pp. 828131.
13. Jiménez, V., Ramírez-Lucas, A., Díaz, J.A., Sánchez, P. & Romero, A. 2012, "CO_2 capture in different carbon materials", Environmental science & technology, vol. 46, no. 13, pp. 7407-7414.
14. Figueroa, J.D., Fout, T., Plasynski, S., McIlvried, H. & Srivastava, R.D. 2008, "Advances in CO_2 capture technology—the US Department of Energy's Carbon Sequestration Program", International journal of greenhouse gas control, vol. 2, no. 1, pp. 9-20.
15. Su, C. & Loh, K.P. 2012, "Carbocatalysts: graphene oxide and its derivatives", Accounts of Chemical Research, vol. 46, no. 10, pp. 2275-2285.

16. Ruiz-Hitzky, E. & Rojo, J. 1980, "Intracrystalline grafting on layer silicic acids", Nature, vol. 287, pp. 28-30.

17. Yu, D. & Dai, L. 2009, "Self-assembled graphene/carbon nanotube hybrid films for supercapacitors", The Journal of Physical Chemistry Letters, vol. 1, no. 2, pp. 467-470.

18. Parida, K.M. & Rath, D. 2009, "Amine functionalized MCM-41: An active and reusable catalyst for Knoevenagel condensation reaction", Journal of Molecular Catalysis A: Chemical, vol. 310, no. 1, pp. 93-100.

19. Yang, S., Feng, X., Wang, L., Tang, K., Maier, J. & Müllen, K. 2010, "Graphene-Based Nanosheets with a Sandwich Structure", Angewandte Chemie, vol. 122, no. 28, pp. 4905-4909.

20. Wang, X., Pei, Y., Lu, M., Lu, X. & Du, X. 2015, "Highly efficient adsorption of heavy metals from wastewaters by graphene oxide-ordered mesoporous silica materials", Journal of Materials Science, vol. 50, no. 5, pp. 2113-2121.

21. Machado, B.F. & Serp, P. 2012, "Graphene-based materials for catalysis", Catalysis Science & Technology, vol. 2, no. 1, pp. 54-75

22. Dreyer, D.R., Park, S., Bielawski, C.W. & Ruoff, R.S. 2010, "The chemistry of graphene oxide", Chemical Society Reviews, vol. 39, no. 1, pp. 228-240

23. Huang, D., Wang, X., Deng, C., Song, G., Cheng, H. and Zhang, X., 2014. Facile preparation of raisin-bread sandwich-structured magnetic graphene/mesoporous silica composites with C18-modified pore-walls for efficient enrichment of phthalates in environmental water. Journal of Chromatography A, 1325, pp.65-71.

24. Merkel, T.C., Lin, H., Wei, X. & Baker, R. 2010, "Power plant post-combustion carbon dioxide capture: an opportunity for membranes", *Journal of Membrane Science,* vol. 359, no. 1, pp. 126-139.

25. Bennaceur, K., Gielen, D., Kerr, T. & Tam, C. 2008, CO_2 capture and storage: a key carbon abatement option, OECD.

26. Klass, A.B. & Wilson, E.J. 2008, "Climate change and carbon sequestration: Assessing a liability regime for long-term storage of carbon dioxide"

27. Zaman, M. & Lee, J.H. 2013, "Carbon capture from stationary power generation sources: A review of the current status of the technologies", Korean Journal of Chemical Engineering, vol. 30, no. 8, pp. 1497-1526.

28. Yang, H., Xu, Z., Fan, M., Gupta, R., Slimane, R.B., Bland, A.E. & Wright, I. 2008, "Progress in carbon dioxide separation and capture: A review", Journal of Environmental Sciences, vol. 20, no. 1, pp. 14-27.

29. Kunze, C. & Spliethoff, H. 2012, "Assessment of oxy-fuel, pre-and post-combustion-based carbon capture for future IGCC plants", Applied Energy, vol. 94, pp. 109-116.

30. Buhre, B., Elliott, L., Sheng, C., Gupta, R. & Wall, T. 2005, "Oxy-fuel combustion technology for coal-fired power generation", Progress in energy and combustion science, vol. 31, no. 4, pp. 283-307.

31. Toftegaard, M.B., Brix, J., Jensen, P.A., Glarborg, P. & Jensen, A.D. 2010, "Oxy-fuel combustion of solid fuels", Progress in energy and combustion science, vol. 36, no. 5, pp. 581-625.

32. Daraboina, N., Ripmeester, J. & Englezos, P. 2013, "The impact of SO_2 on post combustion carbon dioxide capture in bed of silica sand through hydrate formation", International Journal of Greenhouse Gas Control, vol. 15, pp. 97-103.

33. Wang, M., Lawal, A., Stephenson, P., Sidders, J. & Ramshaw, C. 2011, "Post-combustion CO_2 capture with chemical absorption: a state-of-the-art review", *Chemical Engineering Research and Design,* vol. 89, no. 9, pp. 1609-1624.

34. 34 Orr Jr, F.M. 2009, "CO_2 capture and storage: are we ready?", *Energy & Environmental Science,* vol. 2, no. 5, pp. 449-458.

35. Spigarelli, B.P. & Kawatra, S.K. 2013, "Opportunities and challenges in carbon dioxide capture", *Journal of CO_2 Utilization,* vol. 1, pp. 69-87.

36. Sreenivasulu, B., Gayatri, D., Sreedhar, I. & Raghavan, K. 2015, "A journey into the process and engineering aspects of carbon capture technologies", *Renewable and Sustainable Energy Reviews,* vol. 41, pp. 1324-1350.

37. Plaza, M., García, S., Rubiera, F., Pis, J. & Pevida, C. 2010, "Post-combustion CO_2 capture with a commercial activated carbon: comparison of different regeneration strategies", *Chemical Engineering Journal,* vol. 163, no. 1, pp. 41-47.

38. Shannon, M.S., Tedstone, J.M., Danielsen, S.P. & Bara, J.E. 2011, "Evaluation of alkylimidazoles as physical solvents for CO_2/CH_4 separation", *Industrial & Engineering Chemistry Research,* vol. 51, no. 1, pp. 515-522.

39. Rochelle, G.T. 2009, "Amine scrubbing for CO_2 capture", *Science (New York, N.Y.),* vol. 325, no. 5948, pp. 1652-1654.

40. Gao, J., Wang, S., Zhao, B., Qi, G. & Chen, C. 2011, "Pilot-scale experimental study on the CO_2 capture process with existing of SO_2: Degradation, reaction rate, and mass transfer", *Energy & Fuels,* vol. 25, no. 12, pp. 5802-5809.

41. Yeh, J.T., Resnik, K.P. & Pennline, H.W. 2004, "Regenerable aqua ammonia process for CO_2 sequestration", *Prepr. Pap.-Am. Chem. Soc. Div. Fuel Chem,* vol. 49, no. 1, pp. 247-248.

42. Olajire, A. 2013, "CO_2 capture by aqueous ammonia process in the clean development mechanism for Nigerian oil industry", *Frontiers of Chemical Science and Engineering,* vol. 7, no. 3, pp. 366-380.

43. Darted, V., Thomsen, K., van Well, W.J. & Stenby, E.H. 2009, "Aqueous ammonia process for CO_2 capture", *IOP Conference Series: Earth and Environmental Science*IOP Publishing, pp. 172017.

44. 44 Wolken, M.B. 2006, Process and apparatus for generating power, producing fertilizer, and sequestering, carbon dioxide using renewable biomass.

45. 45 Ciferno, J.P., DiPietro, P. & Tarka, T. 2005, "An economic scoping study for CO_2 capture using aqueous ammonia", *Final Report, National Energy Technology Laboratory, US Department of Energy, Pittsburgh, PA*.

46. Olajire, A.A. 2010, "CO_2 capture and separation technologies for end-of-pipe applications–a review", *Energy,* vol. 35, no. 6, pp. 2610-2628.

47. Chen, W., Chen, S. & Hung, C. 2013, "Carbon dioxide capture by single droplet using Selexol, Rectisol and water as absorbents: A theoretical approach", *Applied Energy,* vol. 111, pp. 731-741.

48. Tande, B., Seames, W. & Benson, S. 2013, Efficient Regeneration of Physical and Chemical Solvents for CO_2 Capture.

49. Pevida García, C., González Plaza, M., Arias Rozada, B., Fermoso Domínguez, J., Rubiera González, F. & Pis Martínez, J.J. 2007, "Nitrogen enriched solid sorbents for CO_2 capture".

50. Songolzadeh, M., Ravanchi, M.T. & Soleimani, M. 2012, "Carbon dioxide capture and storage: a general review on adsorbents", *World Academy of Science, Engineering and Technology,* vol. 70, pp. 225-232.

51. Choi, S., Drese, J.H. & Jones, C.W. 2009, "Adsorbent materials for carbon dioxide capture from large anthropogenic point sources", *ChemSusChem,* vol. 2, no. 9, pp. 796-854

52. Gregg, S.J., Sing, K.S.W. & Salzberg, H. 1967, "Adsorption surface area and porosity", *Journal of the Electrochemical Society,* vol. 114, no. 11, pp. 279C-279C.

53. Wang, J., Huang, L., Yang, R., Zhang, Z., Wu, J., Gao, Y., Wang, Q., O'Hare, D. and Zhong, Z., 2014. Recent advances in solid sorbents for CO_2 capture and new development trends. *Energy & Environmental Science*, *7*(11), pp.3478-3518

54. Smirniotis, P.G., Davydov, L. & Ruckenstein, E. 1999, "Composite zeolite-based catalysts and sorbents", *Catalysis Reviews,* vol. 41, no. 1, pp. 43-113

55. Liu, Q., Pham, T., Porosoff, M.D. & Lobo, R.F. 2012, "ZK-5: A CO_2-Selective Zeolite with High Working Capacity at Ambient Temperature and Pressure", *ChemSusChem,* vol. 5, no. 11, pp. 2237-2242.

56. Hong, S., Kim, S.H. & Lee, K.B. 2013, "Adsorption of Carbon Dioxide on 3-Aminopropyl-Triethoxysilane Modified Graphite Oxide", *Energy & Fuels,* vol. 27, no. 6, pp. 3358-3363.

57. Siriwardane, R.V., Shen, M., Fisher, E.P. & Losch, J. 2005, "Adsorption of CO_2 on zeolites at moderate temperatures", *Energy & Fuels,* vol. 19, no. 3, pp. 1153-1159.

58. Lee, K.B., Beaver, M.G., Caram, H.S. and Sircar, S., 2008. Reversible chemisorbents for carbon dioxide and their potential applications. *Industrial & Engineering Chemistry Research*, *47*(21), pp.8048-8062.

59. Hardie, S., Garnett, M., Fallick, A., Rowland, A. & Ostle, N. 2005, "Carbon Dioxide Capture Using a Zeolite Molecular Sieve Sampling System for Isotopic Studies (^ 1^ 3C and^ 1^ 4C) of Respiration", *Radiocarbon,* vol. 47, no. 3, pp. 441.

60. Chatti, R., Bansiwal, A.K., Thote, J.A., Kumar, V., Jadhav, P., Lokhande, S.K., Biniwale, R.B., Labhsetwar, N.K. and Rayalu, S.S., 2009. Amine loaded zeolites for carbon dioxide capture: Amine loading and adsorption studies. *Microporous and Mesoporous Materials*, *121*(1-3), pp.84-89.

61. Shafeeyan, M.S., Daud, Wan Mohd Ashri Wan, Houshmand, A. & Shamiri, A. 2010, "A review on surface modification of activated carbon for carbon dioxide adsorption", *Journal of Analytical and Applied Pyrolysis,* vol. 89, no. 2, pp. 143-151.

62. Qi, G., Wang, Y., Estevez, L., Duan, X., Anako, N., Park, A.A., Li, W., Jones, C.W. & Giannelis, E.P. 2011, "High efficiency nanocomposite sorbents for CO_2 capture based on amine-functionalized mesoporous capsules", *Energy & Environmental Science,* vol. 4, no. 2, pp. 444-452.

63. Liu, Y., Ye, Q., Shen, M., Shi, J., Chen, J., Pan, H. & Shi, Y. 2011, "Carbon dioxide capture by functionalized solid amine sorbents with simulated flue gas conditions", *Environmental science & technology,* vol. 45, no. 13, pp. 5710-5716.

64. y Leon, C.L., Solar, J.M., Calemma, V. and Radovic, L.R., 1992. Evidence for the protonation of basal plane sites on carbon. *Carbon*, *30*(5), pp.797-811.

65. Khatri, R.A., Chuang, S.S., Soong, Y. & Gray, M. 2006, "Thermal and chemical stability of regenerable solid amine sorbent for CO_2 capture", *Energy & Fuels,* vol. 20, no. 4, pp. 1514-1520.

66. Yang, Z., Lu, Y. and Yang, Z., 2009. Mesoporous materials: tunable structure, morphology and composition. *Chemical Communications*, (17), pp.2270-2277.

67. Liang, C., Li, Z. and Dai, S., 2008. Mesoporous carbon materials: synthesis and modification. *Angewandte Chemie International Edition*, *47*(20), pp.3696-3717.

68. Zhao, D., Feng, J., Huo, Q., Melosh, N., Fredrickson, G.H., Chmelka, B.F. and Stucky, G.D., 1998. Triblock copolymer syntheses of mesoporous silica with periodic 50 to 300 angstrom pores. *science*, *279*(5350), pp.548-552.

69. Asaftei, I.V., Bilba, N., Birsa, L.M. and Luchian, C., Sorption Properties of MCM-41 Mesoporous Materials.

70. Hoffmann, F., Cornelius, M., Morell, J. & Fröba, M. 2006, "Silica-based mesoporous organic–inorganic hybrid materials", *Angewandte Chemie International Edition,* vol. 45, no. 20, pp. 3216-325

71. Liu, S.H., Lin, Y.C., Chien, Y.C. and Hyu, H.R., 2011. Adsorption of CO_2 from flue gas streams by a highly efficient and stable aminosilica adsorbent. *Journal of the Air & Waste Management Association*, *61*(2), pp.226-233.

72. Yue, M.B., Sun, L.B., Cao, Y., Wang, Y., Wang, Z.J. and Zhu, J.H., 2008. Efficient CO_2 capturer derived from as-synthesized MCM-41 modified with amine. *Chemistry–A European Journal*, *14*(11), pp.3442-3451.

73. Yue, M.B., Chun, Y., Cao, Y., Dong, X. and Zhu, J.H., 2006. CO_2 capture by as-prepared SBA-15 with an occluded organic template. *Advanced Functional Materials*, *16*(13), pp.1717-1722.

74. Singh, V., Joung, D., Zhai, L., Das, S., Khondaker, S.I. & Seal, S. 2011, "Graphene based materials: past, present and future", *Progres*(Wang et al.., 2014)*s in materials science,* vol. 56, no. 8, pp. 1178-1271

75. Lonkar, S.P., Deshmukh, Y.S. & Abdala, A.A. 2015, "Recent advances in chemical modifications of graphene", *Nano Research,* vol. 8, no. 4, pp. 1039-1074.

76. Compton, O.C. & Nguyen, S.T. 2010, "Graphene Oxide, Highly Reduced Graphene Oxide, and Graphene: Versatile Building Blocks for Carbon-Based Materials", *small,* vol. 6, no. 6, pp. 711-723

77. Dreyer, D.R., Ruoff, R.S. & Bielawski, C.W. 2010, "From conception to realization: an historial account of graphene and some perspectives for its future", *Angewandte Chemie International Edition,* vol. 49, no. 49, pp. 9336-9344

78. Allen, M.J., Tung, V.C. & Kaner, R.B. 2009, "Honeycomb carbon: a review of graphene", *Chemical reviews,* vol. 110, no. 1, pp. 132-145.

79. Novoselov, K. May 2011*, Graphene: 2D carbon* [Homepage of Prof. Kostya Novoselov's], [Online]. Available: http://graphita.bo.imm.cnr.it/graphita2011/graphene.html.

80. Stankovich, S., Dikin, D.A., Piner, R.D., Kohlhaas, K.A., Kleinhammes, A., Jia, Y., Wu, Y., Nguyen, S.T. & Ruoff, R.S. 2007, "Synthesis of graphene-based nanosheets via chemical reduction of exfoliated graphite oxide", *carbon,* vol. 45, no. 7, pp. 1558-1565.

81. Zhu, C., Guo, S., Fang, Y. & Dong, S. 2010, "Reducing sugar: new functional molecules for the green synthesis of graphene nanosheets", *ACS nano,* vol. 4, no. 4, pp. 2429-2437.

82. Wang, G., Yang, J., Park, J., Gou, X., Wang, B., Liu, H. & Yao, J. 2008, "Facile synthesis and characterization of graphene nanosheets", *The Journal of Physical Chemistry C,* vol. 112, no. 22, pp. 8192-8195.

83. Erickson, K., Erni, R., Lee, Z., Alem, N., Gannett, W. & Zettl, A. 2010, "Determination of the local chemical structure of graphene oxide and reduced graphene oxide", *Advanced Materials,* vol. 22, no. 40, pp. 4467-4472.

84. Hontoria-Lucas, C., Lopez-Peinado, A., López-González, J.d.D., Rojas-Cervantes, M. & Martin-Aranda, R. 1995, "Study of oxygen-containing groups in a series of graphite oxides: physical and chemical characterization", *Carbon,* vol. 33, no. 11, pp. 1585-1592.

85. Lee, D. & Seo, J. 2011, "sp2/sp3 carbon ratio in graphite oxide with different preparation times", *The Journal of Physical Chemistry C,* vol. 115, no. 6, pp. 2705-2708.

86. Szabó, T., Berkesi, O., Forgó, P., Josepovits, K., Sanakis, Y., Petridis, D. & Dékány, I. 2006, "Evolution of surface functional groups in a series of progressively oxidized graphite oxides", *Chemistry of materials,* vol. 18, no. 11, pp. 2740-2749.

87. Mermoux, M., Chabre, Y. & Rousseau, A. 1991, "FTIR and 13C NMR study of graphite oxide", *Carbon,* vol. 29, no. 3, pp. 469-474.

88. He, H., Klinowski, J., Forster, M. & Lerf, A. 1998, "A new structural model for graphite oxide", *Chemical Physics Letters,* vol. 287, no. 1, pp. 53-56.

89. Lerf, A., He, H., Forster, M. & Klinowski, J. 1998, "Structure of graphite oxide revisited", *The Journal of Physical Chemistry B,* vol. 102, no. 23, pp. 4477-4482.

90. Johnson, J., Benmore, C., Stankovich, S. & Ruoff, R. 2009, "A neutron diffraction study of nano-crystalline graphite oxide", *Carbon,* vol. 47, no. 9, pp. 2239-2243.

91. Matsuo, Y., Nishino, Y., Fukutsuka, T. & Sugie, Y. 2007, "Introduction of amino groups into the interlayer space of graphite oxide using 3-aminopropylethoxysilanes", *Carbon,* vol. 45, no. 7, pp. 1384-1390.

92. Goeppert, A., Zhang, H., Olah, G.A. and Prakash, G.S., University of Southern California (USC), 2016. *Regenerative adsorbents of modified amines on solid supports*. U.S. Patent Application 14/991,886.

93. Knowles, G.P., Graham, J.V., Delaney, S.W. and Chaffee, A.L., 2005. Aminopropyl-functionalized mesoporous silicas as CO_2 adsorbents. Fuel Processing Technology, 86(14-15), pp.1435-1448.

94. Hicks, J.C., Drese, J.H., Fauth, D.J., Gray, M.L., Qi, G. and Jones, C.W., 2008. Designing adsorbents for CO_2 capture from flue gas-hyperbranched aminosilicas capable of capturing CO_2 reversibly. Journal of the American Chemical Society, 130(10), pp.2902-2903.

95. Zhao, Y., Ding, H. and Zhong, Q., 2012. Preparation and characterization of aminated graphite oxide for CO_2 capture. *Applied Surface Science*, *258*(10), pp.4301-4307.

96. Asenath Smith, E. and Chen, W., 2008. How to prevent the loss of surface functionality derived from aminosilanes. Langmuir, 24(21), pp.12405-12409.

97. Bourlinos, A.B., Gournis, D., Petridis, D., Szabó, T., Szeri, A. & Dékány, I. 2003, "Graphite oxide: chemical reduction to graphite and surface modification with primary aliphatic amines and amino acids", *Langmuir,* vol. 19, no. 15, pp. 6050-6055.

98. Wan, Y.J., Gong, L.X., Tang, L.C., Wu, L.B. and Jiang, J.X., 2014. Mechanical properties of epoxy composites filled with silane-functionalized graphene oxide. *Composites Part A: Applied Science and Manufacturing*, *64*, pp.79-89.

99. Shin, G.J., Rhee, K. and Park, S.J., 2016. Improvement of CO_2 capture by graphite oxide in presence of polyethylenimine. *International Journal of Hydrogen Energy*, *41*(32), pp.14351-14359.

100. Bhagiyalakshmi, M., Yun, L.J., Anuradha, R. and Jang, H.T., 2010. Utilization of rice husk ash as silica source for the synthesis of mesoporous silicas and their application to CO_2 adsorption through TREN/TEPA grafting. Journal of hazardous materials, 175(1), pp.928-938.

101. Sui, Z.Y., Cui, Y., Zhu, J.H. and Han, B.H., 2013. Preparation of three-dimensional graphene oxide–polyethylenimine porous materials as dye and gas adsorbents. ACS applied materials & interfaces, 5(18), pp.9172-9179.

102. Wang, X., Schwartz, V., Clark, J.C., Ma, X., Overbury, S.H., Xu, X. and Song, C., 2009. Infrared study of CO_2 sorption over "molecular basket" sorbent consisting of polyethylenimine-modified mesoporous molecular sieve. *The Journal of Physical Chemistry C*, *113*(17), pp.7260-7268.

103. Zhu, Y., Murali, S., Cai, W., Li, X., Suk, J.W., Potts, J.R. and Ruoff, R.S., 2010. Graphene and graphene oxide: synthesis, properties, and applications. *Advanced materials*, *22*(35), pp.3906-3924.

104. Boukhvalov, D. & Katsnelson, M. 2009, "Chemical functionalization of graphene", *Journal of Physics: Condensed Matter,* vol. 21, no. 34, pp. 344205.

105. Serna-Guerrero, R., Da'na, E. & Sayari, A. 2008, "New insights into the interactions of CO_2 with amine-functionalized silica", *Industrial & Engineering Chemistry Research,* vol. 47, no. 23, pp. 9406-9412.

106. Park, J.Y. & Kim, S. 2013, "Preparation and electroactivity of polymer-functionalized graphene oxide-supported platinum nanoparticles catalysts", *International Journal of Hydrogen Energy,* vol. 38, no. 14, pp. 6275-6282.

107. Chen, J., Yao, B., Li, C. & Shi, G. 2013, "An improved Hummers method for eco-friendly synthesis of graphene oxide", *Carbon,* vol. 64, pp. 225-229.

108. Ferrer, N., 2012. Applications of Fourier transform infrared spectroscopy. *Unitat d'Anàlisi Molecular, CCiTUB, Universitat de Barcelona. Lluís Solé i Sabarís*, pp.1-3.

109. Doyle, W.M., 1992. Principles and applications of Fourier transform infrared (FTIR) process analysis. Process control and quality, 2, p.50.

110. Siesler, H.W., Ozaki, Y., Kawata, S. and Heise, H.M. eds., 2008. Near-infrared spectroscopy: principles, instruments, applications. John Wiley & Sons.

111. Song, J., Wang, X. and Chang, C.T., 2014. Preparation and characterization of graphene oxide. Journal of Nanomaterials, 2014.

112. Lin-Vien, D., Colthup, N.B., Fateley, W.G. and Grasselli, J.G., 1991. The handbook of infrared and Raman characteristic frequencies of organic molecules. Elsevier.

113. Yang, S., Zhan, L., Xu, X., Wang, Y., Ling, L. and Feng, X., 2013. Graphene-Based Porous Silica Sheets Impregnated with Polyethyleneimine for Superior CO_2 Capture. *Advanced Materials*, *25*(15), pp.2130-2134.

114. Frankenburg, W.G., Komarewsky, V.I. and Rideal, E.K., 1952. *Advances in catalysis* (Vol. 4). Academic Press.

115. Loye, Z.H.2013, X-Ray Diffraction: How it works (http://www.chem.sc.edu/faculty/zurloye/xrdtutorial_2013.pdf), University of South Carolina.

116. Chowdhury, S. and Balasubramanian, R., 2016. Three-dimensional graphene-based porous adsorbents for postcombustion CO2 capture. *Industrial & Engineering Chemistry Research*, *55*(29), pp.7906-7916.

117. Navaee, A. and Salimi, A., 2015. Efficient amine functionalization of graphene oxide through the Bucherer reaction: an extraordinary metal-free electrocatalyst for the oxygen reduction reaction. *RSC Advances*, *5*(74), pp.59874-59880.

118. Sawinski, P.K., Meven, M., Englert, U. and Dronskowski R., 2013. Single-crystal neutron diffraction study on guanidine, CN_3H_5. *Crystal Growth & Design*, *13*(4), pp.1730-1735.

119. Dalagan, J.Q. and Enriquez, E.P., 2014. One-step synthesis of mesoporous silica–graphene composites by simultaneous hydrothermal coupling and reduction of graphene oxide. *Bulletin of Materials Science*, *37*(3), pp.589-595.

120. Zhang, L.L., Zhao, S., Tian, X.N. and Zhao, X.S., 2010. Layered graphene oxide nanostructures with sandwiched conducting polymers as supercapacitor electrodes. *Langmuir*, *26*(22), pp.17624-17628.

121. Sanz-Pérez, E.S., Dantas, T.C.M., Arencibia, A., Calleja, G., Guedes, A.P.M.A., Araujo, A.S. and Sanz, R., 2017. Reuse and recycling of amine-functionalized silica materials for CO_2 adsorption. *Chemical Engineering Journal*, *308*, pp.1021-1033.

122. Goldstein, J., Newbury, D.E., Echlin, P., Joy, D.C., Romig Jr, A.D., Lyman, C.E., Fiori, C. and Lifshin, E., 2012. *Scanning electron microscopy and X-ray microanalysis: a text for biologists, materials scientists, and geologists*. Springer Science & Business Media

123. Jeol Manufacturing Company " Basic knowledge for using SEM" *http://www.jeol.co.jp/en/applications/pdf/sm/sem_atoz_all.pdf*, Jeol Ltd.

124. Ngo, P.D., 1999. Energy dispersive spectroscopy. In *Failure Analysis of Integrated Circuits* (pp. 205-215). Springer US.

125. Gurunathan, S., Han, J.W. and Kim, J.H., 2013. Green chemistry approach for the synthesis of biocompatible graphene. *International journal of nanomedicine*, *8*, p.2719.

126. Jia, Z. and Wang, Y., 2015. Covalently crosslinked graphene oxide membranes by esterification reactions for ions separation. *Journal of* Materials *Chemistry A*, *3*(8), pp.4405-4412.

127. Austrian Centre for Electron Microscopy and Nanoanalysis *, The principles of TEM* [Homepage of FELMI-ZFE, Steyrergasse], [Online]. Available:

http://portal.tugraz.at/portal/page/portal/felmi/ResearchN/research/TEM%20and%20Nano analysis/Principles%20of%20TEM.

128. Rouquerol, J., Rouquerol, F., Llewellyn, P., Maurin, G. and Sing, K.S., 2013. Adsorption by powders and porous solids: principles, methodology and applications. Academic press.

129. Nishi, Y. and Inagaki, M., 2016. Gas adsorption/desorption isotherm for pore structure characterization. In *Materials Science and Engineering of Carbon* (pp. 227-247). Butterworth-Heinemann. (adsorption image)

130. Sing, K.S., 2004. Characterization of porous materials: past, present and future. *Colloids and Surfaces A: Physicochemical and Engineering Aspects*, *241*(1), pp.3-7.

131. Sing, K., 2001. The use of nitrogen adsorption for the characterisation of porous materials. *Colloids and Surfaces A: Physicochemical and Engineering Aspects*, *187*, pp.3-9.

132. Leofanti, G., Padovan, M., Tozzola, G. and Venturelli, B., 1998. Surface area and pore texture of catalysts. *Catalysis Today*, *41*(1), pp.207-219

133. Donohue, M.D. and Aranovich, G.L., 1998. Adsorption hysteresis in porous solids. Journal of colloid and interface science, 205(1), pp.121-130.

134. Gao, W., Wan, Y., Dou, Y. and Zhao, D., 2011. Synthesis of partially graphitic ordered mesoporous carbons with high surface areas. *Advanced Energy Materials*, *1*(1), pp.115-123.

135. Chowdhury, D.R., Singh, C. and Paul, A., 2014. Role of graphite precursor and sodium nitrate in graphite oxide synthesis. *RSC Advances*, *4*(29), pp.15138-15145.

136. Eigler, S., Dotzer, C., Hirsch, A., Enzelberger, M. and Müller, P., 2012. Formation and decomposition of CO_2 intercalated graphene oxide. *Chemistry of Materials*, *24*(7), pp.1276-1282.

137. Mishra, A.K. and Ramaprabhu, S., 2011. Carbon dioxide adsorption in graphene sheets. *AIP Advances*, *1*(3), p.032152

138. Hong, S.M. and Lee, K.B., 2014. Solvent-assisted amine modification of graphite oxide for CO_2 adsorption. *RSC Advances*, *4*(100), pp.56707-56712

139. Liu, Y., Li, Y., Li, X. & He, T. 2013, "Kinetics of (3-aminopropyl) triethoxylsilane (APTES) silanization of superparamagnetic iron oxide nanoparticles", *Langmuir,* vol. 29, no. 49, pp. 15275-15282.

140. Matsuo, Y., Sakai, Y., Fukutsuka, T. and Sugie, Y., 2009. Preparation and characterization of pillared carbons obtained by pyrolysis of silylated graphite oxides. *Carbon*, *47*(3), pp.804-811.

141. Chaffee, A.L., Knowles, G.P., Liang, Z., Zhang, J., Xiao, P. & Webley, P.A. 2007, "CO_2 capture by adsorption: materials and process development", *International journal of greenhouse gas control,* vol. 1, no. 1, pp. 11-18.

142. Wang, Z.M., Hoshinoo, K., Shishibori, K., Kanoh, H. and Ooi, K., 2003. Surfactant-Mediated Synthesis of a Novel Nanoporous Carbon− Silica Composite. *Chemistry of materials*, *15*(15), pp.2926-2935.

143. dos Santos, T.C., Bourrelly, S., Llewellyn, P.L., Carneiro, J.W.D.M. and Ronconi, C.M., 2015. Adsorption of CO_2 on amine-functionalised MCM-41: experimental and theoretical studies. *Physical Chemistry Chemical Physics*, *17*(16), pp.11095-11102.

144. , S., Hsiao, W. & Chiang, C. 2012, "Synthesis of Stable tetraethylenepentamine-functionalized mesocellular silica foams for CO_2 adsorption", *Journal of Chemistry,* vol. 2013

145. Yan, X., Zhang, L., Zhang, Y., Yang, G. and Yan, Z., 2011. Amine-modified SBA-15: effect of pore structure on the performance for CO_2 capture. *Industrial & Engineering Chemistry Research*, *50*(6), pp.3220-3226.

146. Goeppert, A., Czaun, M., May, R.B., Prakash, G.S., Olah, G.A. and Narayanan, S.R., 2011. Carbon dioxide capture from the air using a polyamine based regenerable solid adsorbent. *Journal of the American Chemical Society*, *133*(50), pp.20164-20167.